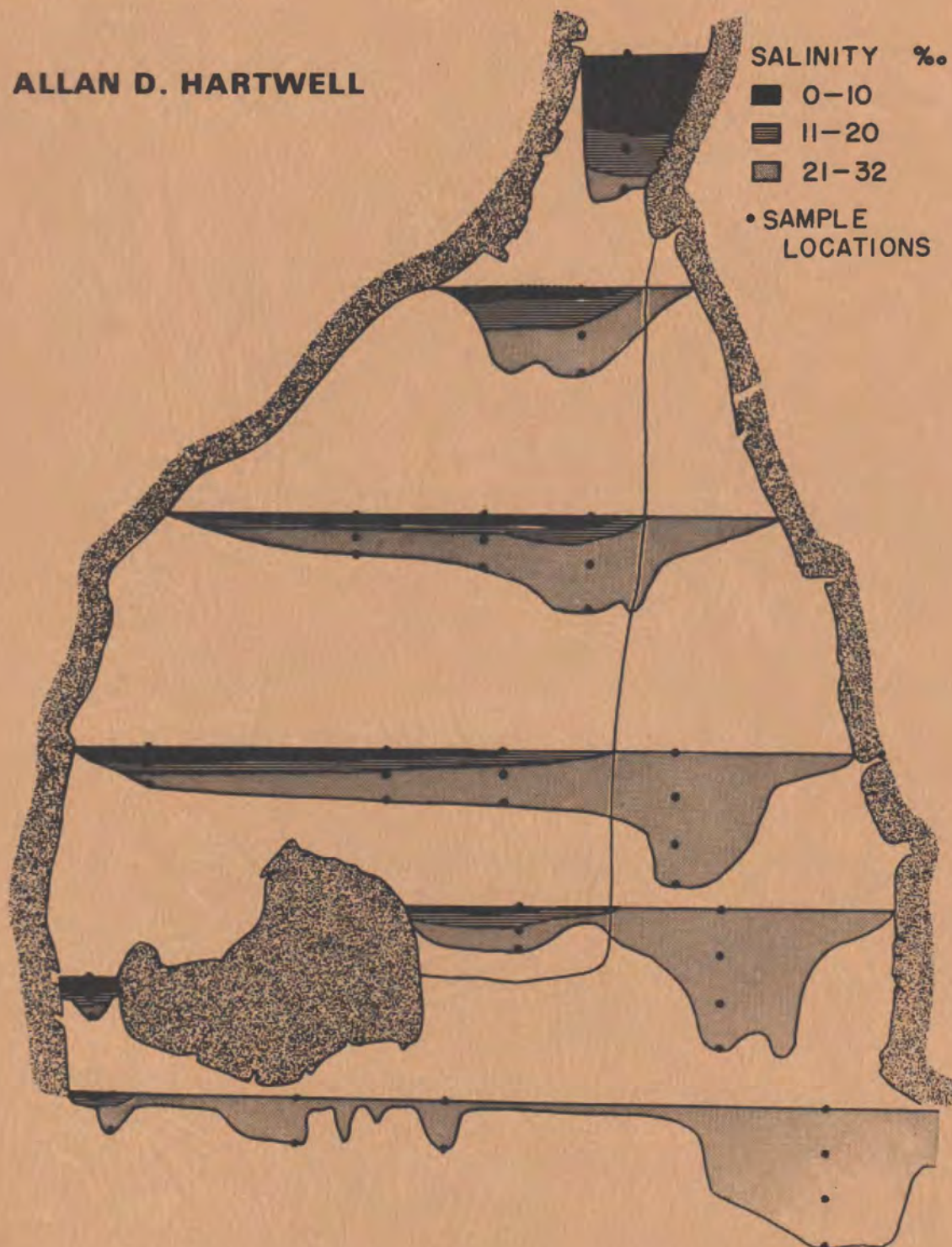


HYDROGRAPHY AND HOLOCENE SEDIMENTATION of the Merrimack River Estuary Massachusetts

ALLAN D. HARTWELL



Contribution No. 5-CRG obtained under Contract No. Nonr
N00014-67-A-0230-0001, Task Order No. NR 388-084 of
the Geography Branch, Office of Naval Research.
Distribution of this document is unlimited.

Contribution No. 5-CRG
Department of Geology
University of Massachusetts
June 1970

HYDROGRAPHY AND HOLOCENE SEDIMENTATION
OF THE MERRIMACK RIVER ESTUARY,
MASSACHUSETTS

Allan D. Hartwell

The contents of this report may be reproduced in whole
or in part for any purpose of the United States Government.
Distribution of this document is unlimited.

TABLE OF CONTENTS

	Page
Abstract.....	1
Introduction.....	4
Acknowledgements.....	11
Hydrography.....	12
Surface circulation pattern.....	13
Stratification and three-dimensional circulation.....	13
Effect of below-normal discharge.....	21
Current velocity.....	34
Current-velocity asymmetry.....	39
Suspended sediments.....	42
Hydrography of the Plum Island River.....	47
Sedimentary environments.....	51
Sediment distribution patterns.....	51
Main channel.....	72
Subtidal channel.....	75
Flood-tidal delta.....	81
Intertidal flats.....	108
Secondary tidal channels.....	123
Major tidal channels.....	123
Minor tidal channels.....	135
Salt marsh.....	136
Recent geologic history of the Merrimack River estuary.....	155

Summary and conclusions.....	160
References cited.....	164

LIST OF ILLUSTRATIONS

Figure	Page
1. Location map for hydrographic sampling locations.....	6
2. Map of sedimentary environments of the estuary.....	8
3. Infrared imagery of hydrographic circulation.....	15
4. Salinity distribution during a tidal cycle: normal discharge conditions.....	18
5. Three-dimensional flood-tide stratification.....	20
6. Salinity variation with depth: low-water.....	23
7. Salinity variation with depth: two hours after low water.....	25
8. Salinity variation with depth: two hours before high water...	27
9. Salinity variation with depth: high water.....	29
10. Salinity variation with depth: four hours after high water...	31
11. Salinity distribution during a tidal cycle: below normal discharge conditions.....	33
12. Hydrographic changes during a tidal cycle at a single station.	36
13. Tidal current-velocity profiles at a single station.....	38
14. Tidal current-velocity profiles at four stations in the main channel.....	41
15. Tidal current-velocity asymmetry.....	44
16. Suspended sediments during a tidal cycle.....	46
17. Hydrographic changes during a tidal cycle in the Plum Island River.....	49
18. Distribution of sediments by type.....	54

19. Distribution of sediments by mean grain size.....	56
20. Distribution of sediments by sorting.....	59
21. Distribution of sediments by inclusive graphic skewness.....	62
22. Scatter plot of inclusive graphic standard deviation versus graphic mean.....	64
23. Scatter plot of inclusive graphic skewness versus graphic mean.....	67
24. Grain-size distribution by frequency percent: main channel...	69
25. Grain-size distribution by frequency percent: secondary tidal channels.....	71
26. Cross-channel bottom profiles of the lower estuary.....	74
27. Cross-channel bottom profiles of the upper estuary.....	77
28. Bottom topography and sediment mean grain size in the main channel.....	80
29. Aerial photograph of the flood-tidal delta.....	84
30. Plane-table map of the flood-tidal delta.....	86
31. Slip-face azimuths of bedforms on the flood-tidal delta during a normal low tide.....	89
32. Slip-face azimuths of sand waves on the flood-tidal delta.....	92
33. Spring-tidal conditions on the flood-tidal delta.....	94
34. Neap-tidal conditions on the flood-tidal delta.....	94
35. Slip-face azimuths of ripples.....	96
36. Histograms of ripple wavelength.....	99
37. Slip-face azimuths of megaripples.....	102

38. Histograms of megaripple wavelength and amplitude.....	104
39. Photographs showing slip-face migration of a flood-oriented sand wave.....	107
40. Sand wave slip-face migration.....	109
41. Photograph of current lineation on intertidal flat.....	112
42. Photograph of intertidal clam flat with bordering mussel bank..	112
43. Photograph of sedimentary structures developed in intertidal flats and secondary tidal channels.....	114
44. Structures developed in intertidal mud flat.....	116
45. Photograph of worm burrows in intertidal flat.....	119
46. Photograph of peat block in intertidal flat.....	119
47. Photograph of mussel bank in intertidal flat.....	121
48. Close-up photograph of mussel bank.....	121
49. Bottom topography and sediment mean grain size along the main channel of the Plum Island River.....	125
50. Rhythmite structures in secondary tidal channel.....	128
51. Plane-table map of point bar.....	130
52. Photograph of ebb scour-megaripples on point bar.....	133
53. Photograph of ebb-current lineation on point bar.....	133
54. Lithology of marsh cores A-T.....	139
55. Lithology of marsh cores J-Q.....	141
56. Peat isopach map of Salisbury Marsh.....	144
57. Peat isopach map of Plum Island River Marsh.....	146
58. Stratigraphic cross sections of Salisbury Marsh.....	149
59. Stratigraphic cross sections of Salisbury Marsh and Plum Island River Marsh.....	151

60. Photograph of ice blocks on bank of Plum Island River.....	154
61. Close-up photograph of ice-rafted sediment deposited on marsh surface.....	154
62. Shoreline changes at the northern end of Plum Island and the southern end of Salisbury Beach.....	158

Abstract: The Merrimack River estuary, situated on glaciated terrain along the coast of northeastern Massachusetts, is representative of the Type B estuary of Pritchard (1955). When the tide floods during periods of normal and high runoffs, a sharp, slightly tilted boundary develops between the intruding salt-water mass and the overriding fresh water. The salt water from the ocean is deflected to the north, or right side of the estuary, while the fresh water ponds up on the south side, where a significant amount of the suspended sediment and pollutant load carried by the river is deposited. When discharge drops below approximately 3000 cfs, the stratification disappears and the estuary becomes partially mixed. Maximum ebb-current velocities, which are frequently twice as strong as flood-current velocities, are concentrated in the upper portion of the water column, whereas maximum flood-current velocities occur near the bottom.

The distribution of bottom sediments is closely related to the hydraulic circulation pattern, tidal current velocities, bottom topography, and sediment source areas. Coarsest sediments are found in the main channel (gravel to gravelly sand; mean -1.06ϕ to 0.95ϕ), where strong tidal currents winnow out fine sand and mud. The inter-tidal flats, which are inhabited by clams, worms, and mussels, are composed of muddy sand to mud (mean 2.1ϕ to 5.4ϕ) that is mostly poorly to very poorly sorted, fine-skewed, and leptokurtic. Sediments of the secondary tidal channels have variable textural parameters. Numerous point bars are present in the channels where sand is abundant and tidal currents are moderate. Sediments in the minor

secondary tidal channels are also variable but are generally fine-grained sand to mud, poorly sorted to very poorly sorted, fine-skewed, and leptokurtic.

The flood-tidal delta near the inlet mouth is a dynamic sediment body composed of well-sorted sand and gravelly sand (mean 1.15 ϕ to 2.54 ϕ) and covered by bedforms. The highest part of the tidal delta forms an ebb shield which protects flood-oriented sand waves along the northeastern margin from modification by ebb currents. The bedforms undergo marked changes in magnitude, orientation, and migration rates in response to variations in estuarine water volume during neap, normal, and spring tides and fluctuations in river discharge.

Characteristic structures are found in each sedimentary environment of the estuary. Included are crossbedding, laminations, worm burrows, clam burrows, hydrogen sulphide cells, organic mottles, rhythmites, and buried flats of large Mya arenaria in life position.

Three types of sand are present in the estuary. A yellow-orange feldspathic suite (modal size 0.5 ϕ to 1.0 ϕ), which contains abundant rock fragments, occupies the main channel and is apparently being transported downstream from an upland glacial outwash source area. A gray feldspathic suite (modal size 1.1 ϕ to 1.5 ϕ), which underlies the marshes of the lower estuary, seems to be derived locally, possibly from the Newburyport Quartz Diorite. A third sand type (modal size 2.4 ϕ to 2.9 ϕ), which is dominantly quartz (86 percent) with subequal amounts of gray and yellow-orange feldspar (5 percent), is common in the central part of the main channel and in some tidal channels; its origin is uncertain.

The fringing salt marshes include intertidal Spartina alterniflora marsh and supratidal high salt marsh dominated by Spartina patens.

Laminations are common in the salt-marsh peat. The stratigraphy and geometry of the marsh deposits document a gradual rise in sea level and infilling of an original open bay environment behind the barrier islands accompanying marine transgression since late Pleistocene.

INTRODUCTION

The hydrography and Holocene sedimentation of the Merrimack River estuary, situated on glaciated terrain along the coast of northeastern Massachusetts (Fig. 1), is of considerable interest from both the practical and scientific points of view. Inasmuch as the Merrimack is highly polluted, the zones of maximum pollution within the estuary are determined by the circulation pattern. From a scientific standpoint, this estuary is a classic Type B estuary of Pritchard (1955), which develops a sharp, slightly tilted boundary between the salt-water wedge and surficial fresh water as the tide floods during periods of normal and high runoff.

Most of the river channel in the upper estuary is narrow, with irregular bottom topography reflecting bedrock control by the underlying Paleozoic igneous and metamorphic rocks (Sears, 1905; Emerson, 1917; Clapp, 1921). Near Newburyport the estuary broadens eastward into a wide embayment with extensive tidal flats and 16.9 km² of salt marsh. Scattered hummocks in the Black Rock Creek marsh and numerous intertidal outcrops (Fig. 2) attest to the shallowness of bedrock. The Newburyport Quartz Diorite of probable Devonian age (Chute, 1964) is the dominant bedrock unit in the study area. The lower estuary is separated from the ocean by two barrier islands, Plum Island on the south and Salisbury Beach to the north. The inlet mouth had undergone marked shoreline changes during historic times, including 1200 m of northward migration since about 1840.

Figure 1. Location map of the study area showing hydrographic sampling stations and channel profiles in the Merrimack River estuary, Massachusetts.

HYDROGRAPHIC SAMPLING LOCATIONS MERRIMACK RIVER ESTUARY

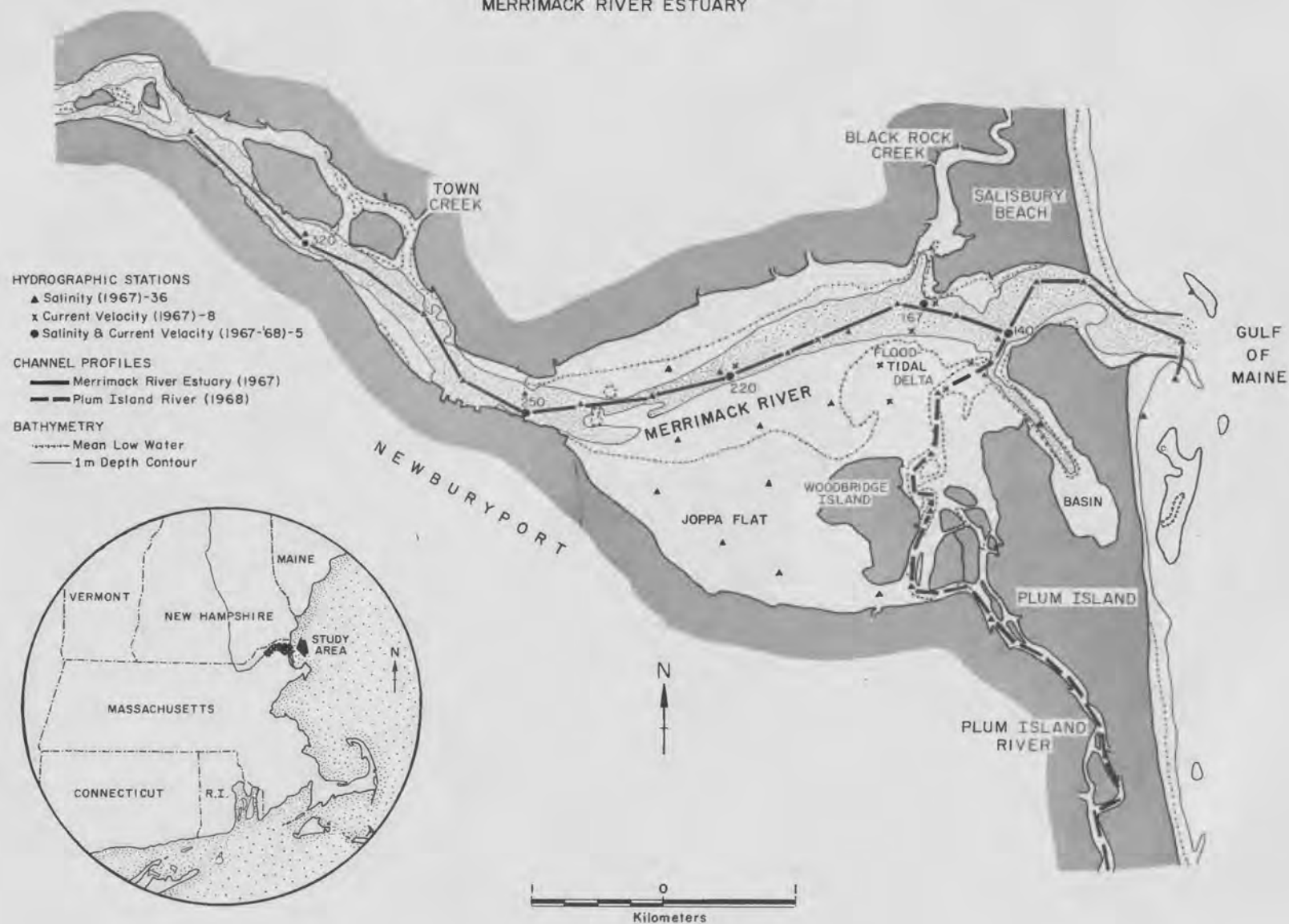


Figure 1

Figure 2. Geographic distribution of the sedimentary environments of the estuary.

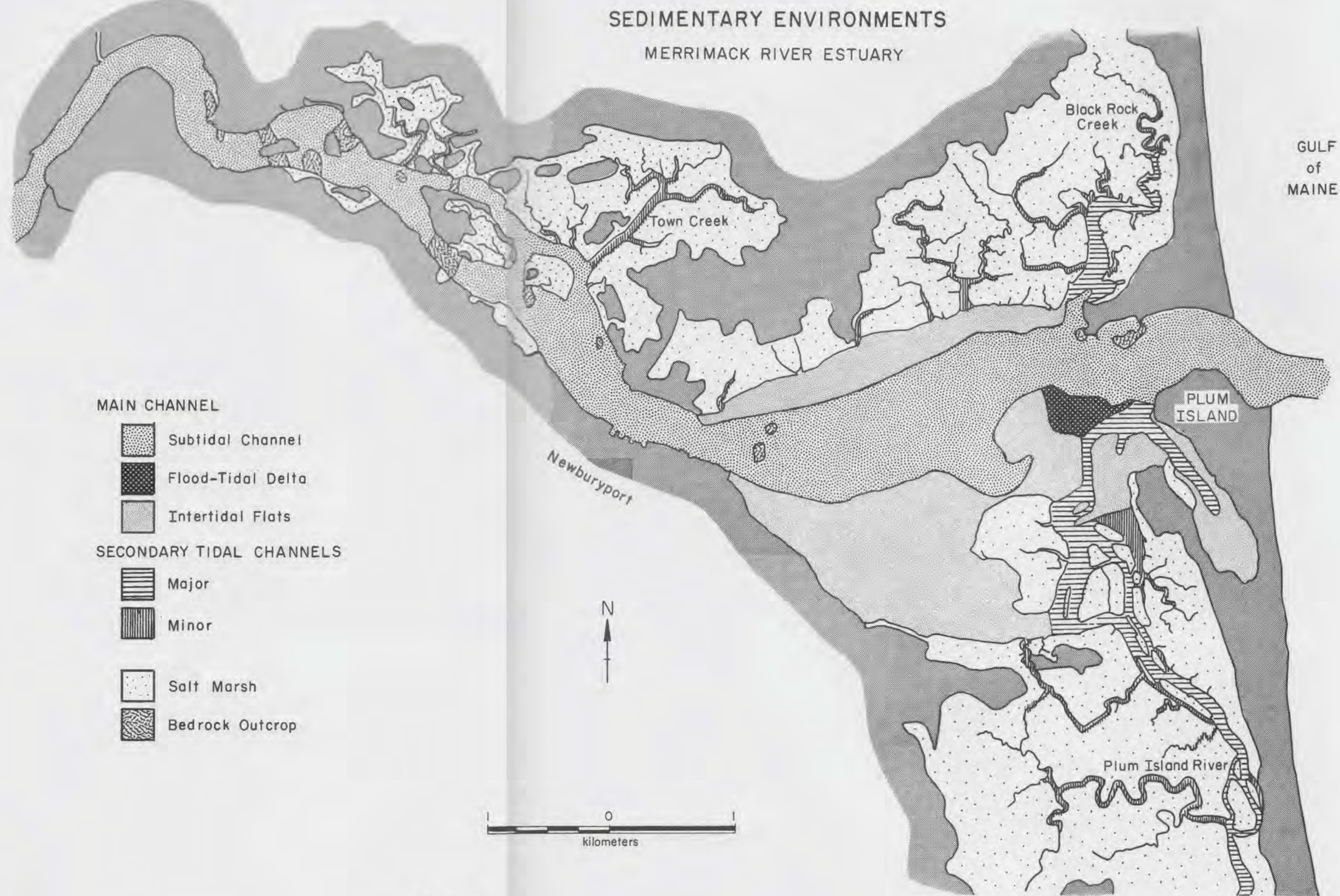


Figure 2

The Merrimack River is the fourth largest river in New England, after the Connecticut, Penobscot, and St. John. It occupies a drainage basin of $12,970 \text{ km}^2$ which extends from the White Mountains of New Hampshire southward into northeastern Massachusetts. The river descends 77.3 m at a generally uniform slope along its 186 km path from Franklin, New Hampshire, to the ocean at Plum Island, Massachusetts.

Annual rainfall in the watershed averages 53 cm (21 in) per year, varying from 76-102 cm (30-40 in) in the extreme north to less than 46 cm (18 in) near the coast. Average daily discharge is about 7000 cfs, ranging from more than 23,000 cfs in the spring to about 1700 cfs in the fall. The lower 35.4 km of the channel are tidal, with a mean tidal range of 2.5 m (8.2 ft) at the mouth and 1.5 m (5.1 ft) at Haverhill. During midsummer of 1967 and 1968, salt water intruded the lower 12.9 km of the river, but salty water probably intrudes further up river during periods of lower discharge. During an average tidal cycle, more than 8 billion gallons of water are exchanged in the estuary (Jerome and others, 1965).

Earlier studies of this portion of the New England coast include those of Johnson (1919; 1925), Chute and Nichols (1941), and Nichols (1942). McIntire and Morgan (1963) established the framework of the stratigraphic history of the Plum Island area as well as the complex series of sea-land level changes that have occurred since 6300 B.P. McCormick (1968) supplemented their work with detailed coring in the Parker River. The report by Jerome and others (1965) is the most comprehensive paper to date on the Merrimack River estuary. Their

study emphasizes the marine resources but includes an excellent summary of surface hydrography and infaunal distribution. The hydrographic circulation pattern was further defined using infrared imagery (Wiesnet and Cotton, 1967) and three-dimensional hydrographic sampling (Coastal Research Group, 1969). Additional data on the Merrimack estuary have been published by the University of Massachusetts Coastal Research Group (1969: in particular see Hartwell and Hayes, hydrography, p. 218-244; Hartwell, Holocene stratigraphy of the salt marshes, p. 428-440; and field trip stop descriptions, p. 34, 176-178, 184-217). Other pertinent work in the area includes surficial mapping by Chute and Nichols (1941) and Sammel (1963), a study by Sammel (1962) on the configuration of bedrock beneath the channel of the lower Merrimack, and a report of the Commonwealth of Massachusetts, Department of Public Health (1964) on sewage disposal in the Merrimack River valley.

Most of the field work for this project relating to the bottom sediments and marsh stratigraphy was conducted between June and September, 1968. However, much of the hydrographic information was collected during the preceding summer by members of the University of Massachusetts Coastal Research Group.

ACKNOWLEDGEMENTS

Most of the funds for this project were obtained under Contract No. Nonr N00014-67-A-0230-001, Task Order No. NR 388-084 of the Geography Branch, Office of Naval Research. Special thanks are extended to Miles O. Hayes, supervisor of the project. Professors Joseph H. Hartshorn and Gregory W. Webb read the manuscript and made many helpful suggestions. David V. Reynolds provided valuable field assistance and the author is especially grateful for his help. Many staff members and graduate students at the University also gave assistance. Eugene G. Rhodes wrote the computer program used in determining the grain-size parameters and helped run fathometer profiles. Robert Gonter from the Research Computing Center was responsible for modifying the computer program to calculate sediment ratios and frequency-percent data. Richard Brown drafted a number of the figures. Sharon A. Greer and Gregory Field assisted in suspended sediment sampling. In addition, Matthew H. Pacillo, Harold Larson, and David M. Atwood from the U.S. Army Cold Regions Research and Engineering Laboratory, Hanover, New Hampshire, provided assistance in drafting and photographic reproduction.

HYDROGRAPHY

The Merrimack River estuary, a representative of the Type B estuary (Pritchard, 1955), is usually well stratified. If discharge is greater than about 3000 cfs, a sharp, slightly tilted boundary develops between the intruding salt-water mass and the overriding fresh water. During the flood period, salt water from the ocean is deflected to the north, or right side of the estuary, whereas the fresh water ponds up on the south side over Joppa Flat (Figs. 1 and 5), where a significant amount of the suspended sediment and pollutant load carried by the river is deposited. Throughout the estuary, the hydrographic circulation pattern strongly affects the distribution of sediments.

Hydrographic measurements were made at 70 locations in the estuary by anchor and drift sampling techniques during 13-hour periods in order to gather data through a complete tidal cycle. During the summer of 1968 a Beckman Induction Salinometer was used to measure salinity and temperature in situ. The 1967 data were measured by standard hydrometer techniques. Current velocity profiles were obtained using a calibrated drag vane and lead weights. Two-hundred suspended sediment samples (each 0.95 liter) were analyzed by Millipore filtration techniques utilizing 1.2 micron cellulose filters. Bottom profiles were obtained with a Raytheon recording fathometer along 34 north-south traverses and a 13 km east-west channel section.

Surface circulation pattern

The surface circulation pattern of the Merrimack estuary is clearly delineated by infrared imagery obtained in August and September, 1966, by D.R. Wiesnet and J.E. Cotton of the Water Resource Division, U.S. Geological Survey, Boston, Mass. The imagery in Figure 3, taken from Wiesnet and Cotton (1967), shows the estuary at ebb tide, low water, flood tide, and high water. This imagery shows that the estuary was filled with high-temperature, low-salinity water at low tide. As the tide began to flood, a wedge of cold salt water moved up the north side of the estuary. At high-water and early into the ebb period, the ponded fresh water on Joppa Flat streamed toward the northeast over the main channel of the estuary; at approximately midtide, the whole surface of the estuary was covered with low-salinity river water.

Stratification and three-dimensional circulation

In order to relate the three-dimensional circulation of the estuary to the surface pattern depicted by the infrared imagery (Fig. 3), a detailed sampling program was undertaken on July 7 and 8, 1967. Thirty-four sampling stations (at high tide) were established. These stations, except for a few that were dry at low water, were sampled at two-hour intervals through a complete tidal cycle. Samples were taken from the surface to the bottom at 1 m intervals. This was accomplished with four field crews in small boats that attempted to collect a "simultaneous" sample over a time span of twenty minutes. The lower

Figure 3. Infrared imagery of the Merrimack River estuary: Plum Island to Newburyport. Upstream is to the left. For orientation, see jetties on the right of the upper diagram and the city of Newburyport on the lower left of the lower diagram (Fig. 1).

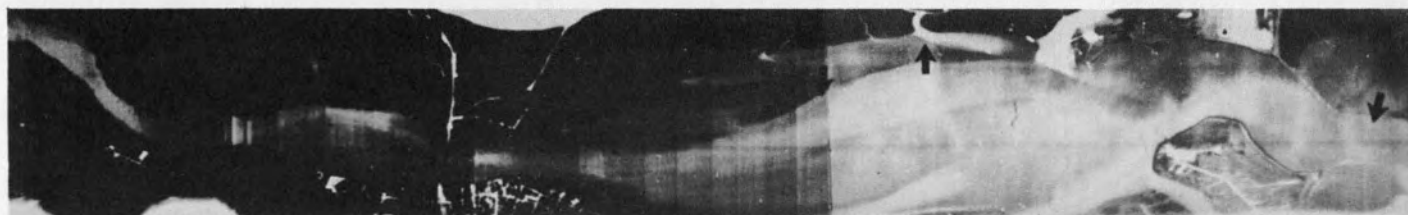
Ebb: Outgoing tide at 0335, Sept. 29, 1966. Whole estuary is full of light-colored, warm, low-salinity water.

Low-water: Low tide at 1922, Sept. 28, 1966. Note uniform tone of the warm estuarine water throughout the entire length of the estuary.

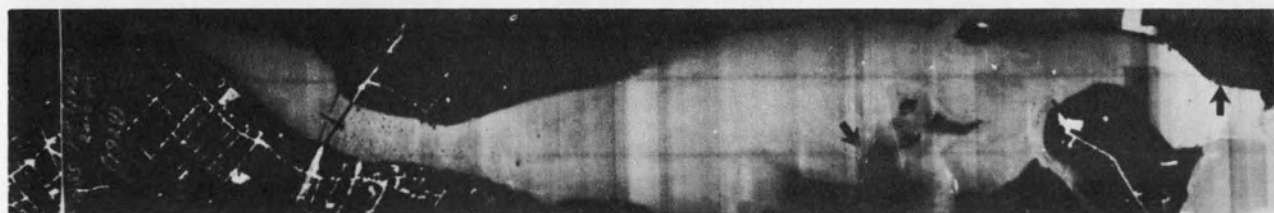
Flood: Incoming tide at 2205, Sept. 28, 1966. Note the surface expression of the salt water (cold water) interface. Arrow at left points to leading edge of the salt-water wedge.

High-water: High tide at 0037, Sept. 29, 1966. Note the spreading of warm (light-colored) estuarine water over the cold ocean water, especially in the area of Joppa Flat.

(From Wiesnet and Cotton, 1967, Fig. 2).



EBB



LOW



FLOOD



HIGH

Figure 3

half of the estuary was sampled on July 7 and the upper half was sampled one hour later at each designated interval on July 8.

From the data of July 7 and 8, 1967, it was possible to construct longitudinal cross sections (for given sampling intervals) of the estuarine water mass from the mouth to 9 km upstream (Figs. 1 and 4). Figure 4, a plot of the salinity data collected through a complete tidal cycle along the axis of the main channel, clearly shows the three-dimensional pattern of flow. Note that these salinity data were collected when the river discharge was nearly normal, about 6300 cfs. At low water, most of the estuary contained fresh water. During early flood, the salt water at the mouth began to intrude upstream along the channel bottom. Two hours after low water, the 5‰ isohaline had moved more than 3 km upstream and some horizontal stratification had developed in the lower estuary. Four hours after low water, the whole upper estuary had a well-developed horizontal stratification, whereas the lower estuary was almost entirely salt water. The fresh water-salt water interface was well developed at high water; however, once the damming effect of the flood current was removed, the boundary moved rapidly seaward and stratification was destroyed. By low water, nearly all the salt water had been flushed out of the main channel.

The entire three-dimensional framework of salinity structure in the estuary at two hours before high water is shown in Figure 5. This diagram indicates that the salt water-fresh water interface is slightly tilted toward the south; hence the estuary falls into the Type B class of Pritchard (1955). The three-dimensional salinity structure of the

Figure 4. Salinity distribution during a complete tidal cycle in a longitudinal cross section along the axis of the main channel (location map, Fig. 1). Data collected July 7-8, 1967, when discharge was about 6300 cfs.

SALINITY DISTRIBUTION DURING A TIDAL CYCLE
MERRIMACK RIVER ESTUARY
JULY 7-8, 1967

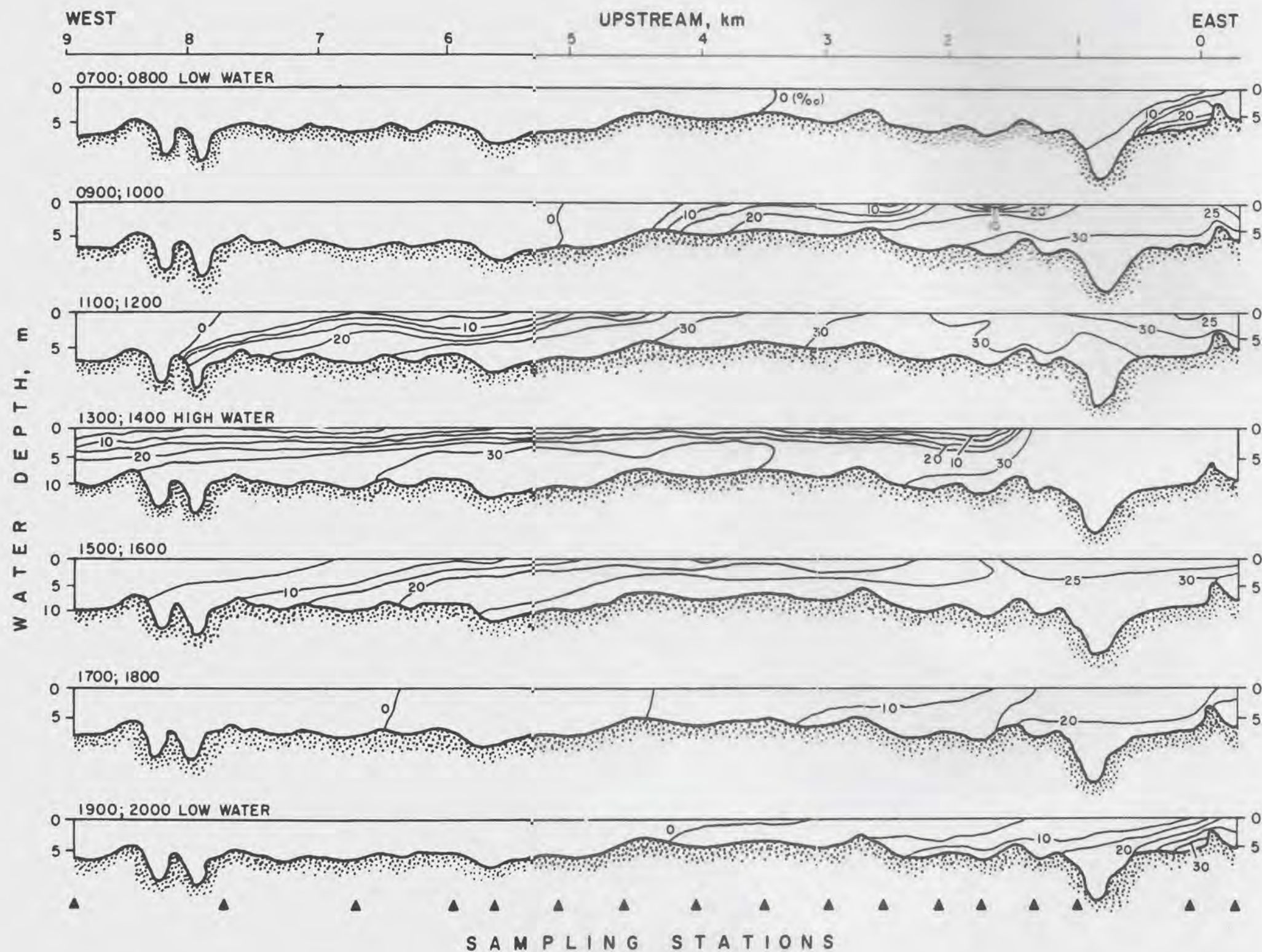


Figure 4

Figure 5. Three-dimensional flood-tide stratification in the lower estuary about 2 hours before high water. Data in the bottom three cross sections collected at 1100 on July 7, 1967; upper three cross sections collected at 1200 on July 8, 1967. Note that salt water from the ocean is deflected to the north, or right side of the estuary, while the fresh water ponds up on the south side where a significant amount of the suspended sediment and pollutant load carried by the river is deposited.

3-D FLOOD-TIDE STRATIFICATION

MERRIMACK RIVER ESTUARY

2 HOURS BEFORE HIGH WATER

11 00 7 JULY, 1967

12 00 8 JULY, 1967

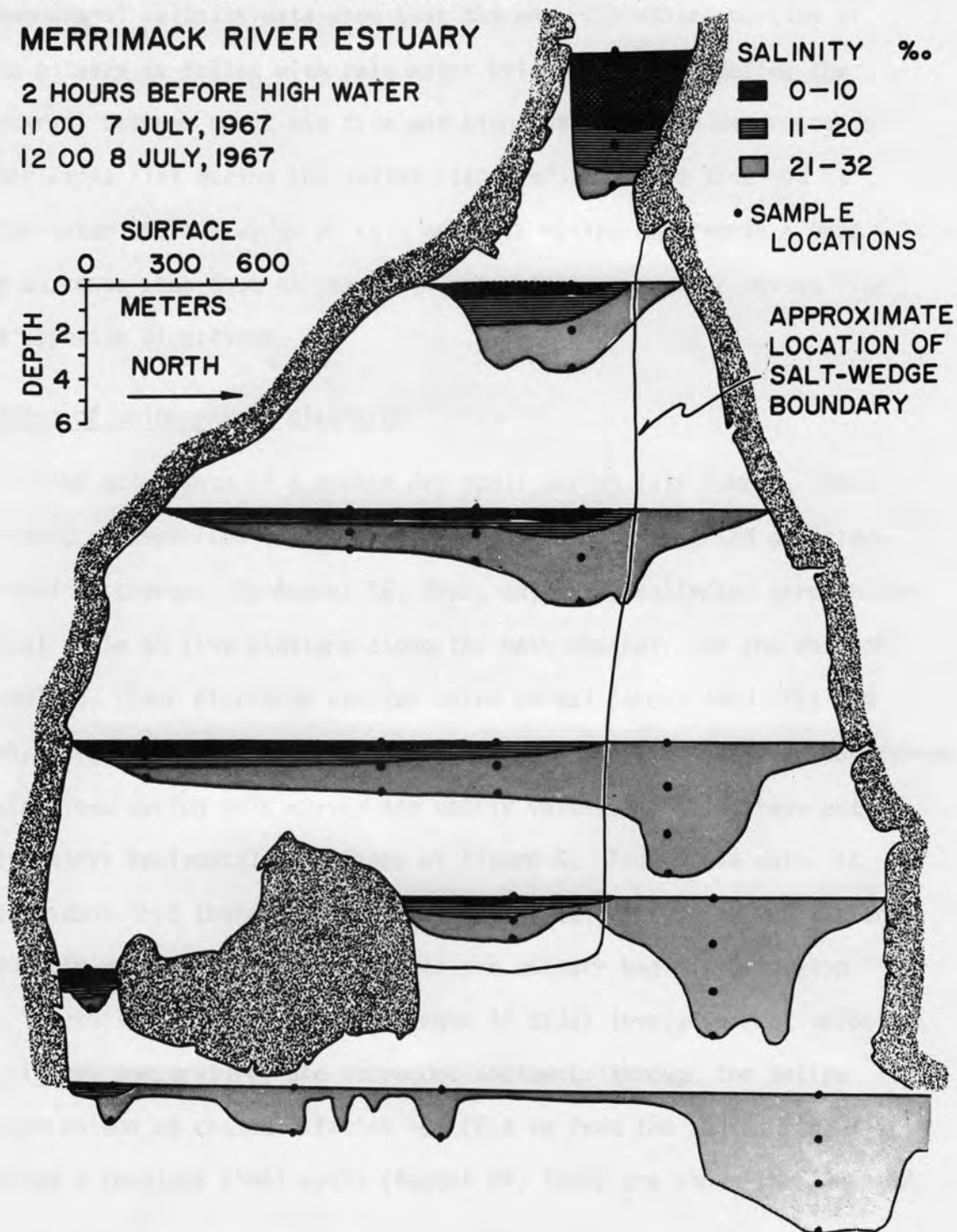


Figure 5

estuary is further delimited in Figures 6 to 10. These three-dimensional salinity data show that the entire southern portion of the estuary is filled with salt water below 2 m depths during the interval between about mid tide and high water. Fresh water stands over Joppa Flat during the latter stages of the flood tide and at high water while a wedge of salt water is moving underneath. Data on currents show that at near high water these two water masses flow in opposite directions.

Effect of below-normal discharge

The occurrence of a modest dry spell during late summer, 1968, allowed a comparison of the July, 1967, data with a period of below-normal discharge. On August 26, 1968, data were collected through the tidal cycle at five stations along the main channel. On the date of sampling, river discharge was far below normal (about 1900 cfs) and only slight stratification developed (Fig. 11). The isohaline boundaries determined during this survey are nearly vertical, in contrast with the nearly horizontal isohalines of Figure 4. From these data, it is evident that there is a critical runoff value between 1900 cfs and 6300 cfs at which stratification in the estuary begins to develop.

Details of thirty-minute changes in tidal level, current velocity, salinity, temperature, and suspended sediments through the entire water column at channel station 167 (2.4 km from the mouth, Fig. 1) during a complete tidal cycle (August 26, 1968) are shown in Figure 12.

Figure 6. Variation of salinity with depth at low water in the estuary. Normal discharge conditions (6300 cfs); July 7 and 8, 1967. Note the almost complete absence, at any depth, of saline water in the estuary.

SALINITY VARIATION WITH DEPTH MERRIMACK RIVER ESTUARY

LOW-WATER

JULY 7, 1967 07 00
JULY 8, 1967 08 00

a. SURFACE

b. 2m DEPTH

c. 4m DEPTH

SALINITY, ‰

0-6

6-12

12-24

24-32

N

0 2 km

Figure 6

Figure 7. Variation of salinity with depth during flood tide, two hours after low water in the estuary. Normal discharge conditions (6300 cfs); July 7 and 8, 1967. Compare the surface water salinity pattern in this diagram with the infrared imagery of Figure 3. Note the intrusion of the salt wedge up the main channel in the northeastern section of the estuary.

SALINITY VARIATION WITH DEPTH MERRIMACK RIVER ESTUARY

2 HRS. AFTER LOW WATER

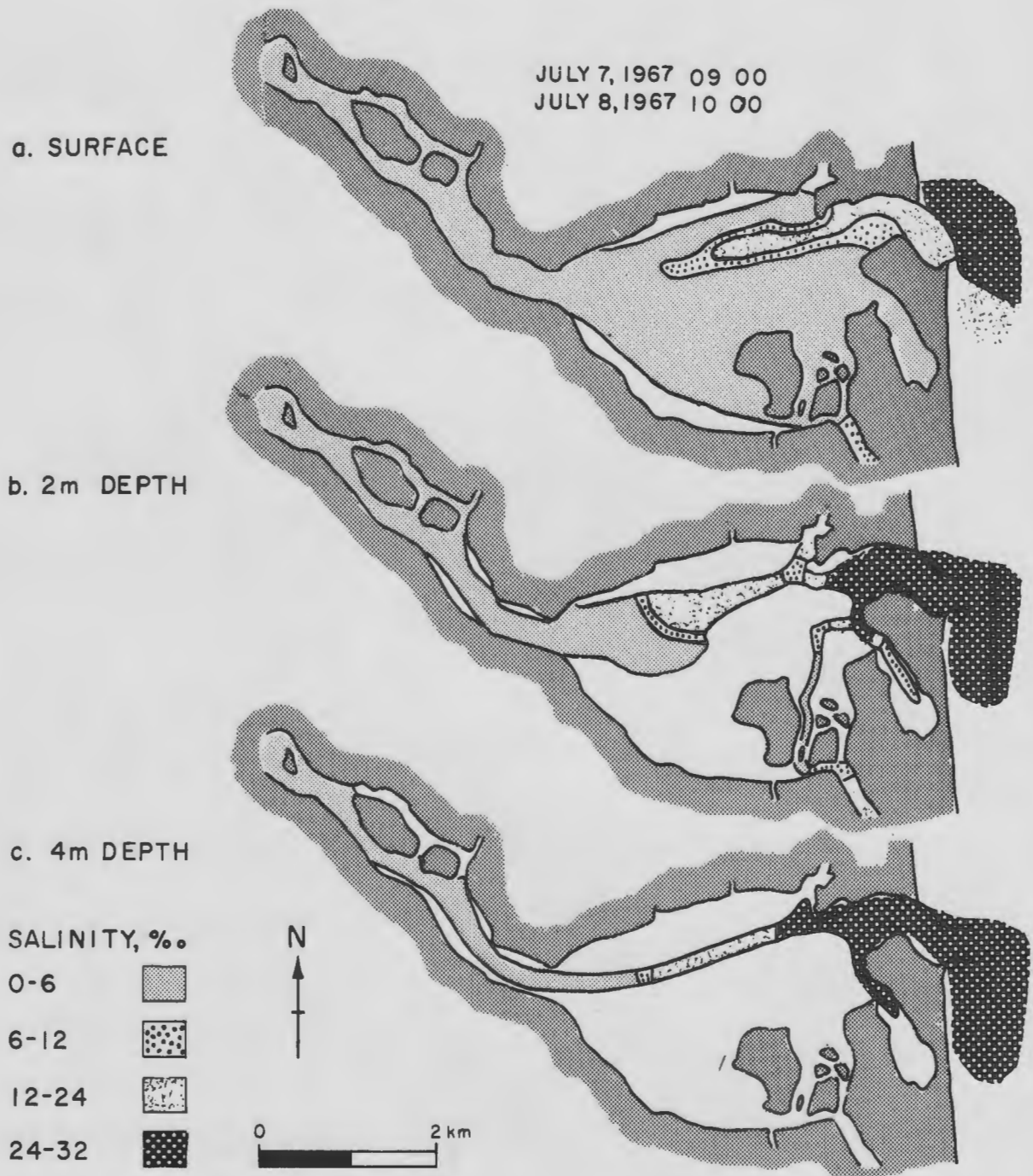


Figure 7

Figure 8. Variation of salinity with depth during flood tide, two hours before high water in the estuary. Normal discharge conditions (6300 cfs); July 7 and 8, 1967. At this stage, the salt wedge has completely intruded the lower half of the estuary. Compare these data with Figure 5, which is based on the same sampling period.

SALINITY VARIATION WITH DEPTH MERRIMACK RIVER ESTUARY

2 HRS. BEFORE HIGH WATER

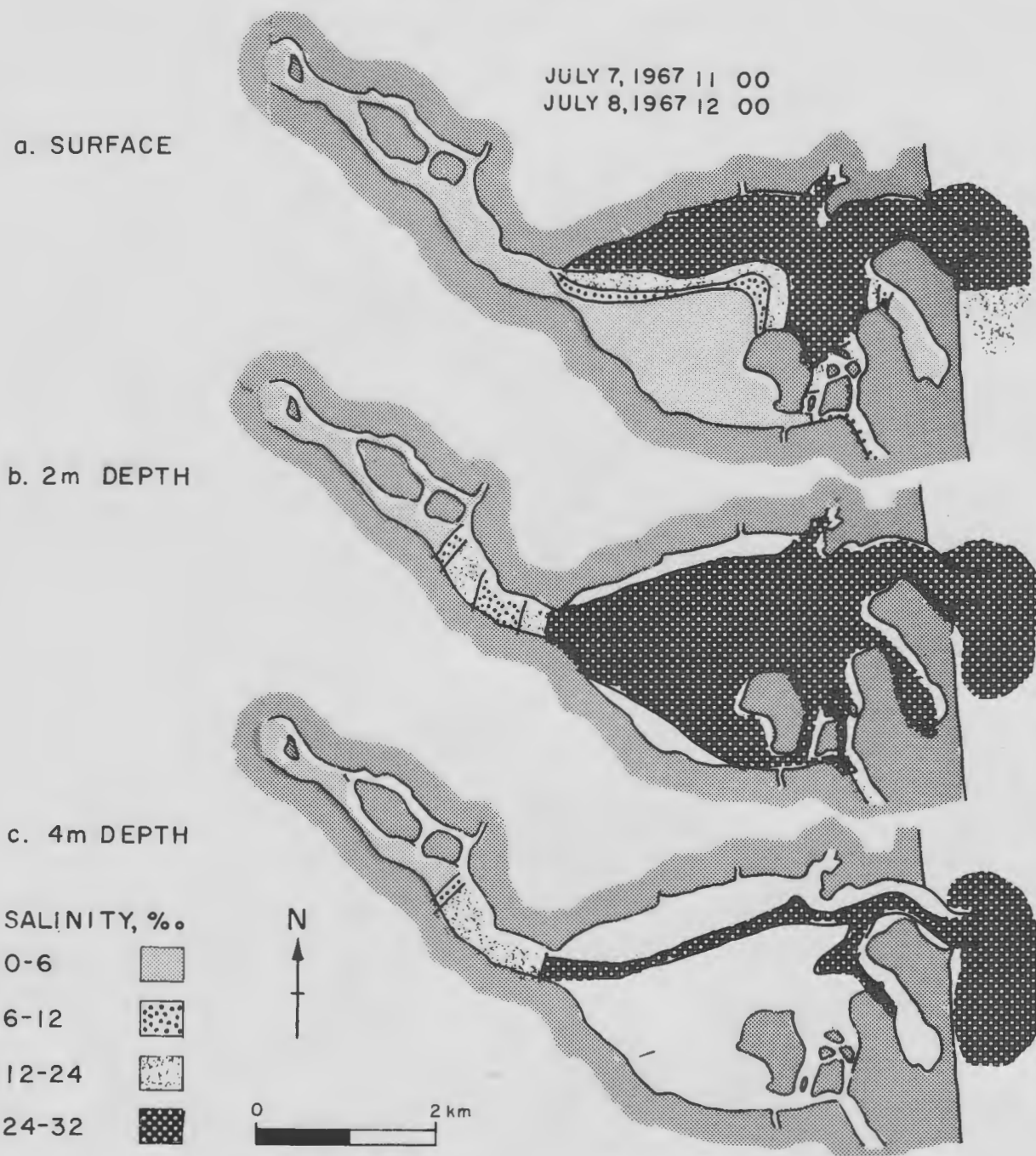


Figure 8

Figure 9. Variation of salinity with depth at high water in the estuary. Normal discharge conditions (6300 cfs); July 7 and 8, 1967. Note that at this stage the fresh water had already begun to drain over the surface of the estuary, even though the lower portions of the water column were still completely saline.

SALINITY VARIATION WITH DEPTH MERRIMACK RIVER ESTUARY

HIGH WATER

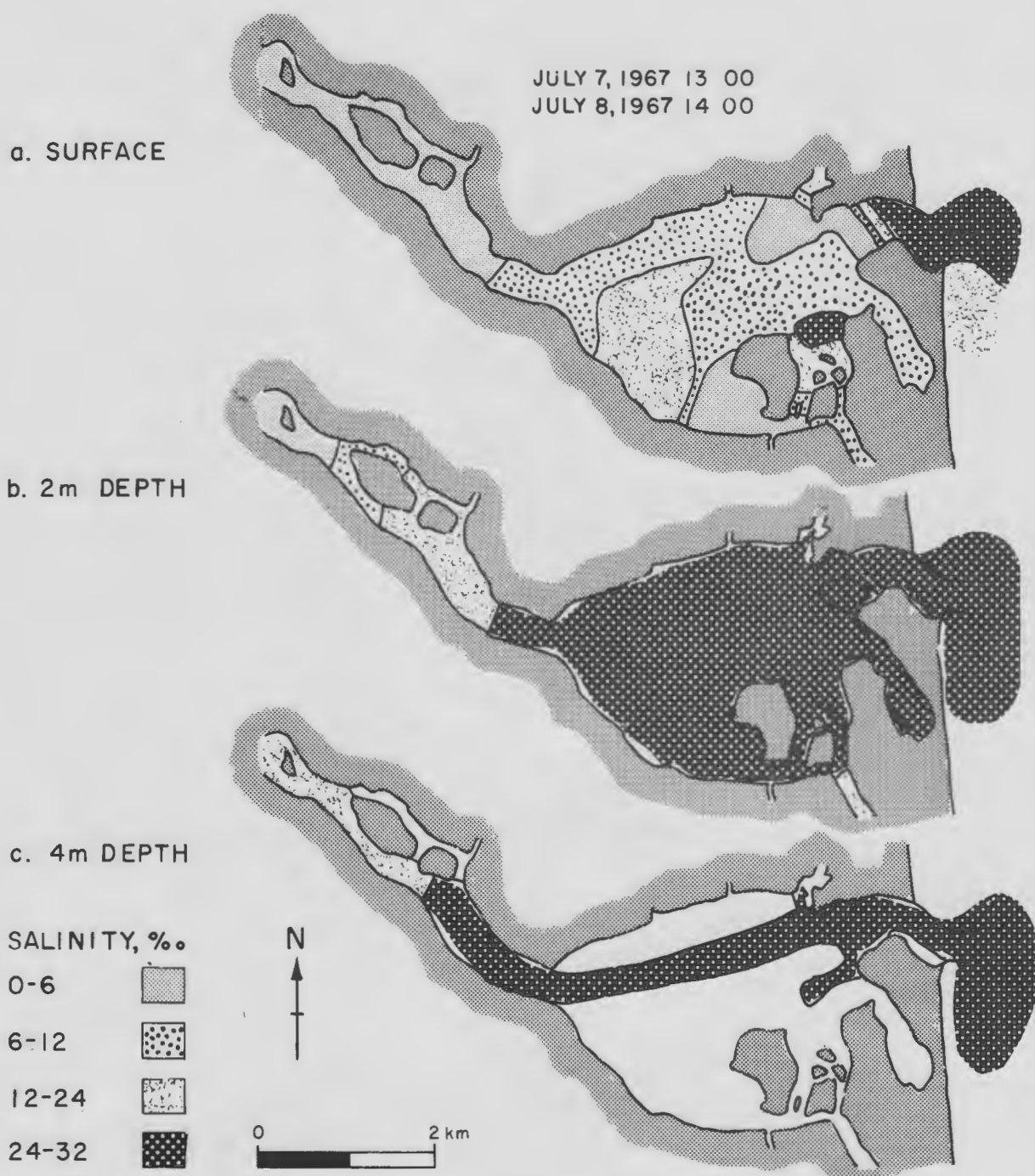


Figure 9

Figure 10. Variation of salinity with depth during ebb tide, four hours after high water in the estuary. Normal discharge conditions (6300 cfs); July 7 and 8, 1967. At this stage, the stratification was almost completely destroyed and most of the saline water had been flushed out of the estuary.

SALINITY VARIATION WITH DEPTH MERRIMACK RIVER ESTUARY

4 HRS. AFTER HIGH WATER

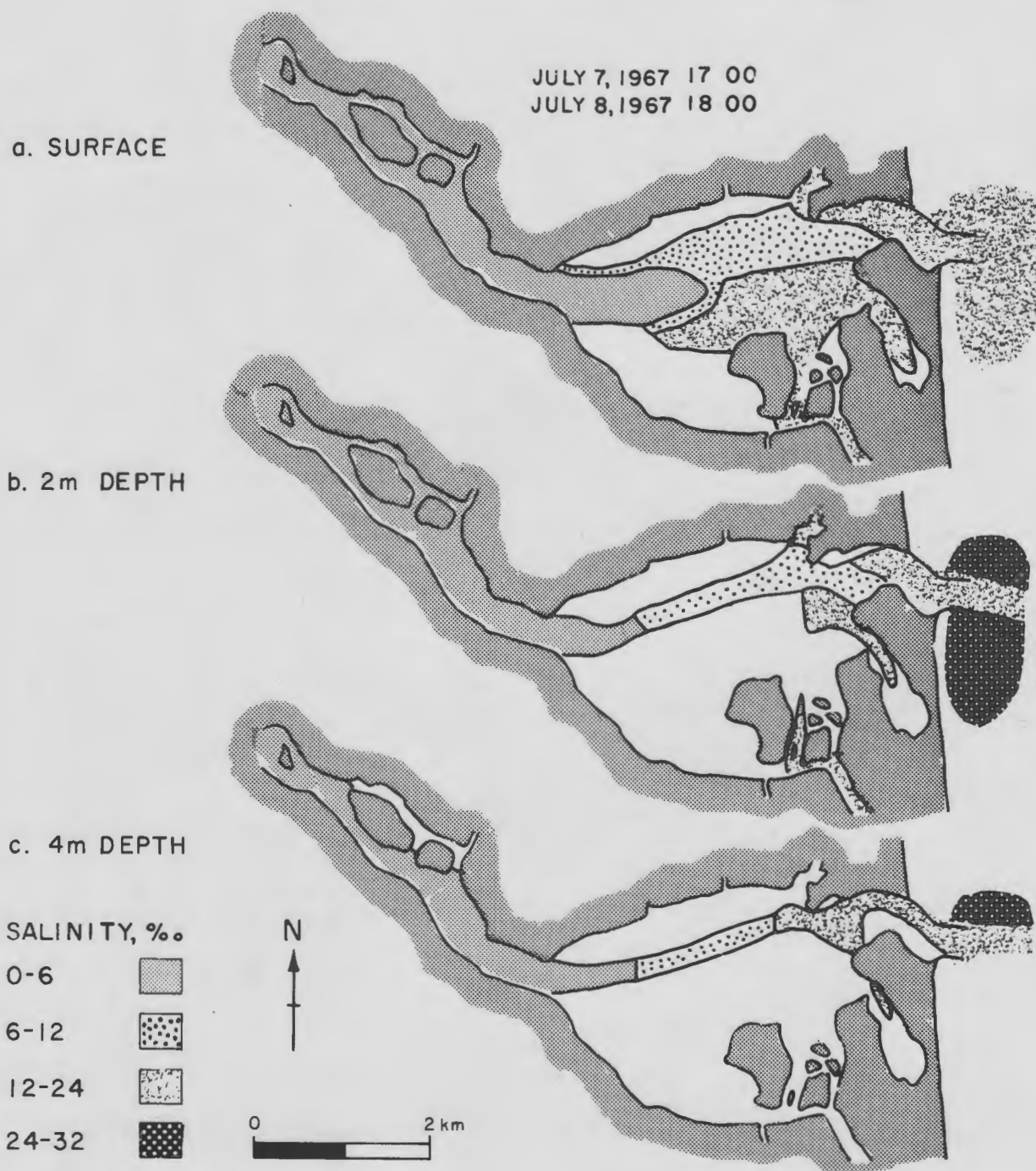


Figure 10

Figure 11. Salinity distribution during a complete tidal cycle in a longitudinal cross section along the axis of the central portion of the main channel (location map, Fig. 1). Data collected August 26, 1968, when river discharge was about 1900 cfs. Note the lack of well-developed stratification of the type that occurred in July, 1967, under normal discharge conditions (Fig. 4).

SALINITY DISTRIBUTION DURING A TIDAL CYCLE
MERRIMACK RIVER ESTUARY
AUGUST 26, 1968

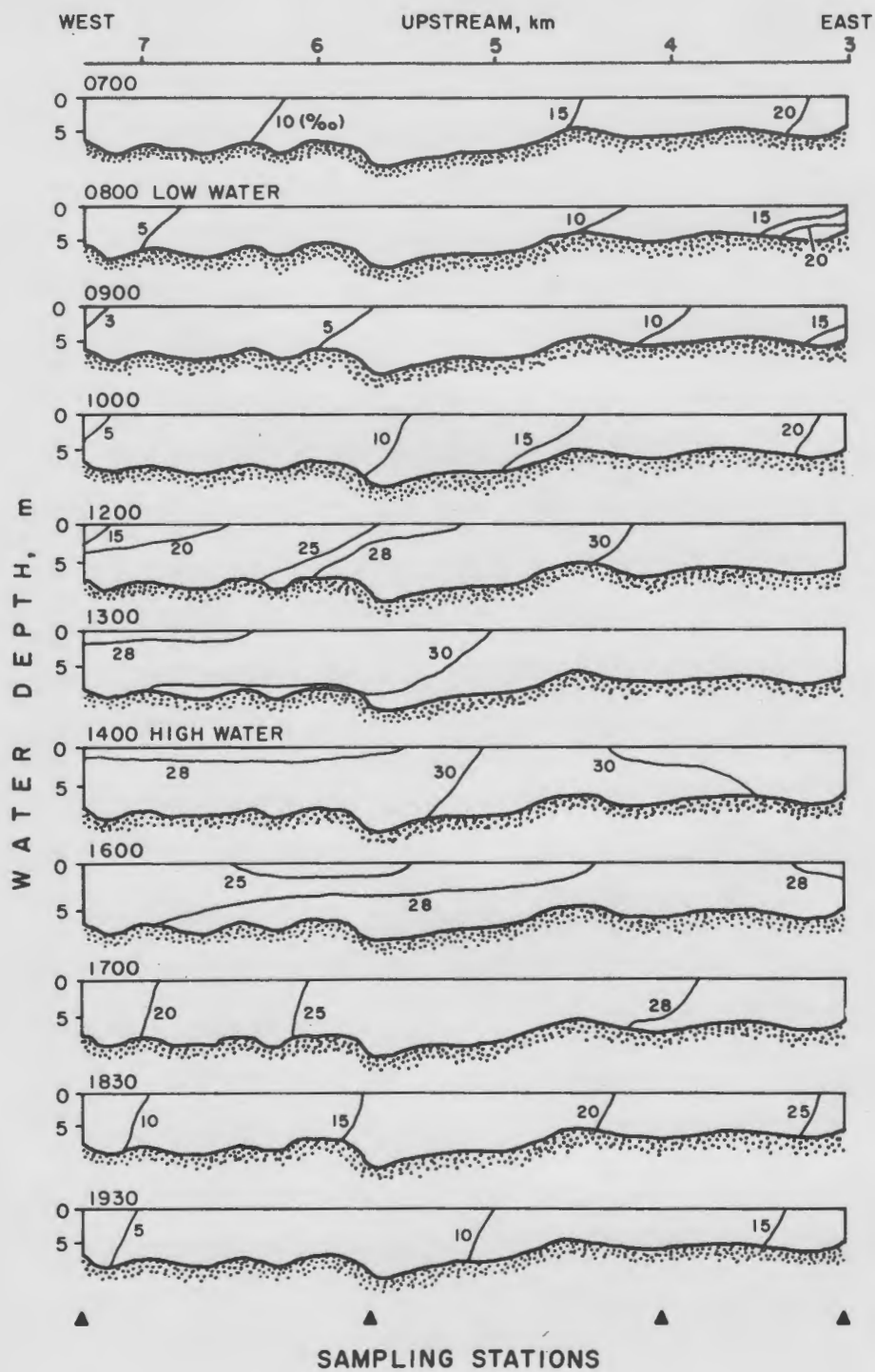


Figure 11

During flood tide, salinity rose sharply while temperature and suspended sediment concentrations steadily decreased to minimum values at about one hour before high water. Changes in temperature and salinity during the ebb period were complicated at this sampling station because of the influence of Black Rock Creek to the north. Current-velocity data reveal that peak flood velocities occurred in pulses along the bottom whereas maximum ebb flow was in the upper part of the water column. Time-velocity asymmetry of tidal currents is evident in that maximum flood velocities occurred two-thirds of the way through the flood period and maximum ebb velocities occurred three-quarters of the way through the ebb period. Low and high-water slack occurred from 30 to 45 minutes later than their respective minimum and maximum points on the tidal curve.

Current velocity

A series of typical current-velocity profiles for the main channel at mid estuary on June 24, 1967, is shown in Figure 13 (station 250, Fig. 1). Note the pronounced time-velocity asymmetry. At 0745 the current was ebbing strongly with maximum velocities in the upper part of the water column. An hour later, at low water (0850), the ebb current was still strong, but velocities at depth were slightly stronger than those at the surface. Slack water did not occur until an hour later (0955), even though the water level had already risen 30 cm. By 1115 the current was flooding but peak velocities were not attained until 1245, nearly three-quarters of the way into the flood

Figure 12. Changes in water level, current velocity, salinity, temperature, and suspended sediments during a complete tidal cycle at a single anchor station in the main channel (station 167, Fig. 1). Below-normal discharge conditions (about 1900 cfs); August 25, 1968.

HYDROGRAPHIC CHANGES DURING A TIDAL CYCLE
MERRIMACK RIVER ESTUARY-STATION 167
AUGUST 25, 1968

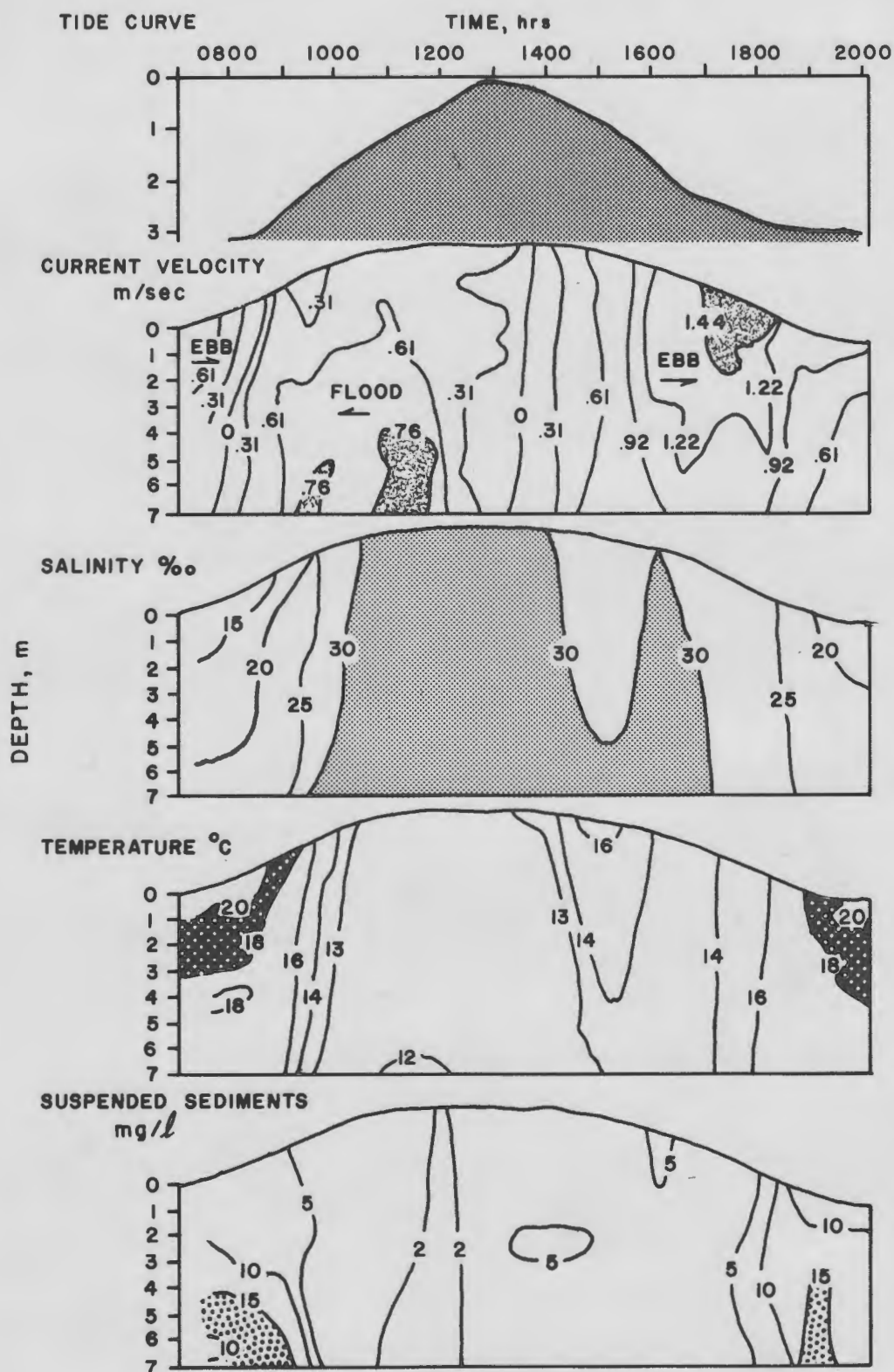


Figure 12

Figure 13. Tidal-current velocity profiles through a complete tidal cycle at station 250 in the main channel (Fig. 1) on June 24, 1967. Some of these data are also shown in Figure 10.

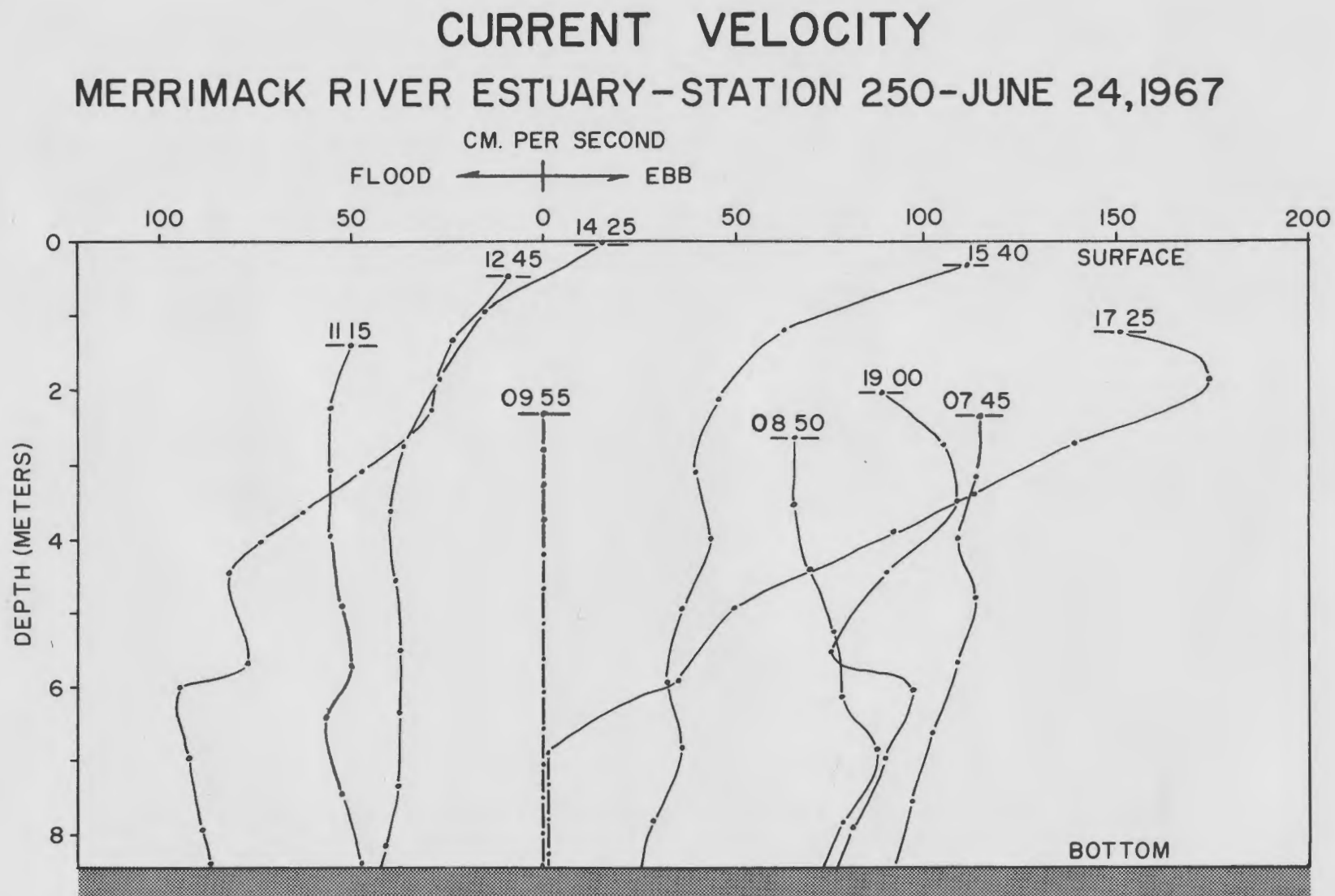


Figure 13

cycle. Note that peak flood velocities occurred near the bottom of the water column. At high water (1425), the surface water had started to ebb while the bottom water continued to flood. Because of continual river discharge in the upper estuary, the entire water column was not slack at high water. Current velocities increased rapidly during ebb, reaching peak values 3 to 4 hours after high water. The slack water near the bottom at 1725 was anomalous; it may have been the result of eddying. Note that maximum ebb velocities occurred near the surface.

Current-velocity profiles for four channel stations along the length of the estuary are shown in Figure 14. These profiles also demonstrate that maximum flood velocities generally occur near the bottom, whereas maximum ebb velocities, which are frequently twice as fast as the flood velocities, occur near the surface.

Current-velocity asymmetry

Tidal-current velocity data from stations in the main channel and near the flood-tidal delta (location map, Fig. 1) show pronounced asymmetry (Fig. 15). In the channel, ebb currents are nearly twice as strong as flood currents; near the flood-tidal delta they are nearly equal. At channel stations, peak flood velocities occur 3 to 4 hours after low water, but peak ebb currents do not occur until 4 to 6 hours after high water. Thus, as the tide begins to flood, it must first overcome a residual ebb current in the channels.

This general time-velocity asymmetry of tidal currents is an important factor in estuarine sedimentation and has been observed

Figure 14. Tidal-current velocity profiles through a complete tidal cycle at four stations in the main channel (140, 220, 250, and 320, Fig. 1). Bottom profile shows station locations and topography of the main channel westward from the river mouth.

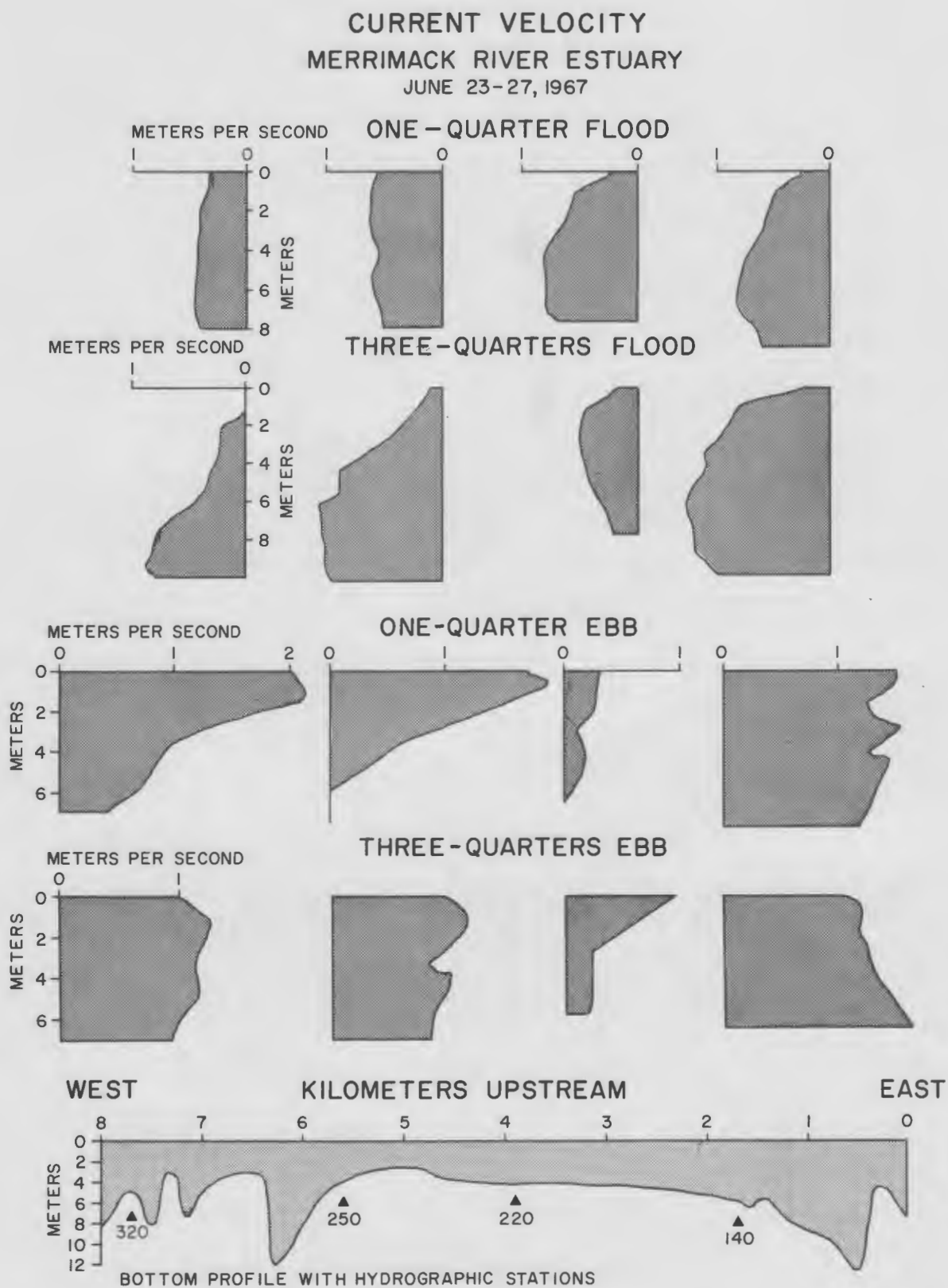


Figure 14

in other local estuaries, including Essex Bay, Parker River estuary, and the Hampton Harbor estuary (Coastal Research Group, 1969), as well as in many European estuaries (Postma, 1967). For both the ebb and flood phase, the tidal-current velocity curve at a fixed point in a tidal channel is asymmetrical, but there is a much longer period of low current velocities around high tide than around low tide (Fig. 15). Because maximum ebb velocities occur near low water, effects of the ebb currents are largely confined to the deeper channels. On the other hand, maximum flood currents occur when most of the estuary is flooded and water is spread horizontally over a large area.

Suspended sediments

Suspended sediment data collected in late August 1968 (Figs. 12 and 16), show that the ocean water carried a relatively small sediment load (maximum values observed were 5 mg/l). Fresh water carried much larger concentrations (up to 19 mg/l), but this probably was a minimal value because of the low discharge (1900 cfs) during the sampling period. Suspended load measured by the U.S. Geological Survey at Lowell, Massachusetts, during 1967, ranged from an average of 2,590,000 kg/day in April to 36,300 kg/day in September (U.S. Geological Survey, 1968). In general, larger suspended sediment concentrations appear to occur during the portions of the tidal cycle when the river influence is greatest. Under low discharge conditions, when the estuary becomes partially mixed, maximum suspended sediment

Figure 15. Tidal-current velocity asymmetry at four stations in the main channel (160, 170, 210, and 220, Fig. 1) and four stations in the vicinity of the flood-tidal delta (173, 175, 180, and 182, Fig. 1).

CURRENT VELOCITY ASYMMETRY MERRIMACK RIVER ESTUARY

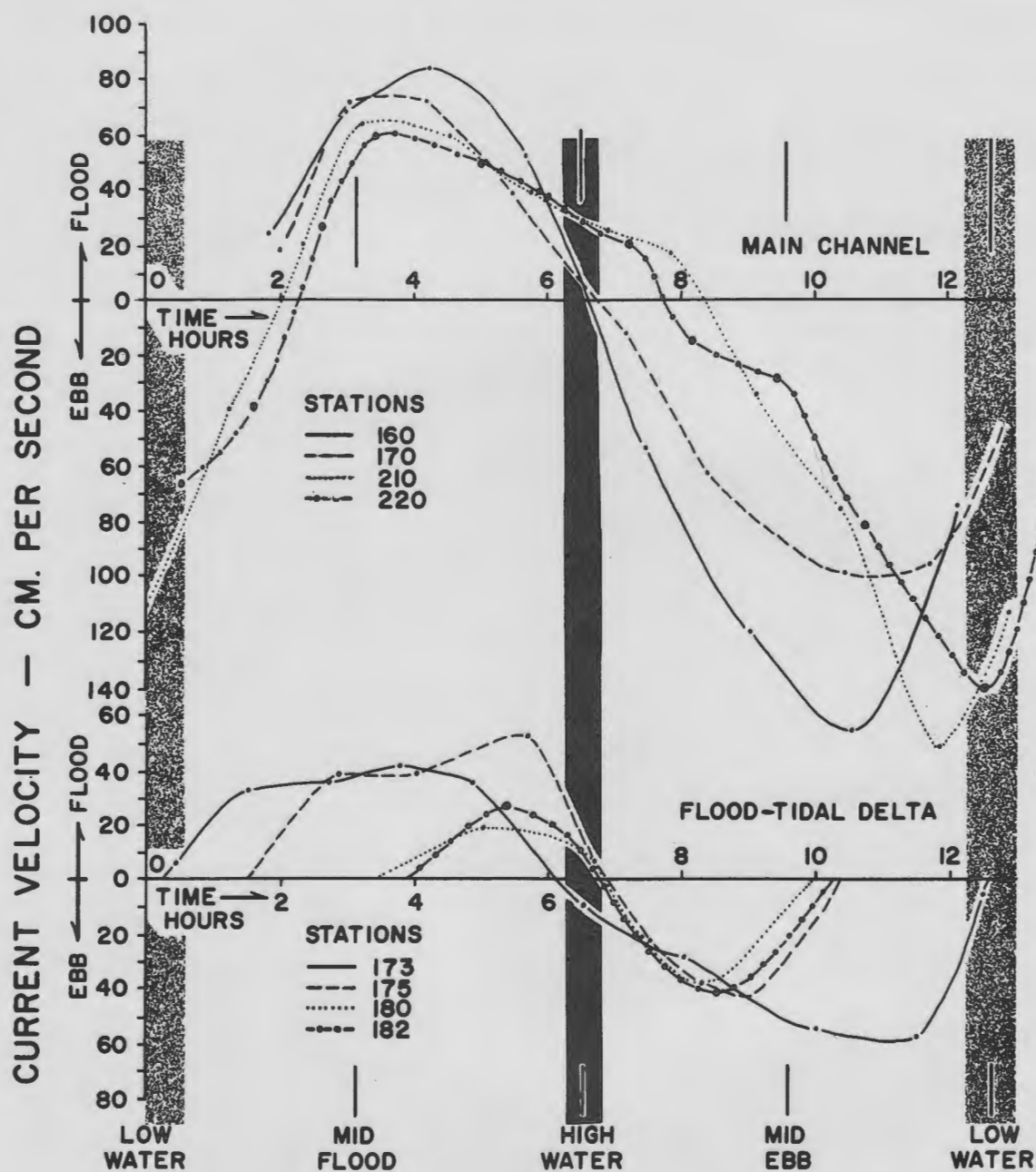


Figure 15

Figure 16. Changes in suspended sediment concentrations (mg/l) during a complete tidal cycle at stations in the main channel on August 26, 1968. Discharge about 1900 cfs.

SUSPENDED SEDIMENTS DURING A TIDAL CYCLE
MERRIMACK RIVER ESTUARY
AUGUST 26, 1968

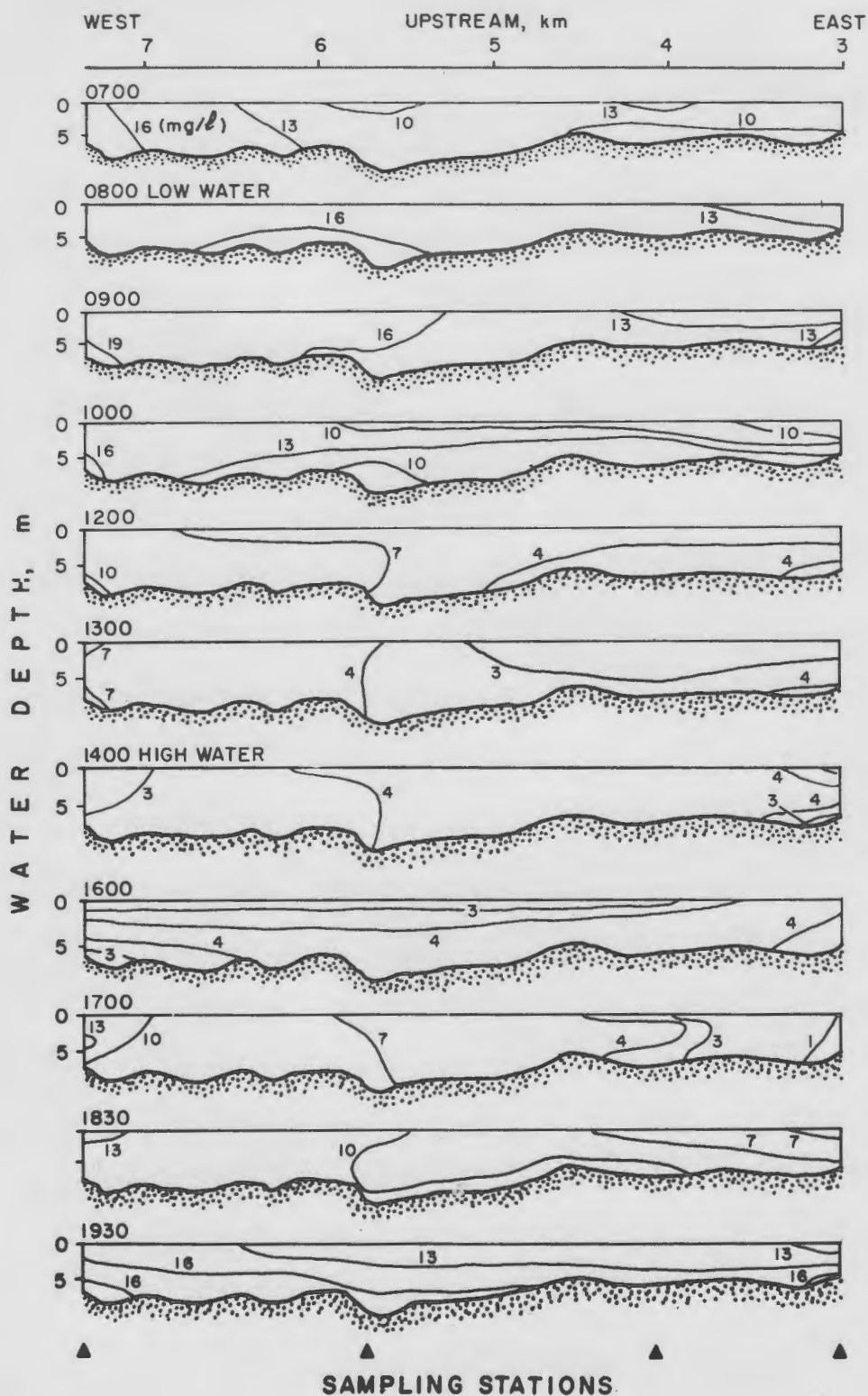


Figure 16

concentrations may occur anywhere in the water column. In view of the estuarine circulation pattern, it is probably that a significant quantity of this suspended sediment load, including pollutants and effluent from the Newburyport sewage plant, is deposited on Joppa Flat. In recent years, rapid shoaling of the channel south of Woodbridge Island and accretion of Spartina alterniflora salt marsh over this accumulating muddy sediment have been observed.

Hydrography of the Plum Island River

The high-discharge, well-stratified Merrimack River estuary contrasts markedly with the low-discharge, well-mixed Parker River estuary to the south (DaBoll, 1969). Salinity-temperature data collected along the Plum Island River, which connects these two estuarine systems (Fig. 1), show how they interacted during a tidal cycle (August 1-2, 1968; Fig. 17). During late ebb (0930 on Fig. 13), warm, high-salinity water flowed north into the Merrimack River. By 1300 the tide had reversed and this same water started flowing south. By midflood, warm, high-salinity water from the Parker had begun to meet the colder, high-salinity water of the Merrimack about 2.3 km south of the Plum Island River bridge. At high water (1700), water of identical salinity filled each end of the river but the Merrimack's contribution was twice as cold (11°C). This marked difference in temperature for water with the same salt content suggests that mixing is more complete in the Parker and that ocean water, which is trapped there for several tidal cycles, is warmed by solar radiation before being returned to the ocean. During the ebb, the river drained to the north but a marked temperature

Figure 17. Changes in salinity and temperature during a tidal cycle in the Plum Island River on August 1-2, 1968.

HYDROGRAPHIC CHANGES DURING A TIDAL CYCLE PLUM ISLAND RIVER AUGUST 1-2, 1968

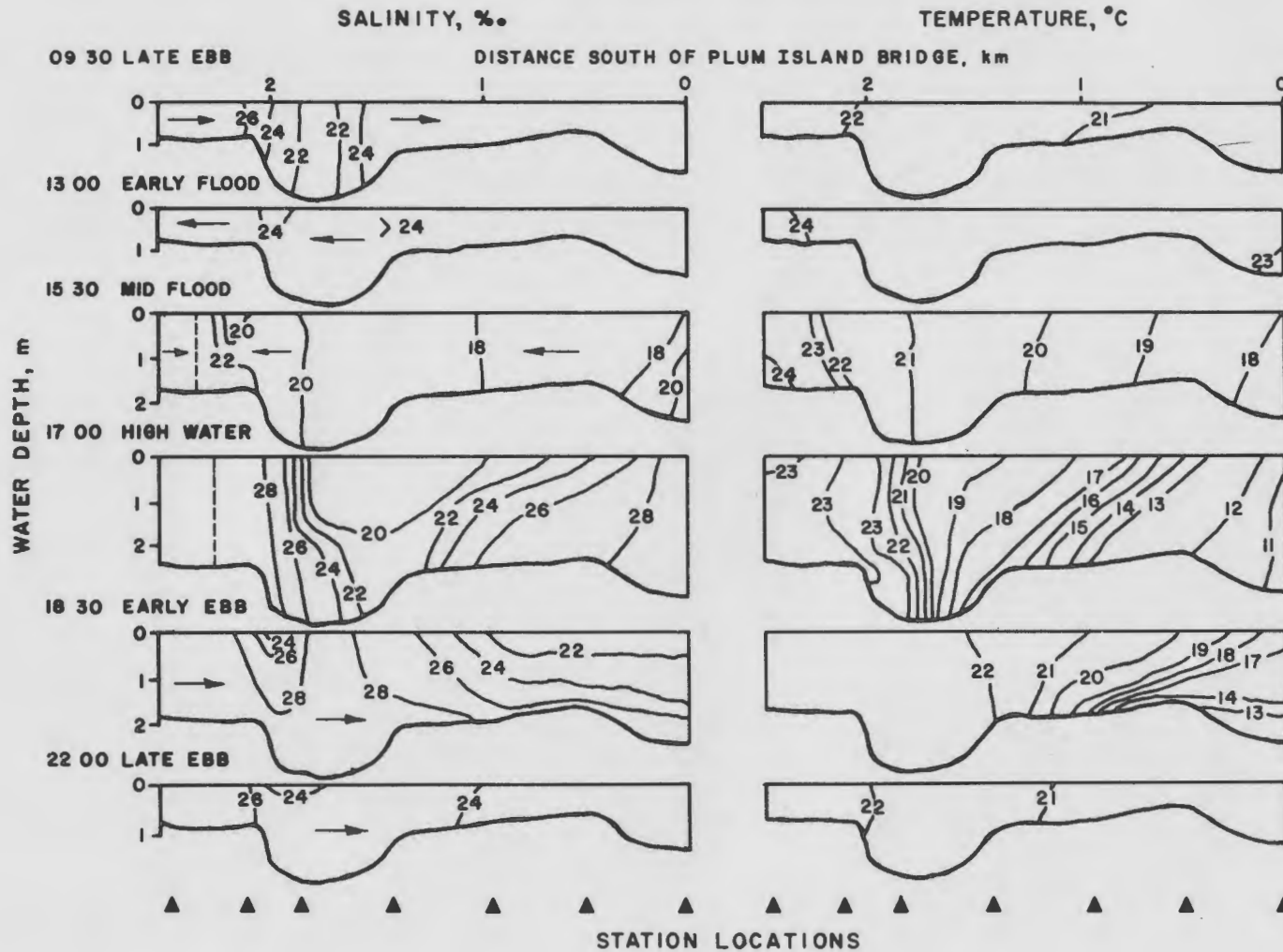


Figure 17

gradient developed as these two water masses mixed.

At the south end of the Plum Island River where these two water masses meet during flood tide (Fig. 17), fine-grained sediments have accumulated to build a natural watershed divide between the two estuarine systems. This sediment deposition appears to be due to settling of silt-size sediments where opposing flood currents meet and the water masses become slack. Since ebb currents flow in opposite directions from this topographic high, sediment tends to become trapped as a settling lag much like that observed in the Wadden Zee (Postma, 1967).

SEDIMENTARY ENVIRONMENTS

For descriptive purposes, the estuary is divided into three main sedimentary environments:

- (1) main channel - a. subtidal channel, b. flood-tidal delta, and c. intertidal flats;
- (2) secondary channels - a. major tidal channels and b. minor tidal channels;
- (3) salt marsh.

The main Merrimack channel dominates the study area (map of geographic distribution of sedimentary environments, Fig. 2). Large intertidal flats border the subtidal channel of the lower estuary. To the south is Joppa Flat (Fig. 1), which contains the largest mud accumulation in the study area. The flood-tidal delta, located 2.2 km west of the inlet mouth, is the only large intertidal sand body along the main channel. Major secondary tidal channels include Black Rock Creek and the Plum Island River, which links the Merrimack estuary to the Parker River estuary in the south. All remaining secondary tidal channels are classified as minor. Bordering the estuary are 16.9 km² of salt marsh.

Sediment distribution patterns

Sediments were collected from 425 locations in the estuary. Intertidal stations were sampled at low tide; subtidal areas were sampled from a small boat by means of a grab sampler. One hundred and fifty oriented box samples were taken for laboratory study of primary structures, using photographic and x-ray radiography techniques. Grain size of 260 samples

was measured using standard sieving and pipetting procedures. Statistical analysis was done by both the method of moments and the Folk and Ward (1957) graphical methods using an IBM 3600 computer.

Sediment types and their geographic distribution (Fig. 18) show excellent correlation with the sedimentary environments and the hydrographic circulation pattern of the estuary. Most of the subtidal portion of the main channel is gravelly sand with several zones of gravel and sandy gravel occurring where scouring is most effective. The intertidal flats are generally muddy sand with a large accumulation of sandy mud and mud on Joppa Flat. The flood-tidal delta is sandy with some slightly gravelly sand occurring along the northeastern margin. The Plum Island River bottom is slightly gravelly sand for most of its length, but muddy sand is present in the southern section and in Little Pine Island Creek. Black Rock Creek sediment is almost entirely muddy sand. Most of the minor tidal channels have muddy bottoms.

Mean grain size (Fig. 19) shows similar correlation with the various sedimentary environments. Gravel and sand coarser than 1.00 are confined to the main channel, to several places near the Basin (Fig. 1), where the mouth of the Merrimack was located as recently as 1827, and along the western side of the Plum Island River where glacial outwash is being eroded from under the marsh. Medium to fine sand (mean 1.010 - 2.500) is abundant along the main channel in the center of the estuary, in the Plum Island River, on the flood-tidal delta, in the Basin, on scattered shoal areas, and in some of the minor secondary tidal channels. Sediments

Figure 18. Distribution of sediments by type. Classification scheme after Folk (1968).

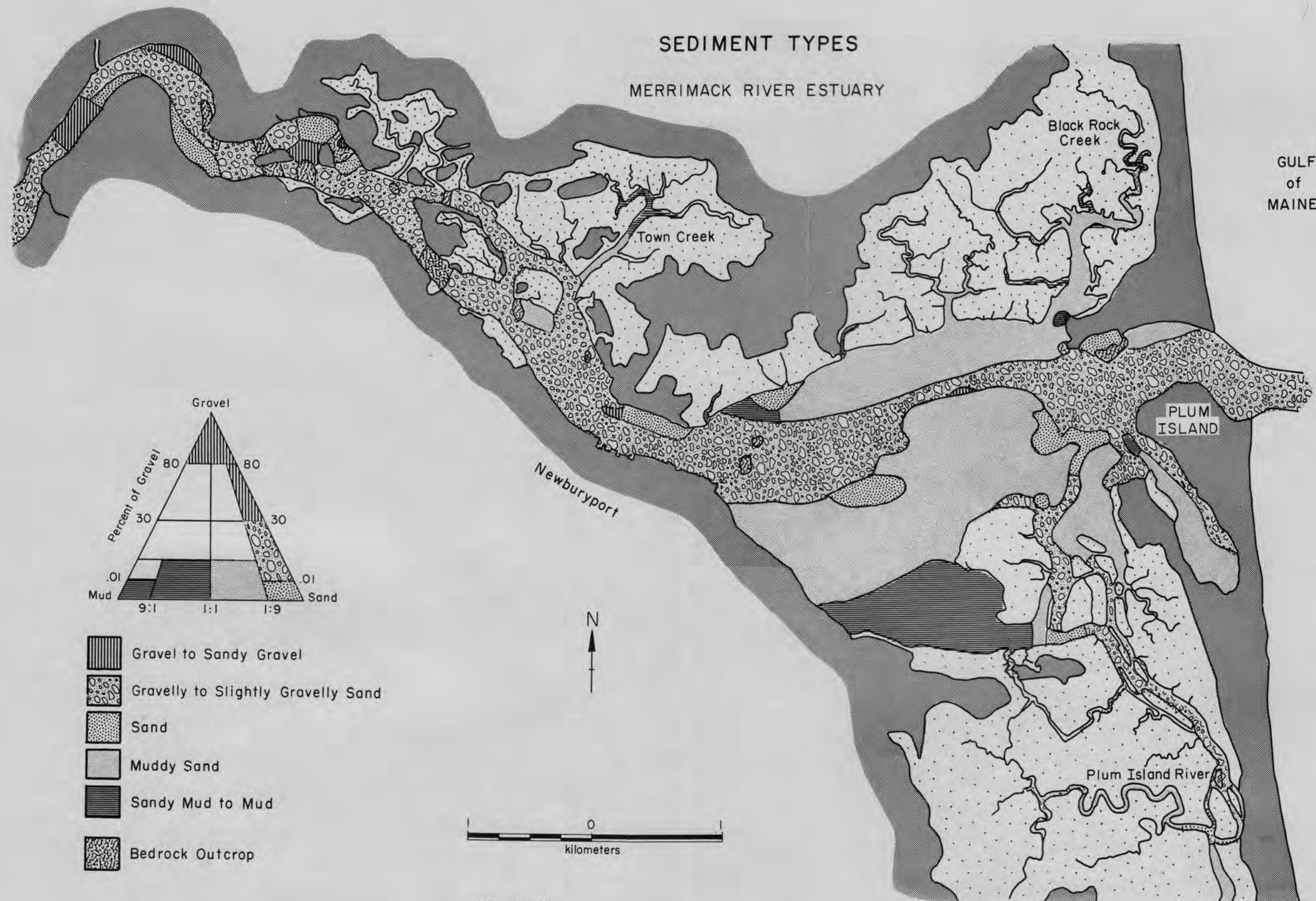


Figure 18

Figure 19. Distribution of sediments by mean grain size.
Textural parameters calculated by method of
moments.

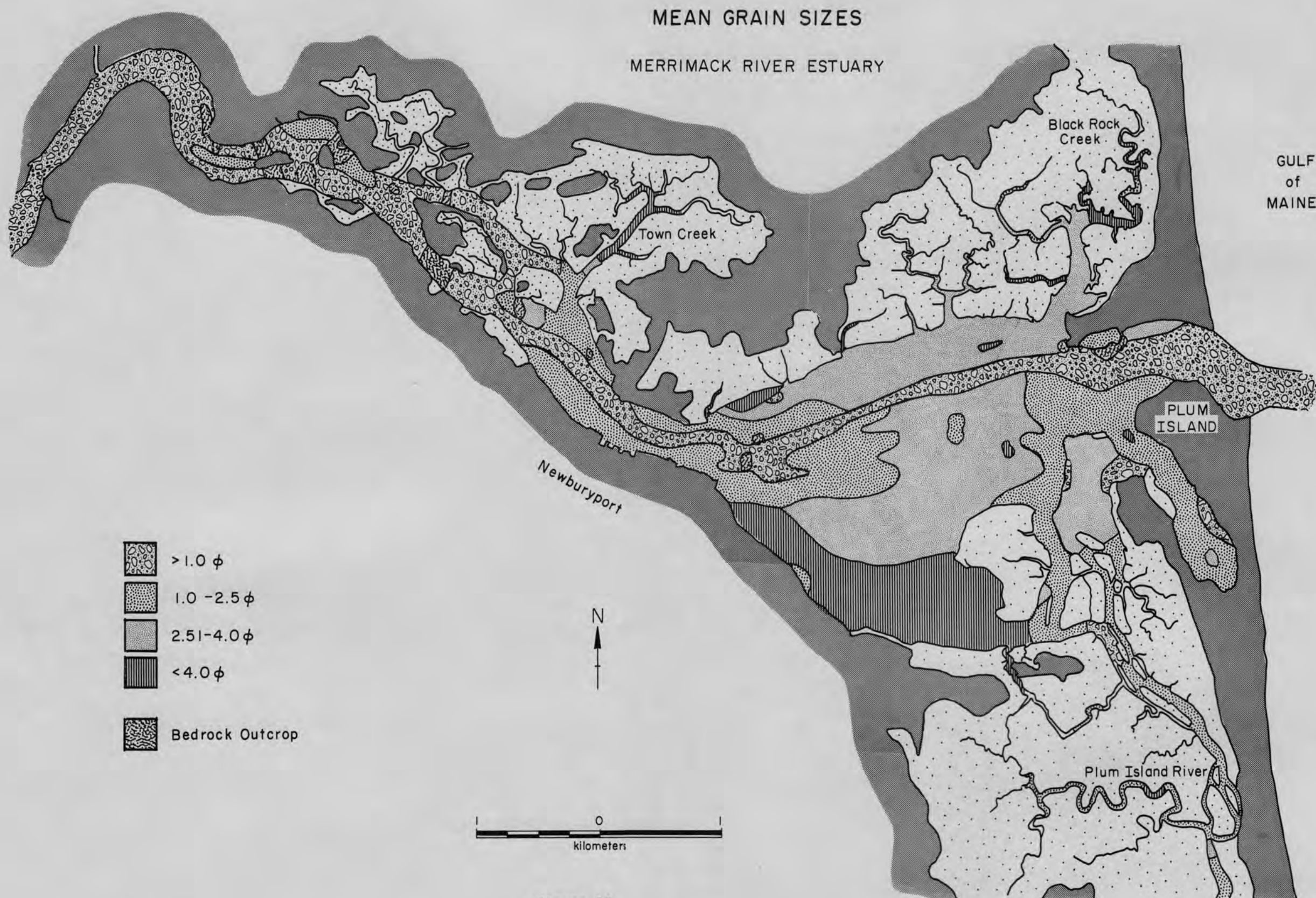


Figure 19

in most of the lower estuary, including intertidal clam and worm flats and mussel banks, are fine sand to very fine sand (mean 2.51 ϕ - 4.00 ϕ). Mud (finer than 4.00 ϕ) covers parts of Joppa Flat and the bottom of a number of small tidal channels and hollows.

Sediment standard deviation or sorting calculated by the method of moments (Fig. 20) correlates well with the distribution of mean grain size (Fig. 19). Moderately to well-sorted sediments occur in the main channel, on the flood-tidal delta, and in parts of the Basin and the Plum Island River. Most of the sediments in the rest of the estuary are poorly sorted (1.00 - 2.00), while very poor sorting (>2.00) is limited to Joppa Flat and to scattered hollows, shoal areas, and small tidal channels throughout the study area.

Inclusive graphic skewness (Fig. 21) shows good correlation with sediment type (Fig. 18), mean grain size (Fig. 19), and sorting (Fig. 20). The main channel samples are generally coarse-skewed to near-symmetrical, probably because of stronger tidal currents and the winnowing of finer grained sediments. Several zones of fine-skewed sediment are present near bedrock outcrops where fine sand and mud have accumulated as current shadows. Most of the Plum Island River sediments are near-symmetrical, possibly due to moderate tidal currents and northward transport of a moderately well-sorted, medium- to fine-grained sand (mean 0.80 - 1.75 ϕ) of unknown origin. Sediments in the remainder of the estuary, including the intertidal flats and minor secondary tidal channels, are fine-skewed presumably because tidal currents are not strong enough to carry in coarse sediment or to resuspend fine sediment deposited during high water.

Figure 20. Distribution of sediments by sorting or standard deviation. Textural parameters calculated by method of moments.

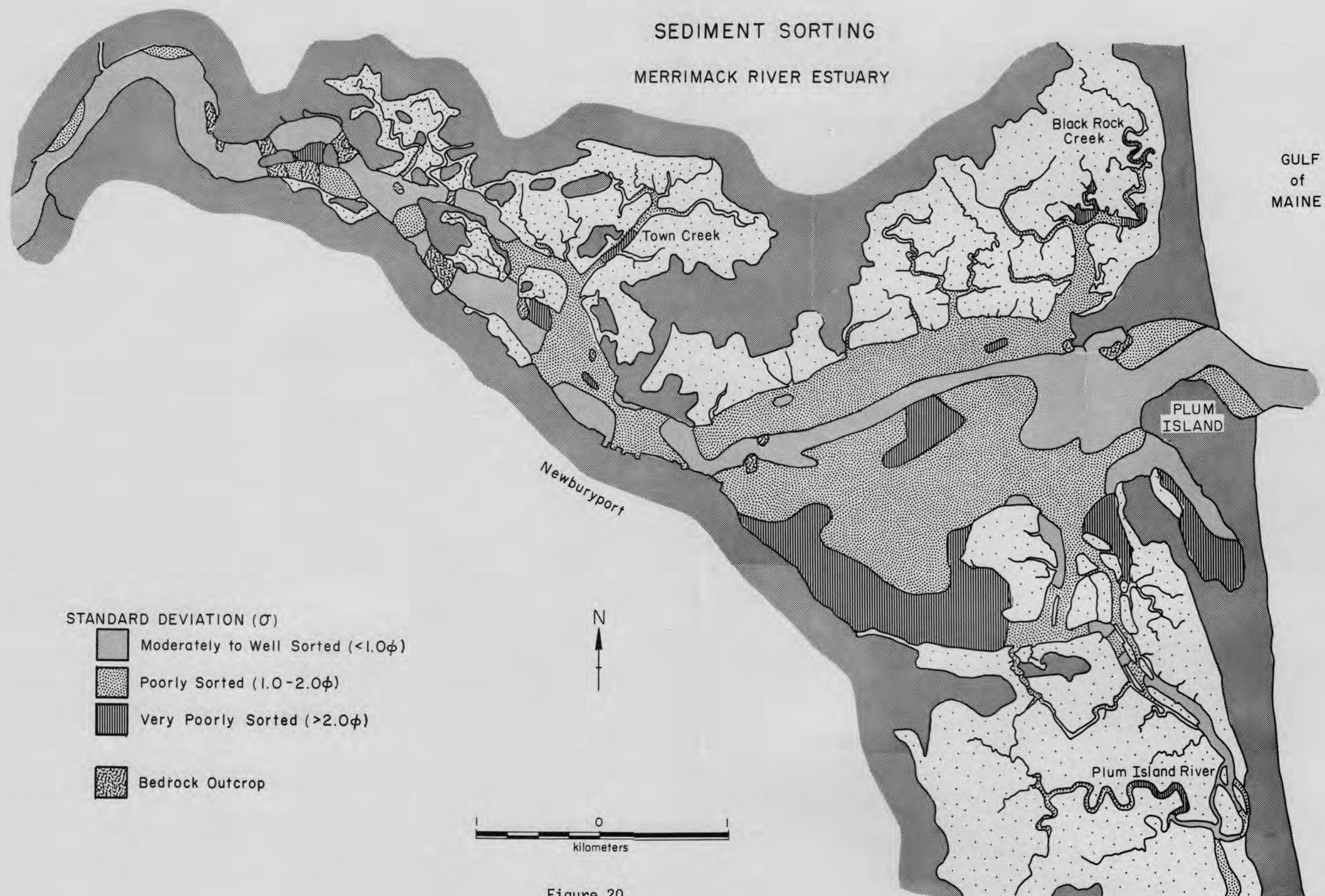


Figure 20

Graphic kurtosis also shows good correlation with the sedimentary environments (Fig. 2), sediment type (Fig. 18), grain size parameters (Figs. 19-21) and distribution of sand modes in the estuary (Figs. 24 and 25). The main channel sediments are generally mesokurtic (0.90 - 1.11), presumably reflecting the more effective sorting by stronger currents. Many samples from the upper estuary, the subtidal channel near Newburyport, and the Basin are platykurtic (0.54 - 0.88) because of marked bimodality, possibly due to the mixing of two previously well-sorted sand suites. Sediments on the flood-tidal delta and in parts of the Plum Island River are mesokurtic. The remainder, including those on the intertidal flats and in small tidal channels, are leptokurtic (1.11 - 3.52).

It should be noted that values of skewness and kurtosis calculated by the method of moments showed poor visual correlation with the distribution of other sediment textural parameters. This phenomenon is possibly due to analytical sampling problems or to mathematical problems in calculation of textural parameters. This is, gravel and mud in the tails were analyzed at 1.00 and 0.50 intervals respectively, while the sand fraction was analyzed at 0.25 intervals.

A scatter plot of sorting (inclusive graphic standard deviation) versus graphic mean for 233 surface sediment samples (Fig. 22) shows much scatter, but a general trend is evident. The coarsest sediments (graphic mean - 0.50 to 1.50) are best sorted, with sorting getting poorer in the finer sizes. These results would appear to agree with the suggestion of Folk and Ward (1957) that grain-size textural parameters usually plot in the form of a large sine curve when plotted on a scatter plot due to the

Figure 21. Distribution of sediments by inclusive graphic skewness. Textural parameters calculated by the graphical methods of Folk and Ward (1957).

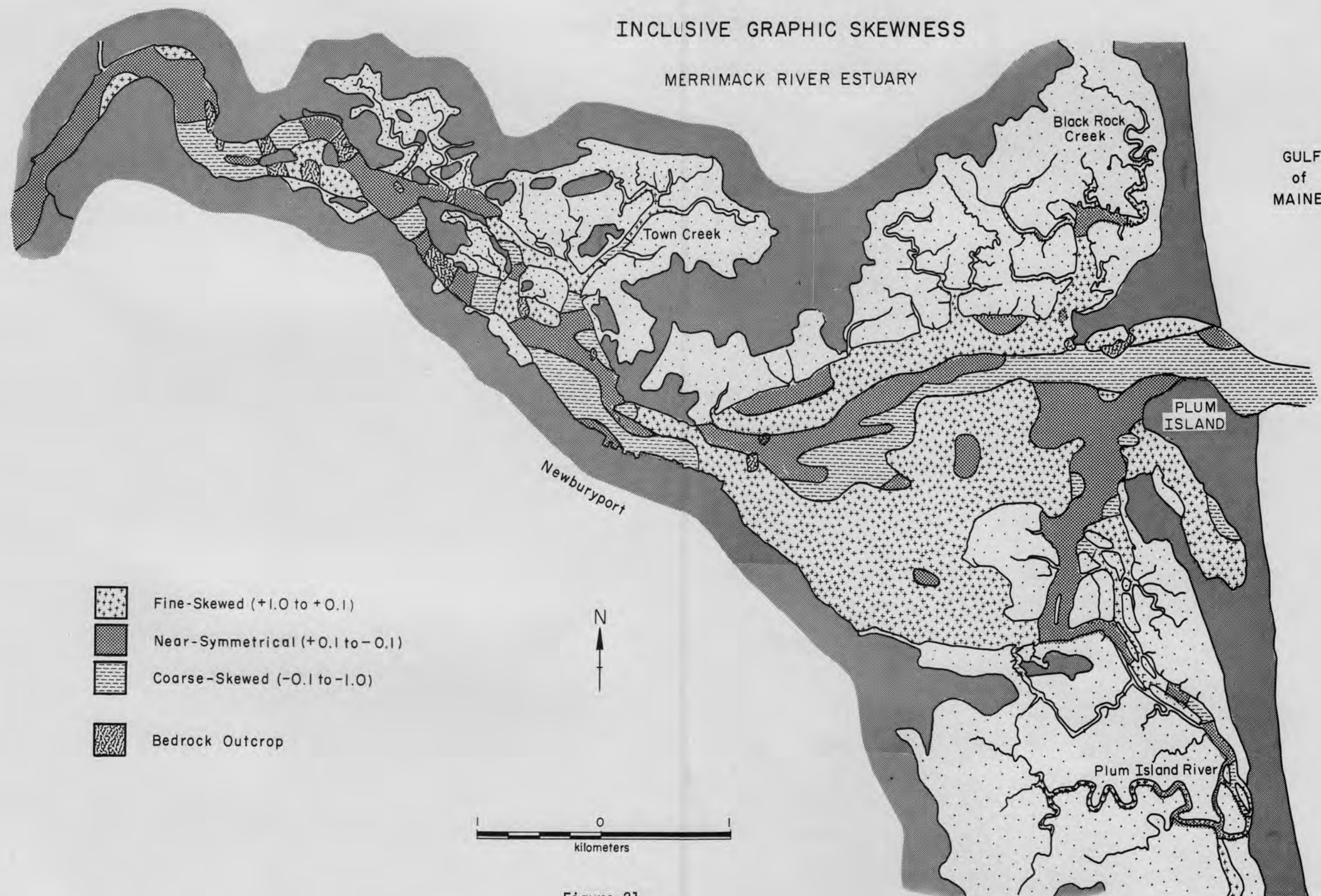


Figure 21

Figure 22. Scatter plot of inclusive graphic standard deviation versus graphic mean for 233 samples from throughout the entire estuary.

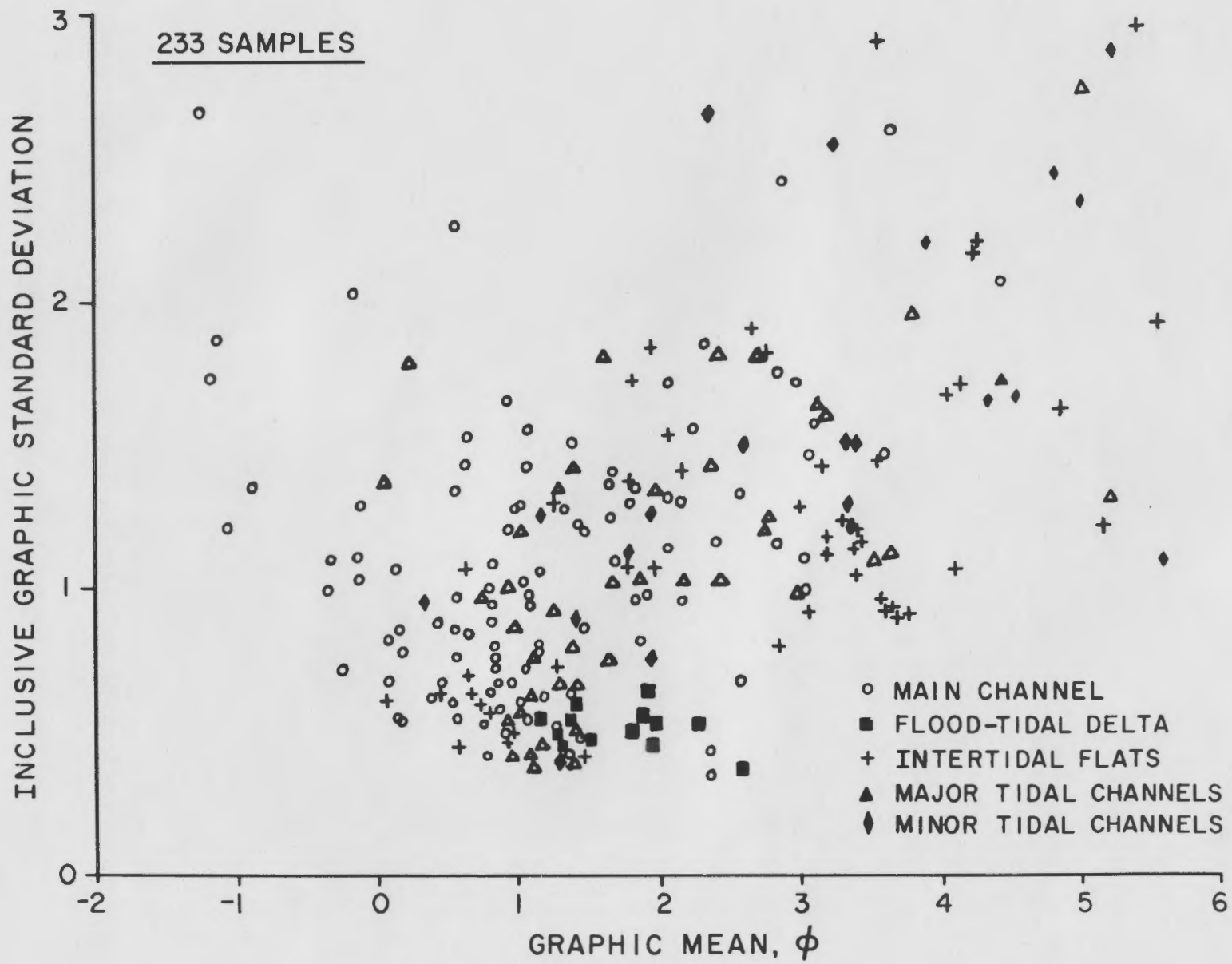


Figure 22

mixing of grain-size modes. Thus in the coarse sediments of Figure 22, the sand mode predominates and sorting is good; however, with decreasing mean size, more of the mud mode is being added and sorting gets worse.

When inclusive graphic skewness is plotted against graphic mean (Fig. 23), a similar sine curve results; but the wavelength is much shorter than that in Figure 22. As graphic mean increases, skewness changes from negative to near-symmetrical to positive and back to near-symmetrical. This relationship appears to be due to mixing of gravel, sand, and mud modes. That is, when a single mode is present or when two modes are present in equal proportions, the distribution is near-symmetrical; however, the occurrence of modes in unequal proportion imparts a coarse or fine tail to the sample and skewness becomes negative or positive respectively. Some of the scatter in these plots is due to the presence of several sand modes in the estuary.

At least three different types of sand have been recognized in the estuary (frequency-percent graphs, Figs. 24 and 25). The coarsest sand (modal size, 0.50 - 1.00), which is present in all of the main channel sediments and portions of the Plum Island River, has an average mineralogy (average of several estimates) of: 48 percent quartz, 9 percent gray feldspar, 26 percent yellow-orange feldspar, 16 percent rock fragments, and 1 percent coal (probably debris from steamships that operated in the river). This yellow-orange feldspathic suite, which occupies the entire main channel, is apparently being transported from an upland source area or from local glacial outwash, kame terraces, and kame ridges (Chute and Nichols, 1941).

Figure 23. Scatter plot of inclusive graphic skewness versus graphic mean for 233 samples from throughout the entire estuary. Note that sediments in the main channel and on the flood-tidal delta are negatively skewed to near-symmetrical whereas those on the intertidal flats and in the tidal channels are generally positively skewed.

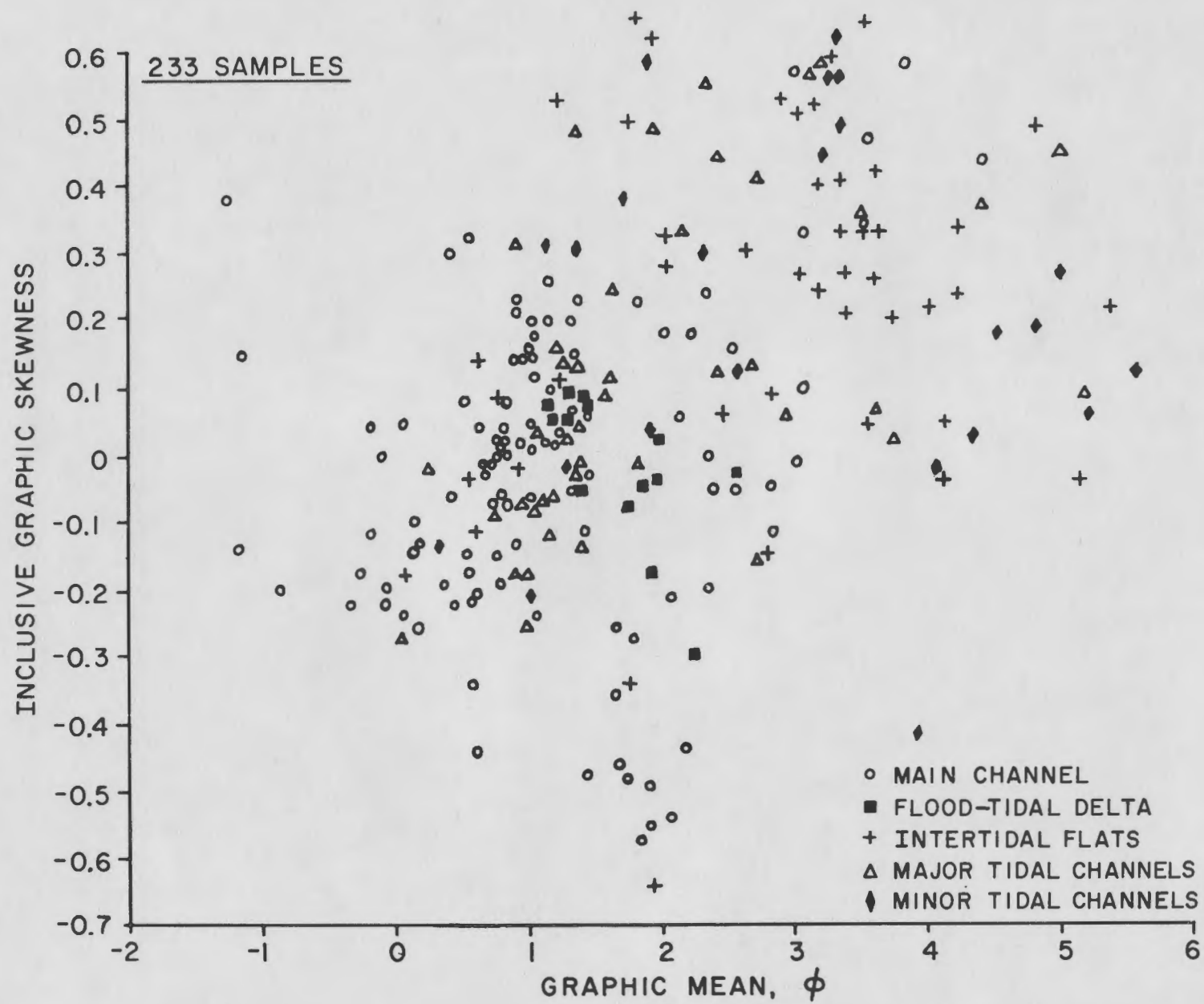


Figure 23

Figure 24. Grain-size distribution by frequency percent of sediments from three locations in the main channel (166, 2.4 km upstream of mouth; 358, 5 km upstream; 660, 7 km upstream; Fig. 1).

GRAIN-SIZE DISTRIBUTION

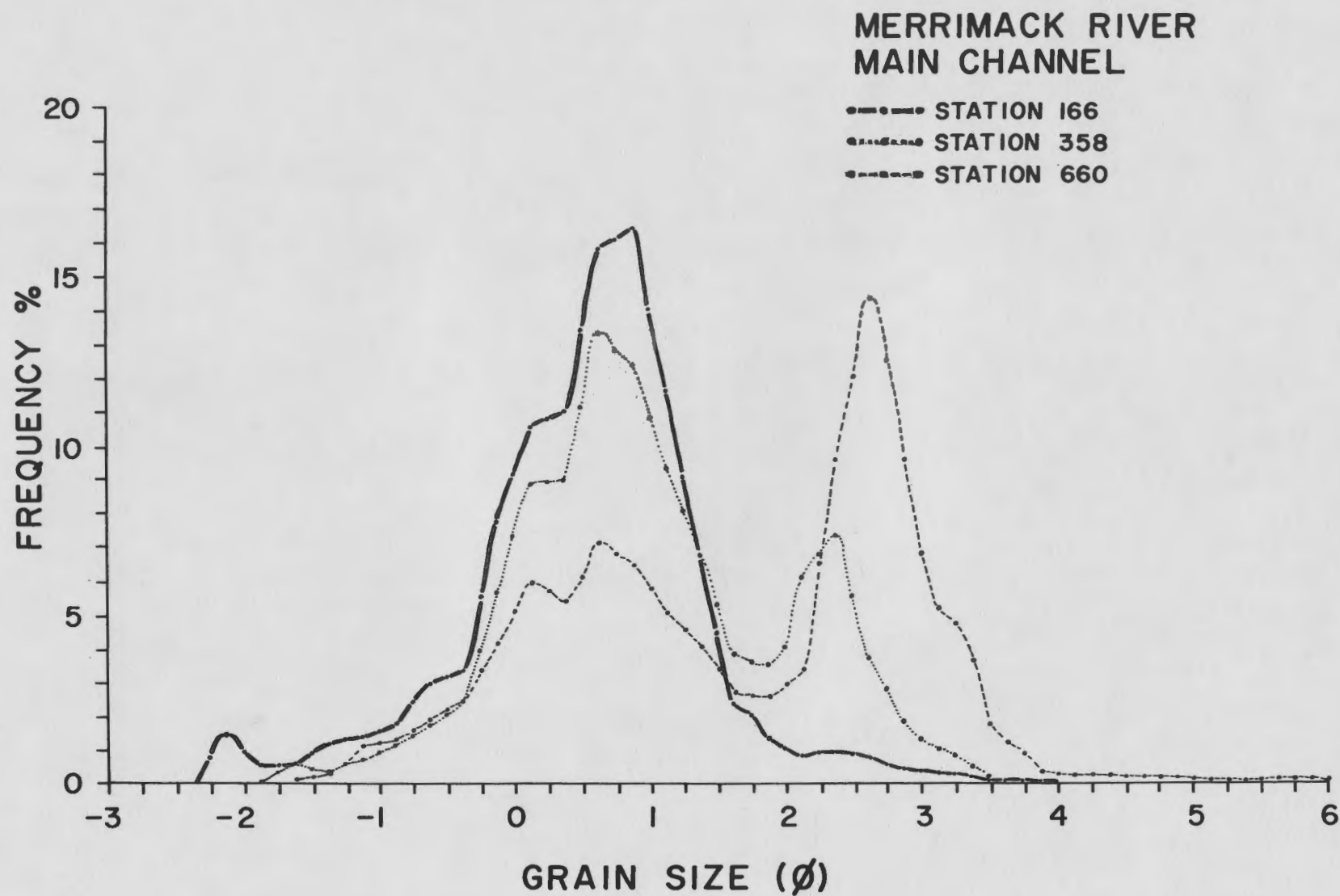


Figure 24

Figure 25. Grain-size distribution of frequency percent of sediments from three locations in secondary tidal channels (264 and 820 from the Plum Island River; 412 from Black Rock Creek; Fig. 1).

GRAIN-SIZE DISTRIBUTION

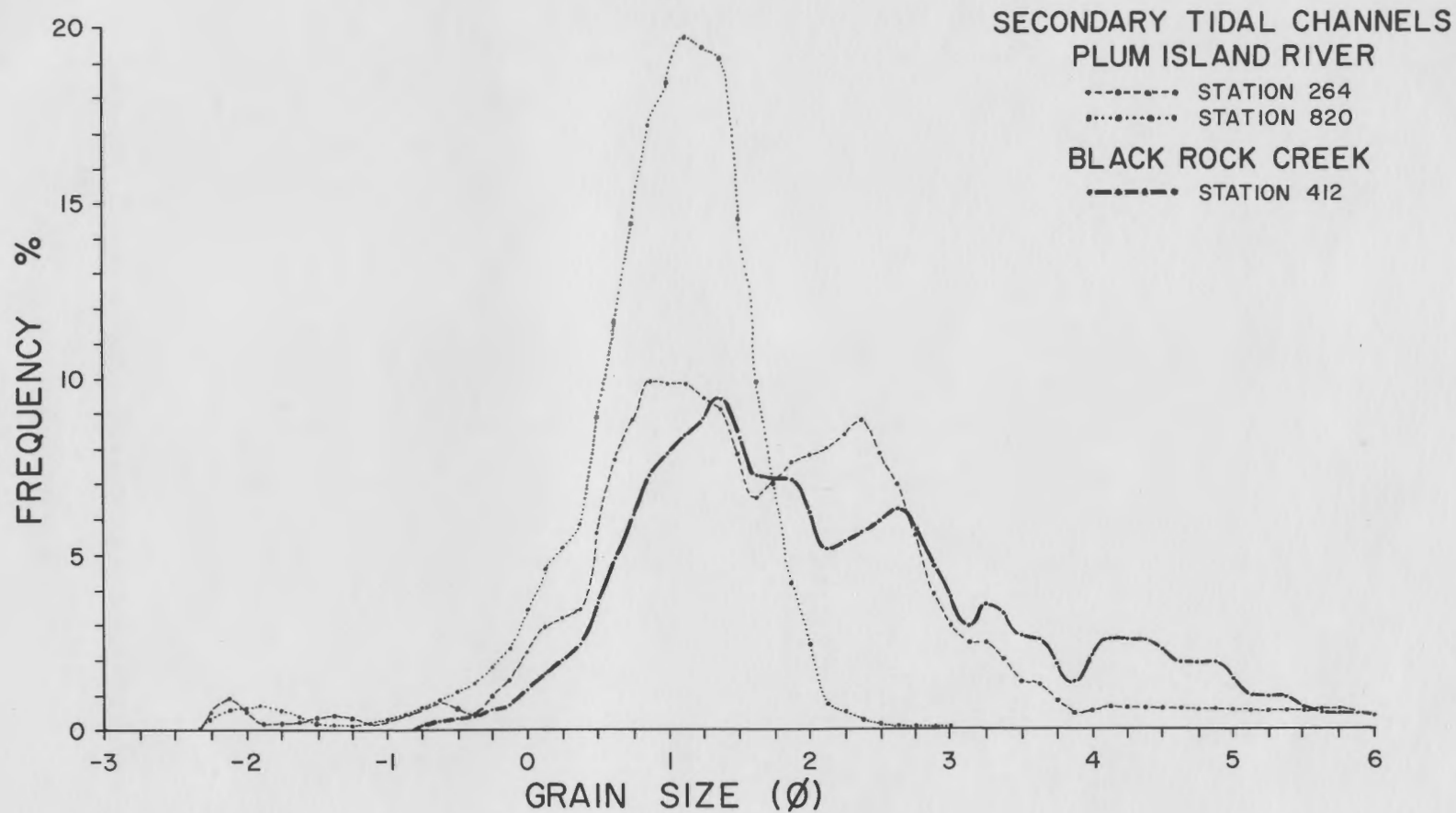


Figure 25

The second sand, which is found in the Plum Island River, east of Woodbridge Island, and on the flood-tidal delta, is slightly finer (modal size, 1.0 ϕ - 1.5 ϕ ; Fig. 25) but quite different mineralogically. Average estimated composition is: 79 percent quartz, 13 percent gray feldspar, 4 percent yellow-orange feldspar, 4 percent rock fragments and a trace of garnet. The paucity of yellow-orange feldspar and rock fragments in this sand suggests that its source was quite different from that of the coarser mode. This gray feldspathic suite seems to underlie the marsh deposits, suggesting that it was derived locally, possibly from erosion of the Newburyport Quartz Diorite.

The finest sand (modal size 2.38 ϕ - 2.88 ϕ) is common in the central part of the main channel near Newburyport and in tidal channels of the Black Rock Creek marsh. Estimated mineralogy is dominantly quartz (86 percent) with subequal amounts of gray feldspar and yellow-orange feldspar (5 percent), 1 percent rock fragments, and traces of mica, coal, and garnet. The origin and source area of this sand are uncertain at this time.

Main channel

The main channel of the Merrimack River estuary consists of three different sedimentary environments: subtidal channel, flood-tidal delta, and intertidal flats (Fig. 2). The geometry of the main channel and the relationship between bottom topography and mean grain size in these various environments is shown in Figures 26 to 28. Coarsest

Figure 26. Cross-channel bottom profiles of the lower estuary showing the relationship between bottom topography and mean grain size (ϕ). Topography reconstructed from fathometer profiles made on October 12, 1968.

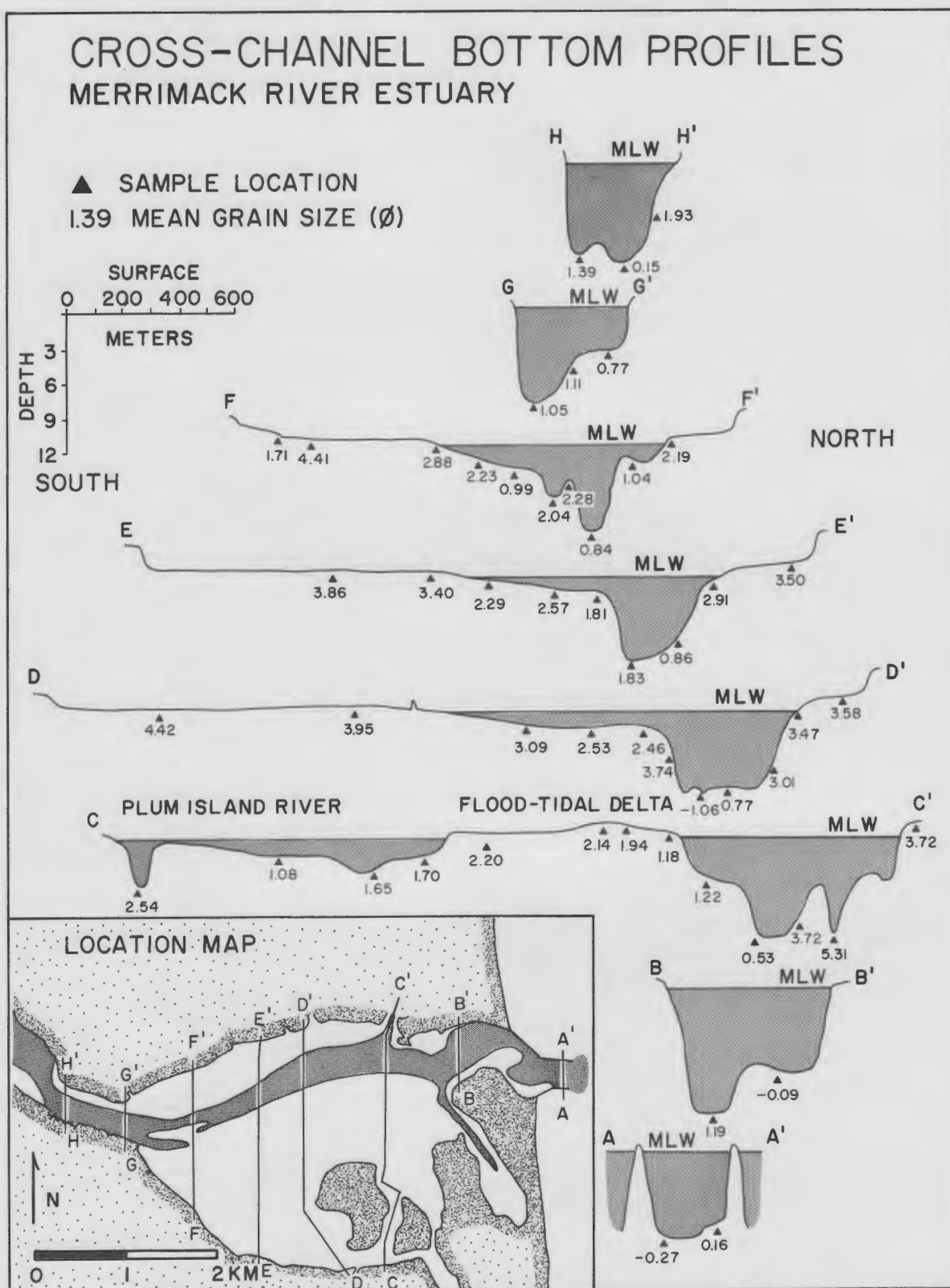


Figure 26

sediments occupy the subtidal channel, while mean grain size decreases and sorting gets poorer further away from the channel on the intertidal flats. Notable mud accumulations occur seaward of bedrock outcrops in the upper estuary, in deep hollows at the mouth of the Black Rock Creek, and on Joppa Flat (Fig. 18).

Subtidal channel. The subtidal channel follows a nearly straight path 13.5 km long across the entire study area. Major elements of this environment include channel bottom, sloping channel sides, and large, permanent bedforms. The channel bottom is subject to periodic dredging, such as at the mouth (June, 1968) and 0.8 km of the subtidal channel east of Newburyport (November, 1957). In the lower estuary, the channel is close to the northern shore, with the largest areas of intertidal flats and mud accumulation located to the south (Fig. 26). This geometry is probably due to active scouring of the subtidal channel bottom by strong tidal currents and deposition of fine-grained sediments in the adjacent shoal areas (note sections D, E, and F; Fig. 26). From Newburyport 0.6 km eastward, the channel is bifurcated because of scouring around an intertidal bedrock outcrop. West of Newburyport the channel is somewhat sinuous with irregular bottom topography due to bedrock control (Fig. 28). From Ram Island westward, the channel is also bifurcated, but the southern portion is generally deeper (note sections K to M, Fig. 27). The northern channel appears to be filled with local glacial outwash (section K-k, Fig. 27).

Figure 27. Cross-channel bottom profiles of the upper estuary showing the relationship between bottom topography and mean grain size (ϕ). Topography reconstructed from fathometer profiles made on October 24, 1968.

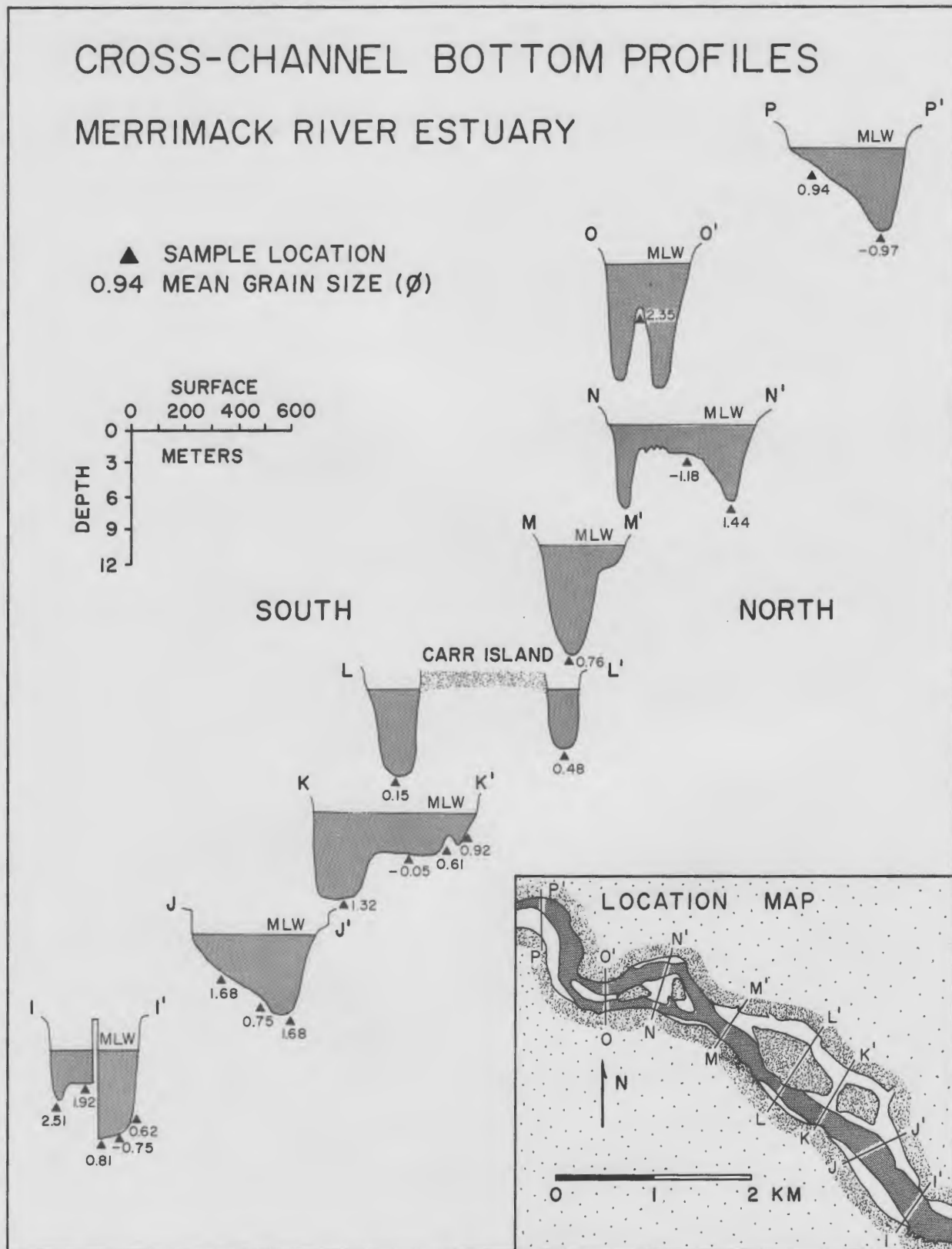


Figure 27

Sediments on the sloping subtidal channel sides are finer grained than those on the adjacent channel bottom (Figs. 26 and 27), apparently due to weaker tidal currents. Large midchannel bars are present east and west of several islands in the upper estuary and a few km west of the study area.

The relationship between channel-bottom topography and mean grain size is demonstrated in Figure 28. Coarsest sediments occur at the river mouth (-0.125ϕ to 0.0ϕ) across a shallow zone where strong currents have built large bedforms. This bottom profile, which was made at high water in early October, 1968, when river discharge was below normal (about 2500 cfs), reveals that these bedforms were symmetrical; however, they may become asymmetric in response to ebb-tidal currents and to periods of higher discharge. The 16 m-deep hole located 0.5 km upstream from the mouth is probably a result of strong scouring along the northern breakwater. From 1 to 1.5 km the bottom is coarse grained (0.6ϕ - 0.8ϕ) with several large permanent ebb-oriented bedforms. The channel from 2 to 5 km is about 4 m deep with coarse sand (0.5ϕ - 0.9ϕ) and small mussel mounds. In two zones, at 4.75 and 5.8 km, sediment becomes coarser, probably due to stronger current velocities. Note that the downstream zone is apparently flood dominated, while the upstream zone reflects ebb-current activity. From 6 to 11 km, deep hollows occur near bedrock outcrops. Sediments in the hollows are generally fine-grained whereas coarse sand and gravel and flood bedforms are present on the seaward sides of the bedrock. The fine sand under the Interstate 95 bridge at 10.3 km

Figure 28. Relationship between bottom topography and sediment mean grain size along the main channel. Topography reconstructed from fathometer profiles made at high water on October 12 and 21, 1968. River discharge about 2500 cfs. Arrows show orientation of bottom bedforms at time of profiling.

BOTTOM TOPOGRAPHY AND MEAN GRAIN SIZE MAIN CHANNEL—MERRIMACK RIVER ESTUARY

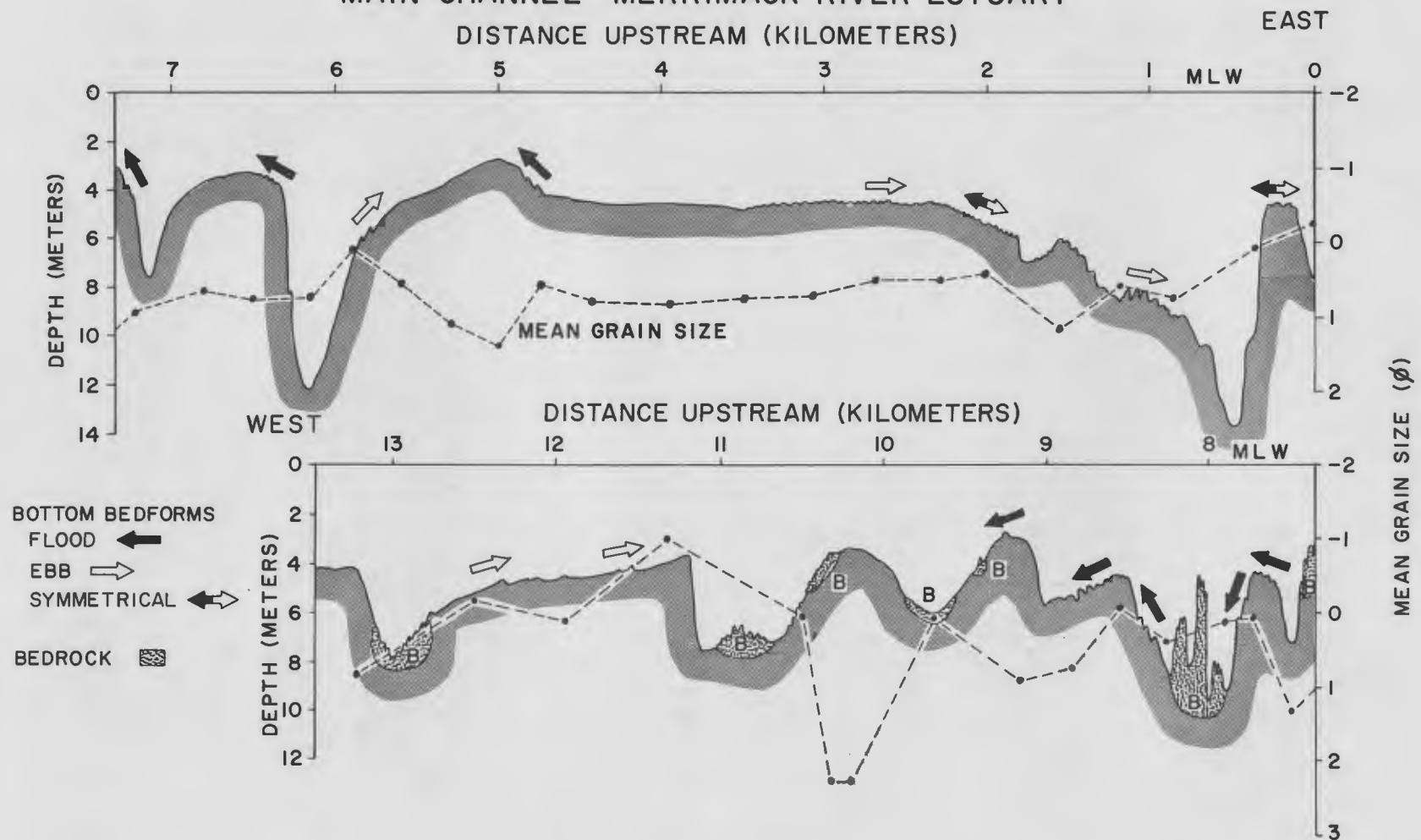


Figure 28

is part of a midchannel bar. Ebb dominance with marked seaward sediment transport by tidal currents is apparent at 11.25 and 13.25 km. Thus, coarse sand and gravel is present along the entire channel, with coarsest material occurring in zones of strong tidal-current activity on topographic highs.

At several locations in the subtidal channel, layers of coarse sand overlying organic debris were observed. The organic detritus may have been carried into the estuary during periods of above-normal discharge and later buried by estuarine sediments. Mussel clumps present in much of the lower estuary channel act as traps for fine-grained sediment and organic debris. Small-scale ripples were observed in medium-grained sand at several locations along sloping channel sides.

Flood-tidal delta. The only major intertidal sand body in the main channel is the flood-tidal delta¹ located 2.2 km west of the estuary mouth (Fig. 1; section C - C', Fig. 26). Although this sand body is

¹ Definitions from Coastal Research Group (1969).

Flood-tidal delta: Sediment accumulation formed inside an inlet by flood-tidal currents.

Ebb spit: Spit formed in an estuary as a result of ebb currents. Commonly found attached to the borders of flood-tidal deltas.

Ebb shield: Topographically high rim or margin around a sand body that protects portions of the sand body from modification by ebb-currents.

similar in morphology and structure to those found in nearby estuaries, such as the Parker River, Essex Bay, and Hampton Harbor (Coastal Research Group, 1969), one important difference is that this delta is strongly influenced by the large volume of fresh water that Merrimack River discharges into the estuary. The aerial photograph (Fig. 29) and plane-table map (Fig. 30) of the flood-tidal delta show the main features, which include a large ebb spit, flood sand-wave field, ebb shield, and northwest sand-lobe area. The ebb shield forms a topographic high 1.0 - 1.5 m below mean sea level. The southwestern and western portions of the delta are covered with mussel banks.

During the summer of 1968, the tidal delta was visited 23 times at low tide to observe bedforms, minor sedimentary structures, sediment distribution, infauna, and migration of sand waves. In late June, an east-west range line was established and a plane-table map prepared (Fig. 30). Approximately every 6 days for the remainder of the summer, bedform azimuths, wavelengths, and amplitudes were measured at low tide

Bedforms:

Ripples: Asymmetric bedforms formed by unidirectional flow. Wavelength less than two feet.

Megaripples: Asymmetrical bedforms formed by unidirectional flow. Wavelength between two and twenty feet.

Linear-megaripples: Megaripples with straight crests.

Scour-megaripples: Megaripples with undulatory to cusped crests and well-developed scour pits in front of the slip faces.

Sand waves: Asymmetric bedforms formed by unidirectional flow. Wavelength greater than twenty feet.

Figure 29. Vertical aerial photograph of Merrimack flood-tidal delta. Note the exceptionally large ebb shield on the western side of the delta (estuary mouth is to the right). Compare photograph with plane-table map (Fig. 30). Photograph taken on April 18, 1968; courtesy of U.S. Army Corps of Engineers.

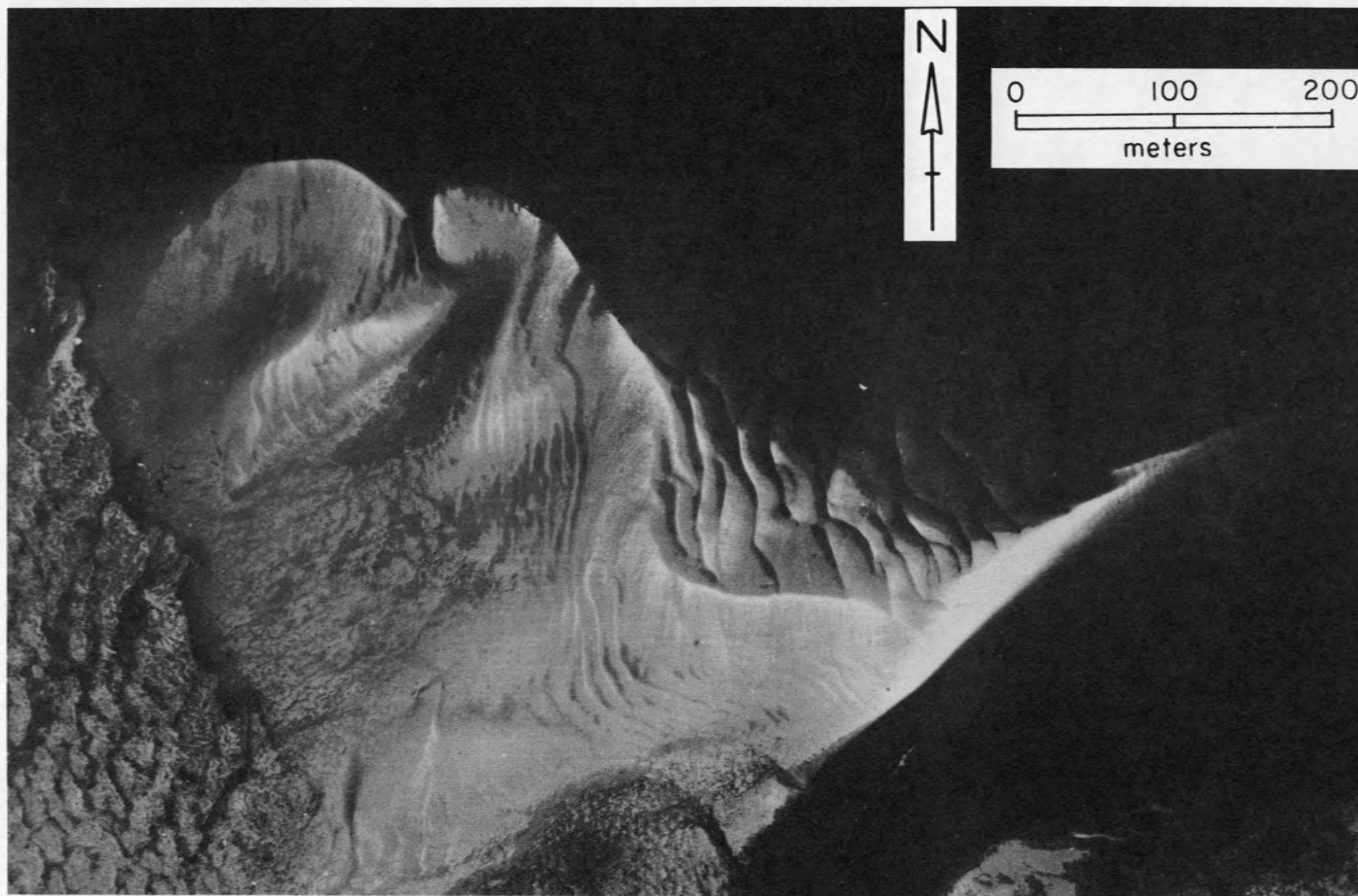


Figure 29

Figure 30. Plane-table map of the Merrimack flood-tidal delta on July 13, 1968. Compare with aerial photograph in Figure 29. Datum is mean sea level; contour interval 0.5 m.

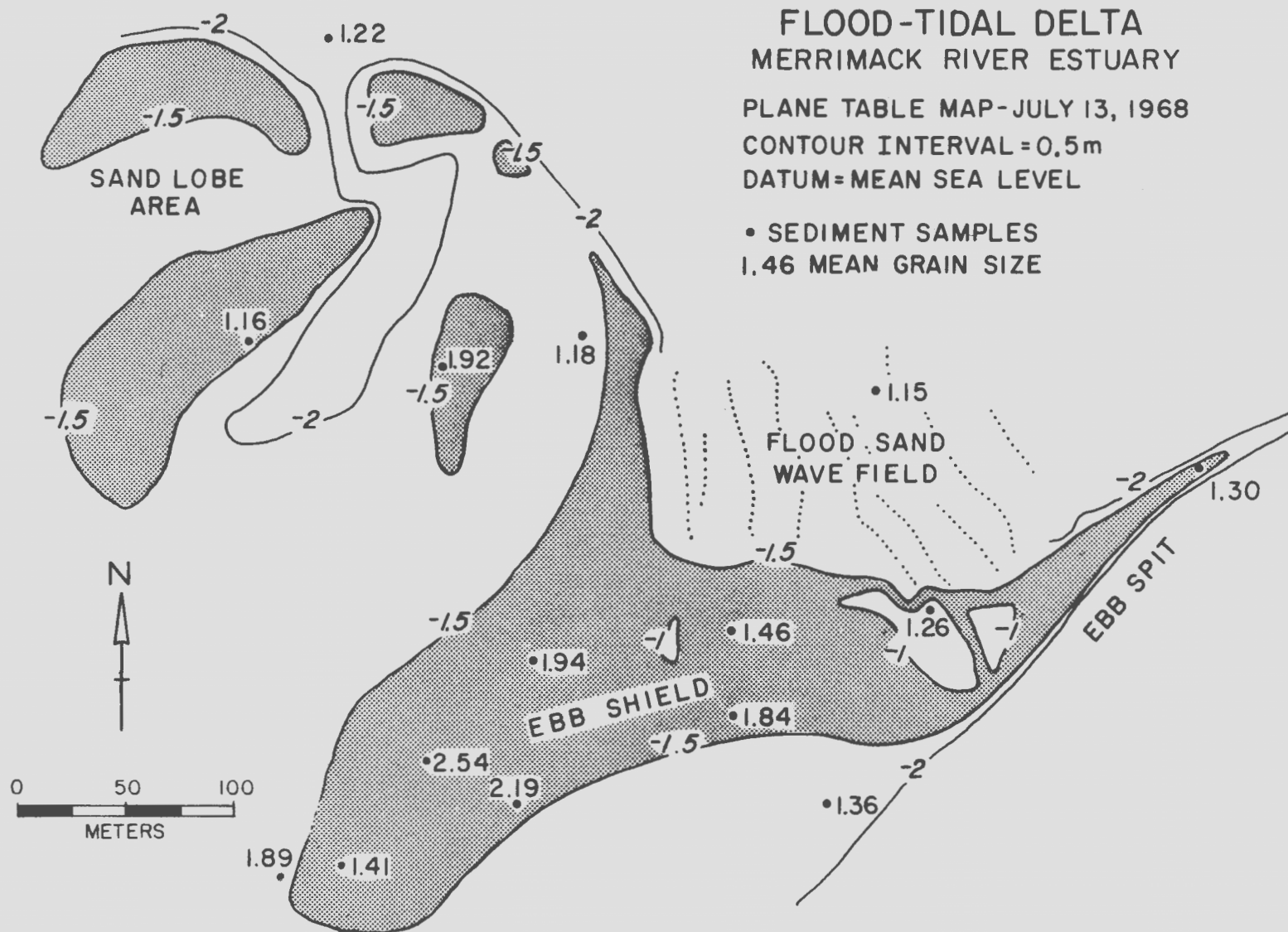


Figure 30

on a 30 m grid across most of the delta. An attempt was made to gather data representative of spring, normal, and neap tides and of high and low discharge conditions. The delta was remapped at the end of the summer and the location of each flood-oriented sand wave determined.

The rose diagram in Figure 31 shows the distribution of the azimuths of slip-face orientations on bedforms during a normal low tide (range 2.5 m). Ripples and megaripples show ebb orientation toward the northeast, whereas sand waves are bimodal, reflecting the flood dominance on the larger sand waves located along the northeastern margin of the delta and the influence of ebb currents during a falling tide on the smaller ones located on the ebb shield (Fig. 29). That is, flood-tidal currents have built a series of large sand waves (Fig. 39) in the topographic low along the northeastern margin of the ebb shield. As flood currents flow up onto the ebb shield during periods of below-normal discharge, they destroy ebb-oriented bedforms left from the previous tidal cycle and cause flood modification of low-amplitude, ebb-oriented sand waves. After the tide turns, the ebb shield becomes covered with ebb-oriented bedforms (Figs. 33 and 34) and acts as a topographic shield to prevent ebb modification of the large sand waves along the northeastern margin. Note also that the maximum ebb-current velocities are not attained until 4 to 6 hours after high water (Fig. 15) when the entire tidal-delta complex is out of the water and flow is restricted to the main channels. Thus, the

Figure 31. Rose diagram of slip-face azimuths of sand waves, megaripples, and ripples (182 readings) on the flood-tidal delta. Data collected during a normal low tide on July 15, 1968.

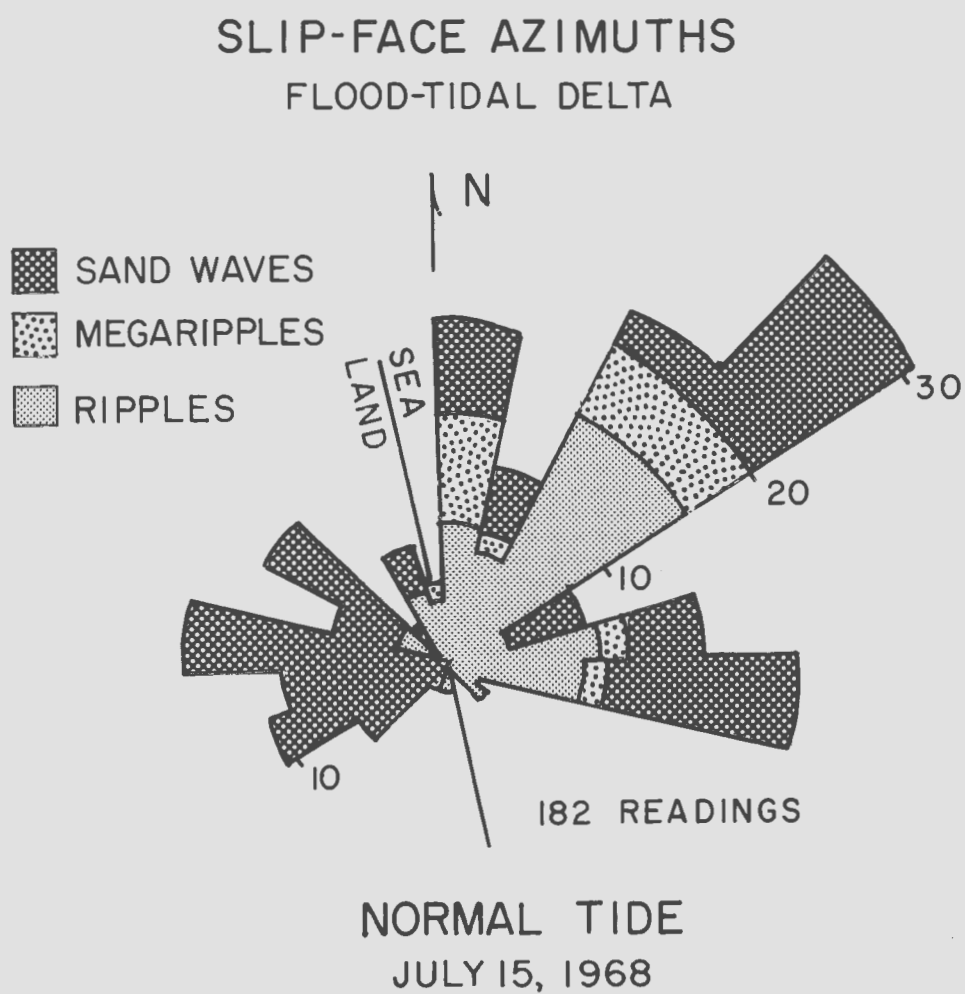


Figure 31

slip-face azimuths of sand waves on the flood-tidal delta show a bimodal orientation (Fig. 32).

One of the most striking aspects of the flood-tidal delta is the differing response of bedforms to neap, normal, and spring tidal conditions. The normal tidal range is 2.5 m (8.2 ft), spring tides reach 3.5 m (11.7 ft), and neap tides may be as small as 1.5 m (5.0 ft). During normal low tides most of the ebb shield is covered with ebb-oriented ripples, while the ebb spit and the northern end of the ebb shield have ebb-oriented megaripples and scour-megaripples. During spring tides, larger volumes of water enter the estuary, so current velocities are stronger. The resulting low-tide bedforms are large megaripples and scour-megaripples across much of the ebb shield (Fig. 33). In contrast, the small water volume of neap tides forms small ebb-oriented ripples (Fig. 34) on the ebb shield at low tide with megaripples being almost nonexistent. The flood-oriented sand waves along the northeastern margin of the ebb shield are unaffected by ebb currents, whereas sand waves on the ebb shield are ebb-oriented except when below-normal discharge permits flood modification.

Details of the changes in bedforms in response to differing tidal ranges, current velocities, and river discharges are documented in Figures 35 to 40. All of the low-tide ripples (Fig. 35) show ebb orientation, but those formed during spring and normal tides are more strongly bimodal due to changes in current direction across the ebb shield. Ripples formed during neap tides have the longest wavelengths, with 27 percent in the 21.3 to 24.4 cm (0.7 to 0.8 ft) class

Figure 32. Composite rose diagram summarizing sand-wave azimuths collected at low tide during spring, normal, and neap tides (total of 92 readings) from June to August, 1968.

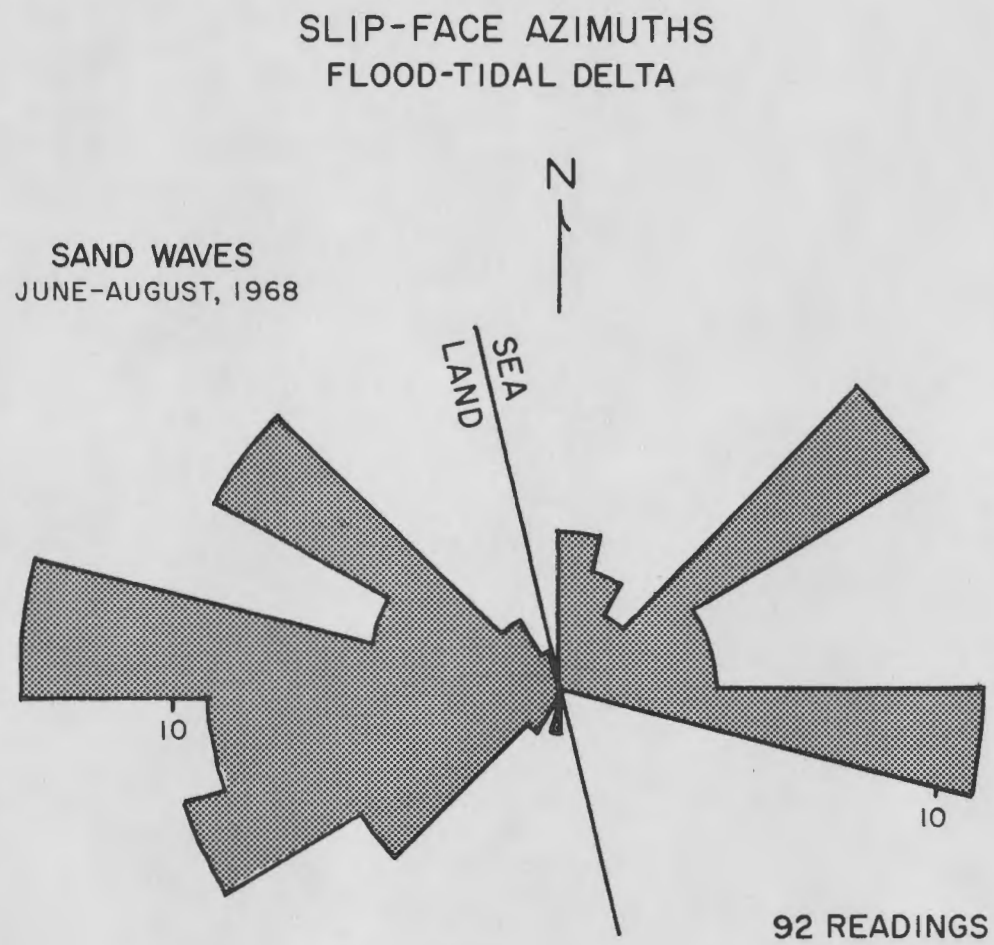


Figure 32

Figure 33. Spring-tidal effects on the flood-tidal delta. View looking northwest across the central portion of the ebb shield at low tide, June 13, 1968. Tidal range 3.2 m (10.8 ft.); note large scour-megaripples and ripples.

Figure 34. Neap-tidal effects on the flood-tidal delta. Approximately the same view as Figure 33; July 22, 1968; tidal range 1.7 m (5.7 ft). Note well-developed ripples but absence of scour-megaripples due to low current velocities.



Figure 33



Figure 34

Figure 35. Rose diagrams showing slip-face azimuths of ripples measured at low tide on the flood-tidal delta during three tidal phases: spring (July 11, 1968), normal (July 15, 1968), and neap (July 22, 1968).

RIPPLE SLIP-FACE AZIMUTHS

FLOOD-TIDAL DELTA

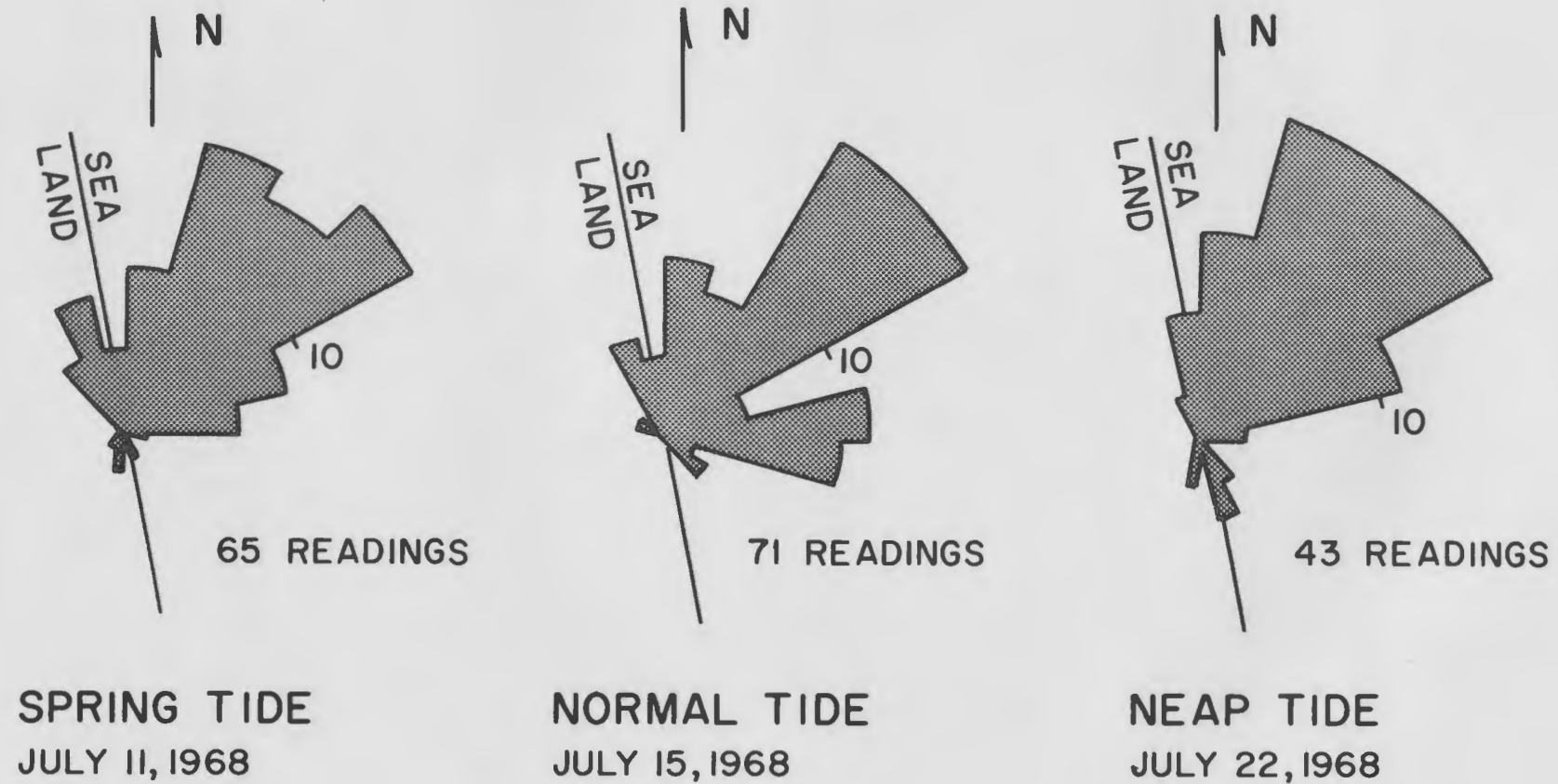


Figure 35

(Fig. 36). Ripples formed during normal and spring tides show three peaks in wavelength (Fig. 36) at 9.2 to 15.2 cm (0.3 to 0.5 ft), 18.3 to 24.4 cm (0.6 to 0.8 ft), and 24.4 to 30.5 cm (0.8 to 1.0 ft). The ripples represented by the first and third peaks probably were formed under higher flow-regime conditions in the scour pits of megaripples. The middle peak corresponds to the smaller ripples that develop on the southwestern side of the ebb shield.

Rose diagrams of megaripples' slip-face azimuths (Fig. 37) reveal that those formed during spring and neap tides are nearly uniformly oriented toward the northeast. During normal tides, a distinct bimodality is evident, reflecting current flow to the north across the ebb spit and to the northeast across the northern end of the ebb shield. Histograms of wavelength (Fig. 38) show that megaripples formed during spring tides are largest (0.6 to 2.8 m; 2 to 10 ft). Normal-tide megaripples are smaller with peaks at 0.9 to 1.2 m (3 to 4 ft) and 1.5 to 1.8 m (5 to 6 ft). Megaripples are rare during neap tides but 66 percent of the wavelengths measured are 0.9 to 1.2 m (3 to 4 ft). Histograms of amplitudes (Fig. 34) reveal a similar trend; that is, spring-tide megaripples are largest with peaks at 6.1 to 9.2 cm (0.2 to 0.3 ft) and 18.3 to 21.3 cm (0.6 to 0.7 ft). During normal and neap tides, most of the amplitudes are between 3.0 and 6.1 cm (0.1 to 1.2 ft).

The migration rates of flood sand waves along the northeastern margin of the ebb shield are also related to the monthly tidal cycle. Stakes were placed at the slip-face base of selected sand waves in

Figure 36. Histograms showing wavelengths (ripple spacing) for ripples occurring on the flood-tidal delta at low tide during three tidal phases (spring, normal, and neap). This is a composite diagram of all ripples measured during the summer of 1968.

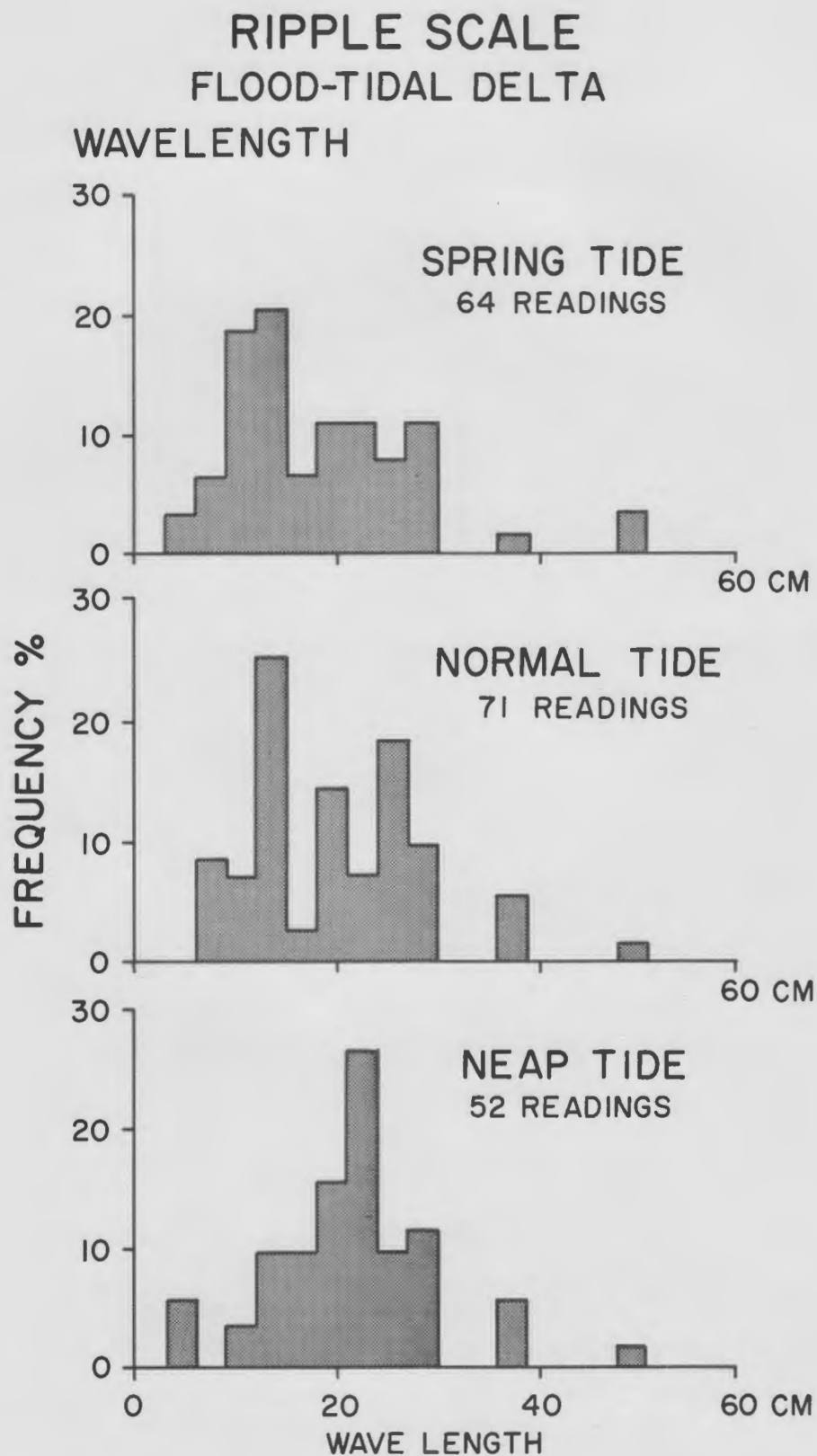


Figure 36

order to monitor changes during the summer of 1968. The photo sequence in Figure 39 illustrates more than 8.5 m of westward migration of one sand wave during a 54-day period starting in late June. Highest migration rates occurred during spring tidal conditions (Fig. 40).

A rapid decrease in fresh-water discharge in early July 1968, had profound effects on large bedforms and ebb-shield morphology. During late June, when discharge was two to three times above the annual mean of 7000 cfs, the numerous sand waves on the ebb shield showed ebb orientations at low tide with active seaward slip-face migration. During the first 10 days of July, discharge dropped from 21,300 to 5760 cfs and flood currents began to dominate the entire delta. The old, ebb-oriented slip faces were largely destroyed and replaced by westward-migrating ones. Thus, many of the larger sand waves on the ebb shield that had previously been ebb-oriented at low tide began to migrate westward and assume a flood-oriented asymmetry. Additional work is necessary to monitor these changes on an annual basis.

The sediment distribution on the flood-tidal delta is closely related to bottom topography and current velocities. The coarsest sediments (slightly gravelly sand, mean 1.150 - 1.460) are found on the topographic high along the northeastern margin of the delta, on the ebb spit, in the flood sand-wave field, and on the topographic high in the southeastern part of the ebb shield (Fig. 30). Fine sand (mean 2.120 to 2.60) is present in a zone of clam flats on the south-

Figure 37. Rose diagrams showing slip-face azimuths of megaripples measured at low tide on the flood-tidal delta during three tidal phases: spring (July 11, 1968), normal (July 15, 1968), and neap (July 22, 1968).

MEGARIPPLE SLIP-FACE AZIMUTHS FLOOD-TIDAL DELTA

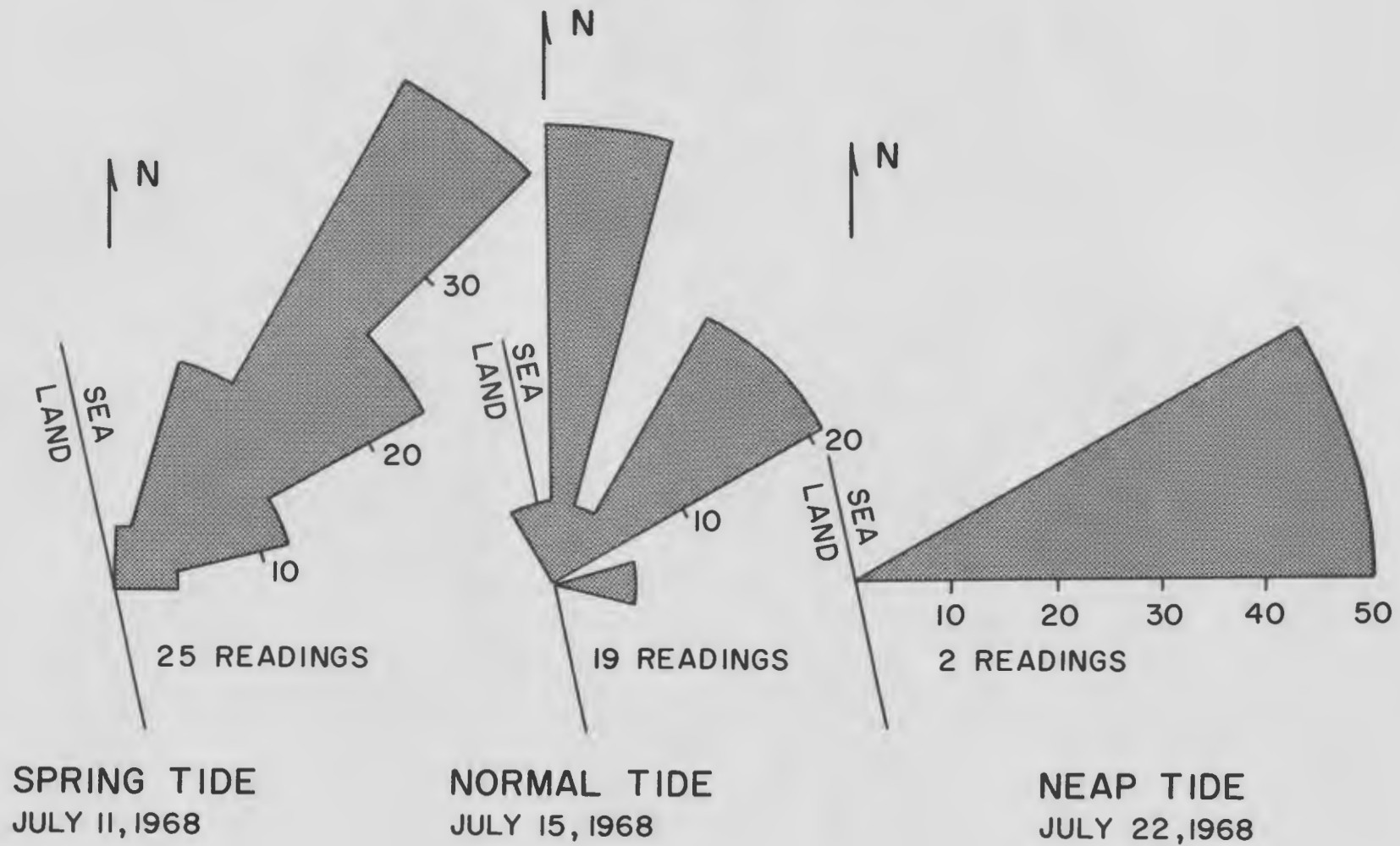


Figure 37

Figure 38. Histograms showing wavelengths and amplitudes of megaripples occurring on the flood-tidal delta at low tide during three tidal phases: spring, normal, and neap. This is a composite diagram of all megaripples measured during the summer of 1968.

MEGARIPPLE SCALE

FLOOD-TIDAL DELTA

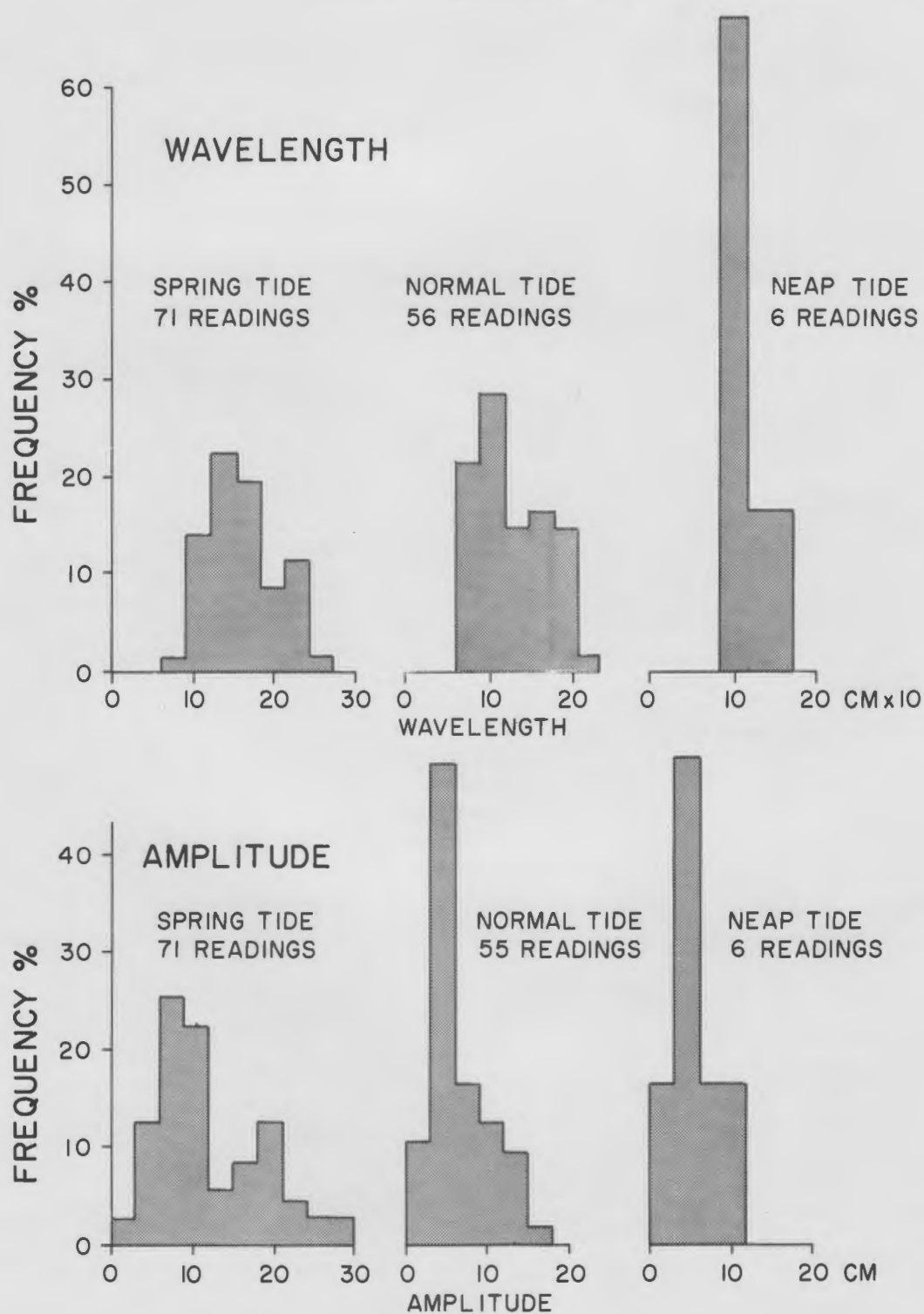


Figure 38

western part of the ebb shield. The remainder of the delta consists of medium sand (mean $1.2\phi - 1.9\phi$). Sediments in the northeastern part of the delta are well sorted ($\sigma .45-.5\phi$) while sorting gets poorer toward the southwest ($\sigma .6-.63\phi$). All of the flood-tidal delta sediments are near-symmetrical and mesokurtic.

The sediment distribution on the flood-tidal delta appears to be the result of selective size sorting and tidal-current velocity asymmetry. Coarsest sediments are found on the topographic highs and along the northeastern edge of the delta where strong flood currents deposit sand from the main channel and winnow out finer grained material. The topographic highs are areas where transport capacity of the currents are increased as a result of decreased depths, or higher Froude numbers. The finest sand on the delta occurs in a topographic depression on the southwestern part of the ebb shield. Because of the current-velocity asymmetry, ebb currents are not as effective on the delta as they could be. That is, maximum ebb velocities are not attained until most of the delta has been uncovered.

Crossbedding is the characteristic sedimentary structure on the delta. Most of the large sand waves produce high angle crossbedding ($27^\circ - 32^\circ$), while smaller sand waves on the ebb shield have low-angle crossbeds ($5^\circ-8^\circ$ and occasionally $10^\circ-15^\circ$). At one location near the ebb spit, herringbone crossbedding with opposing dips, built by ebb and flood currents, was observed. In the clam-flat

Figure 39. Series of photographs (taken at low tide during the summer of 1968) illustrating the rate of movement of the slip face of a flood-oriented sand wave with respect to a permanent stake. Location is the flood sand-wave field along the northeastern margin of the flood-tidal delta (Fig. 30). Compare with graph of the same data (Fig. 40). All photographs were taken looking northwest. Date for each photograph is:

A. June 25
C. July 11
E. July 31

B. July 8
D. July 13
F. August 8

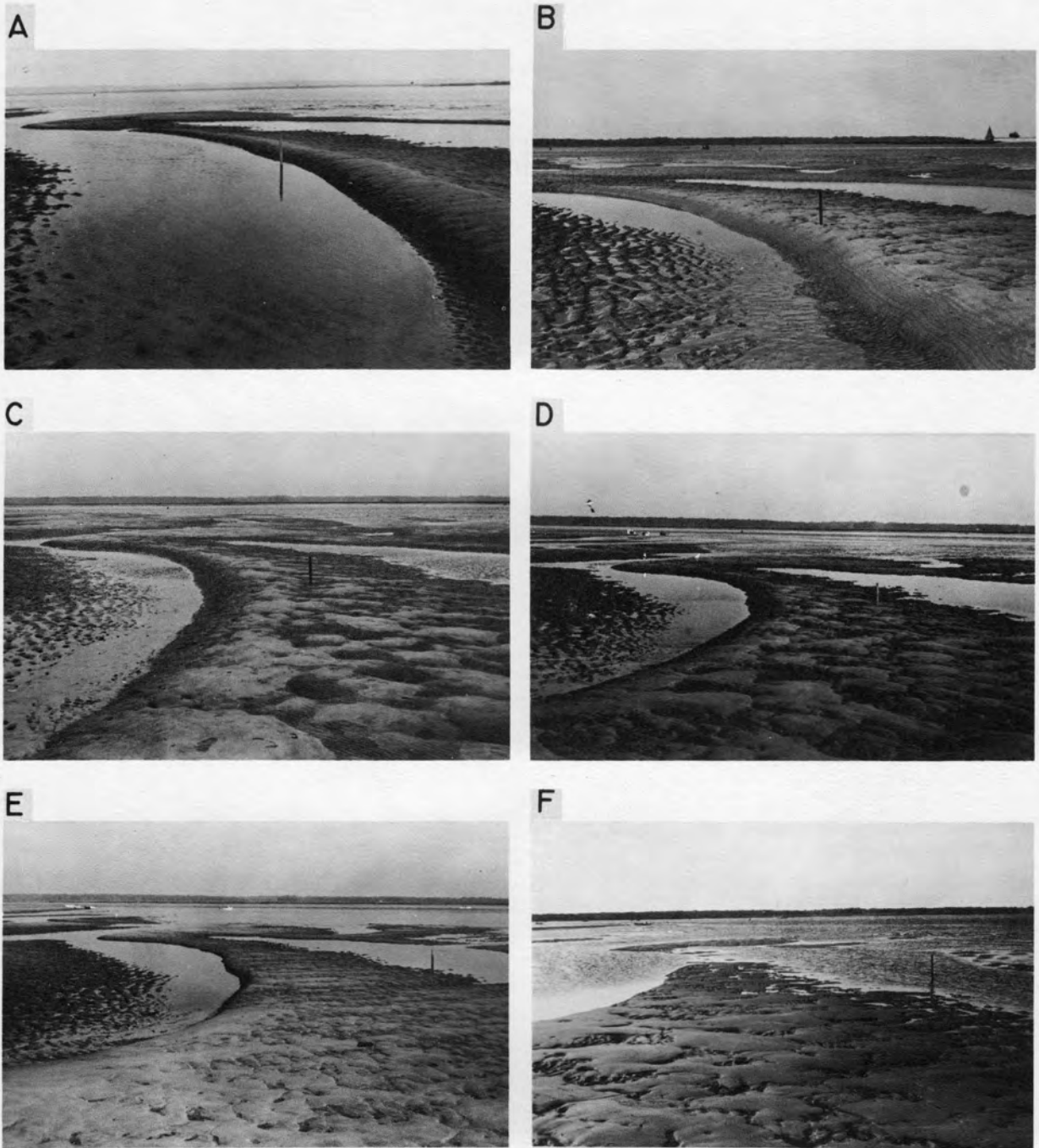


Figure 39

area on the southwestern part of the delta, clam burrows, hydrogen sulphide cells (caused by chemical reduction of buried organic matter), and mottling are present.

Intertidal flats. Intertidal flats border most of the main channel in the lower estuary (Fig. 2). Clams and worms are abundant along both sides of the main channel, along the northern shore of Woodbridge Island, and along the margin of the western prong of Plum Island. Although mussels are found at many scattered locations in the lower estuary, the only extensive mussel banks are adjacent to the southwestern portion of the flood-tidal delta and along the northwestern margin of Plum Island. The sediment in these intertidal environments is generally muddy sand (mean grain size 2.72ϕ - 3.95ϕ ; Fig. 19); however the southern portion of Joppa Flat is sandy mud to mud (Fig. 18). These sediments are poorly sorted to very poorly sorted (1.1 - 2.6ϕ), fine-skewed ($.13$ - $.65$), and leptokurtic (1.17 - 2.04).

Throughout most of the lower estuary, clam and worm flats slope gently toward the main channel (Fig. 26). The surfaces of these flats are soft, muddy sand (mean 3.5ϕ - 4.0ϕ ; at depth, the sediment is slightly coarser (mean 3.5ϕ) with abundant large Mya arenaria shells in life position. Flats located along the northeastern margin of Woodbridge Island and the northwestern margin of Plum Island are coarser grained (mean 1.8ϕ - 3.0ϕ), more compact, and have numerous shell fragments on the surface. These flats are subjected to effective

Figure 40. Graph showing slip-face migration of the flood-oriented sand wave illustrated in Figure 39. Migration rates were greatest during the periods of spring-tidal conditions (July 8-13, and August 5-8, 1968).

SAND-WAVE SLIP-FACE MIGRATION FLOOD-TIDAL DELTA

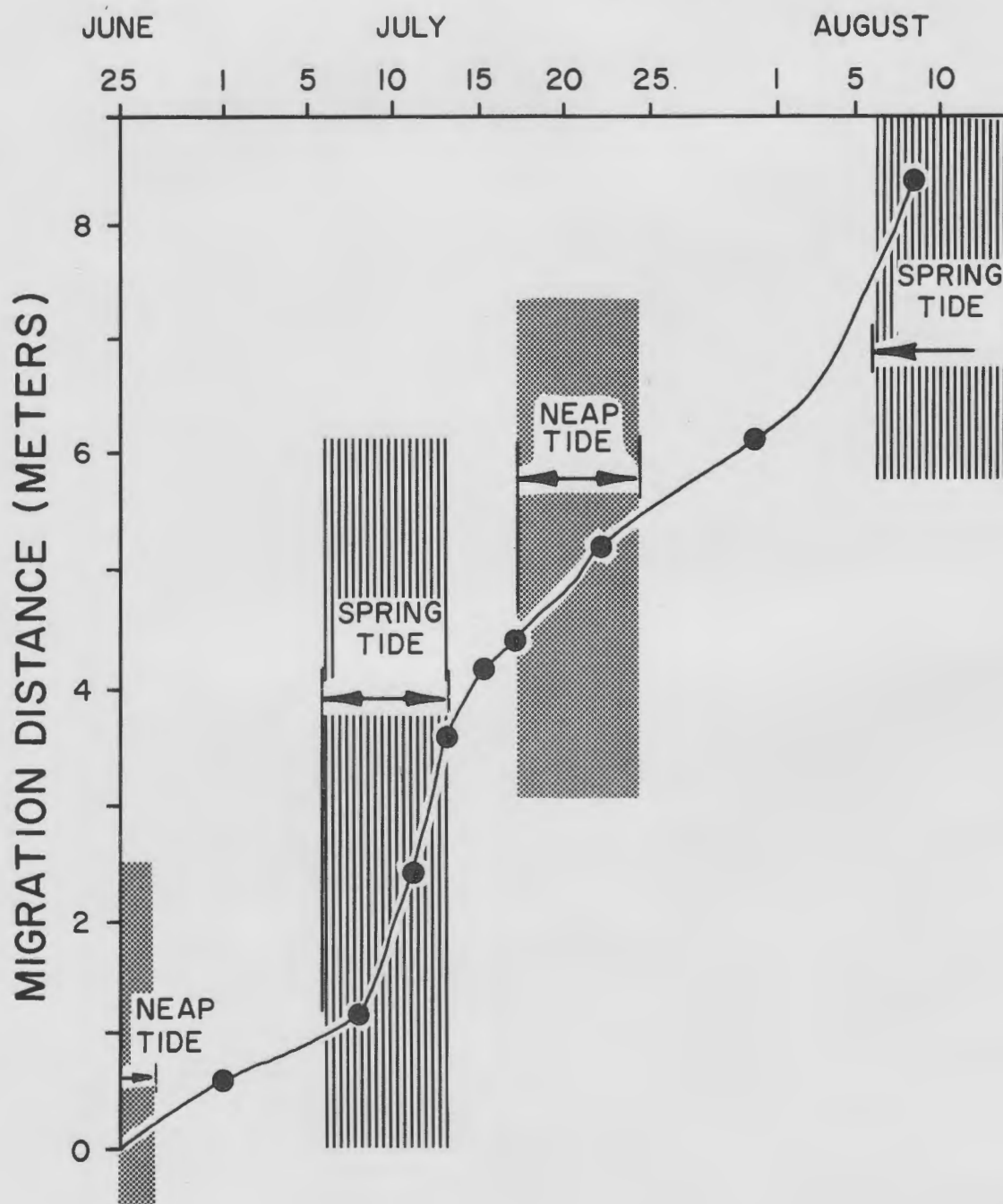


Figure 40

scouring by tidal currents and frequently have well-developed ebb-current lineations (Figs. 41 and 42). At several locations north of Woodbridge Island, tidal-current erosion has exposed abundant large Mya arenaria shells in life position.

Inorganic sedimentary structures in the clam and worm flats include black hydrogen sulphide cells and layers caused by chemical reduction of buried organic matter and laminations (Fig. 43). Most samples have well-developed organic structures. Burrowing and reworking of the sediment by infauna causes irregular mottles of sand and organic matter and disruption of horizontal laminations (Fig. 43A-43C). Commonly individual sand grains and lighter colored mud cells are visible in X-ray radiographs (Fig. 44). Many samples reveal individual burrows of local fauna such as the soft clam (Mya arenaria), clam worm (Nereis virens), duck clam (Macoma balthica), and the bloodworm (Glycera disbranchiata) (Fig. 44). Note how well X-ray radiograph techniques delineate burrows which are not apparent to the naked eye. Many of the smaller burrows have brown linings of oxidized sediment, suggesting active oxygen circulation through the burrows (Fig. 45). Other burrows have turned black from the reduction of trapped organic matter. In many areas clam and worm burrows with oxidized linings that cut across black sulphide cells were observed.

Many of these clam and worm flats overlie a buried zone of Mya arenaria shells in life position. Depth is variable (0.75 - 1.5 m), but the clams are almost always large and tightly packed.

Figure 41. Intertidal clam flat located at the northern end of the Plum Island River. Low-tide view looking due east toward northern tip of Plum Island. Note scattered mussel clumps and well-developed ebb-current lineation toward the northeast. Sediment mean grain size 1.73 ϕ .

Figure 42. Intertidal flat along northeastern margin of Woodbridge Island. Low-tide view looking northwest. Note well-developed current lineation on the clam flat and abundant shell fragments of Mya arenaria unearthed by eroding tidal currents. Border of fringing mussel bank in foreground. Sediment mean grain size 1.8 ϕ .



Figure 41



Figure 42

- Figure 43. Sedimentary structures developed in intertidal flats and secondary tidal channels:
- A. Clam flat in Plum Island River; well-developed laminations disrupted by clam.
 - B. Clam flat at mouth of Black Rock Creek; horizontal laminations, organic mottling, mud lenses, hydrogen sulphide cells, and shell fragments.
 - C. Clam flat in Plum Island River showing finely-laminated rhythmite layers (Reineck, 1967) disrupted by worm (?) burrow (see Fig. 50).
 - D. Clam flat in Plum Island River showing well-developed black hydrogen sulphide layer in coarse sand.

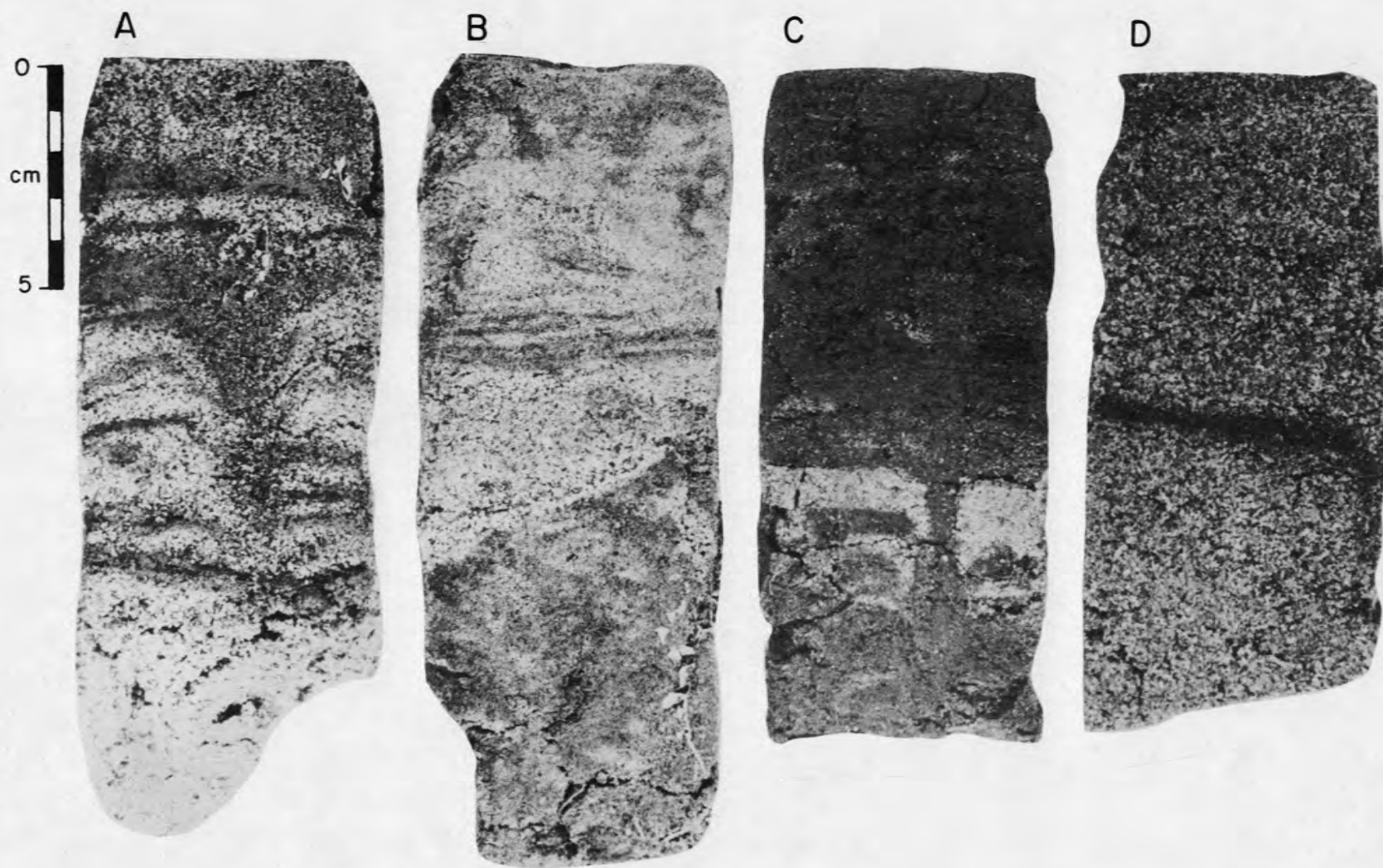


Figure 43

- Figure 44. Structures developed in intertidal mud flats in the western end of Joppa Flat:
- A. Photograph showing large Mya arenaria soft clam in life position. Smaller worm burrows are present but hard to distinguish.
 - B. X-ray radiography of the same sample showing well-developed burrowing by small worms (probably Nereis virens). Note the success of x-ray radiography techniques in delineating structures that would otherwise be indistinguishable (also see Fig. 50).

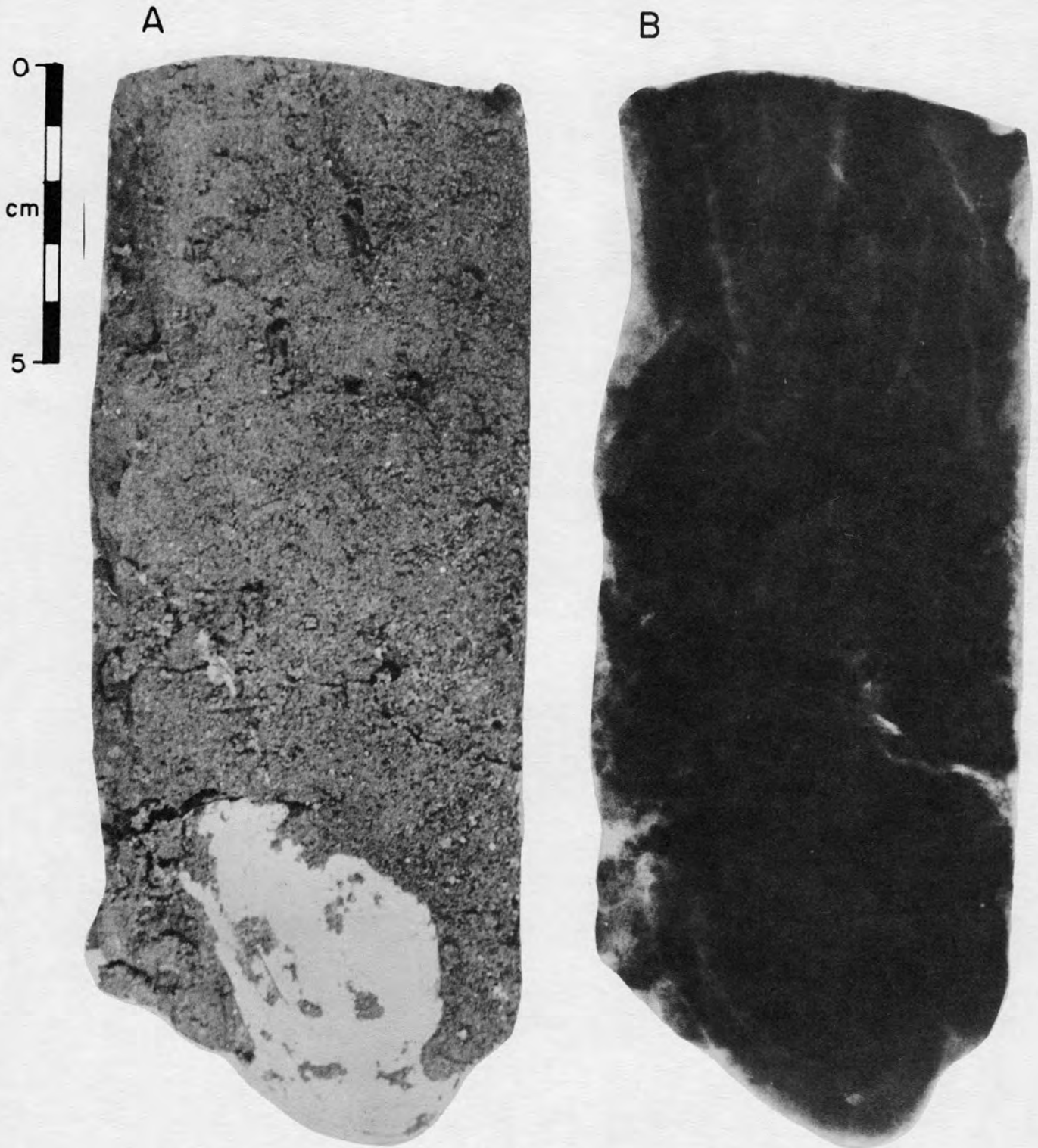


Figure 44

According to Jerome and others (1965), the large size of these paired shells (up to 12 cm) is indicative of mortality by old age. But, the ubiquitous nature of this layer suggests the possibility of a large-scale kill throughout the estuary, possibly as a result of industrial pollution at some time in the past several hundred years. Clams are presently abundant in the lower Merrimack, but most flats are closed to digging because of pollution.

Another significant feature of this environment is the presence of scattered peat blocks, probably carried in by ice rafting during the winter (Fig. 46). If the Merrimack River estuary sediments were to be preserved in the rock record, these vegetal masses could possibly be preserved as coal deposits in shale or mudrock.

The mussel banks, which differ markedly from the clam and worm flats, are located in less active hydraulic zones adjacent to the flood-tidal delta and along the northwestern margin of Plum Island. The mussels grow in irregular clumps, forming mounds or ridges which are out of water for part of every tidal cycle (Fig. 47). Empty shells and organic debris become incorporated into the clumps to form substrata for young mussels (Fig. 48). The mussels originally established themselves on a firm bottom of intertidal sand (Dexter, 1947), but have now become an effective trap for organic material and fine-grained sediments. This process of sediment accumulation on banks of sessile filter-feeding molluscs was termed "biodeposition" by Haven and Morales-Alamo (1969). Mean grain size is very fine sand to mud

Figure 45. Well-developed burrows of the worm Nereis virens in sediment of Joppa Flat. Burrows are lined with a brown oxidized layer suggesting active oxygen circulation from the atmosphere. Kitchen knife for scale. Sample unearthed by shovel.

Figure 46. Salt marsh peat block lodged on intertidal flat (central portion of Joppa Flat). Probably transported by ice rafting during the winter.



Figure 45



Figure 46

Figure 47. Mussel banks at the mouth of the Plum Island River in the vicinity of the flood-tidal delta. Low-tide view looking due south.

Figure 48. Close-up photograph of mussel bank shown in Fig. 47. Note abundance of mussel shells that provide substrate for young mussels and act as a sediment trap. Note barnacles and thin mud deposit; mean grain size 3.38 ϕ . Pencil for scale.



Figure 47



Figure 48

(3.30 - 3.80; Figs. 18 and 19) with poor sorting (1.30 - 1.70; Fig. 20). Sediments of depth are slightly acidic (pH 6.6) and generally black with abundant hydrogen sulphide, indicating active chemical reduction of buried organic matter. Characteristic structures at depth include mussel-shell clumps and worm burrows with brown oxidized linings.

Mud has accumulated in portions of the main channel where tidal currents are weak. Muddy sand (mean 3.20 - 3.30) occurs as ebb-current shadows east of bedrock outcrops in the upper estuary and at the mouth of Black Rock Creek. Euxinic black mud (mean 4.60 - 5.30) fills hollows near the mouth of Black Rock Creek and at the Basin on Plum Island. The largest mud flat in the estuary is Joppa Flat, where sandy mud to mud (mean 4.10 - 5.80) and pollutants carried downstream by the Merrimack River have accumulated as a result of the hydraulic circulation pattern. These sediments are poorly sorted to very poorly sorted (1.70 - 3.20), fine-skewed (.2 - .63), and leptokurtic (1.30 - 3.08).

Conditions are euxinic in the hollows and on much of Joppa Flat because of weak tidal currents, poor oxygenation, abundant organic material, chemical reduction, and abundant hydrogen sulphides. The sediment surface is generally light brown to gray due to weak oxidation, but sediments are universally black at depth. Dominant sedimentary structures include worm burrows on parts of Joppa Flat and hydrogen sulphide cells in sandier areas. The accumulation of sediment and pollutant material on Joppa Flat has contributed to the

recent shoaling of the channel south of Woodbridge Island and rapid accretion of the Spartina alterniflora marsh.

Secondary tidal channels

The two main types of secondary channels in the Merrimack River estuary are major tidal channels and minor tidal channels. The major channels, which are hydraulically significant to estuarine circulation, include the Plum Island River and Black Rock Creek (Fig. 1). All of the other tidal channels are classified as minor. Sediment type, mean grain size, sorting, and graphical skewness are variable in these environments, while most sediments are leptokurtic.

Major tidal channels. Major tidal channels have a significant influence on the hydraulic circulation pattern of the estuary. Major elements of this environment include the channel bottom, sand bodies (such as point bars), and intertidal flats.

The largest major tidal channel is the Plum Island River, which connects the Merrimack River with the Parker River estuary to the south. Although there is considerable hydraulic exchange between the two estuaries (Fig. 17), numerous point-bar complexes with large trailing ebb spits and poorly developed flood slip faces suggest that ebb-tidal currents are more dominant. The channel bottom is uniformly shallow (Fig. 49), consisting of slightly gravelly sand (mean 0.8 ϕ - 1.75 ϕ), except near the Plum Island River bridge where coarser gravelly

Figure 49. Relationship between bottom topography and sediment mean grain size along the main channel of the Plum Island River. Topography reconstructed from fathometer profiles made on October 12, 1968 and from coastal chart 213, U.S. Coast and Geodetic Survey.

BOTTOM TOPOGRAPHY AND MEAN GRAIN SIZE

MAIN CHANNEL — PLUM ISLAND RIVER

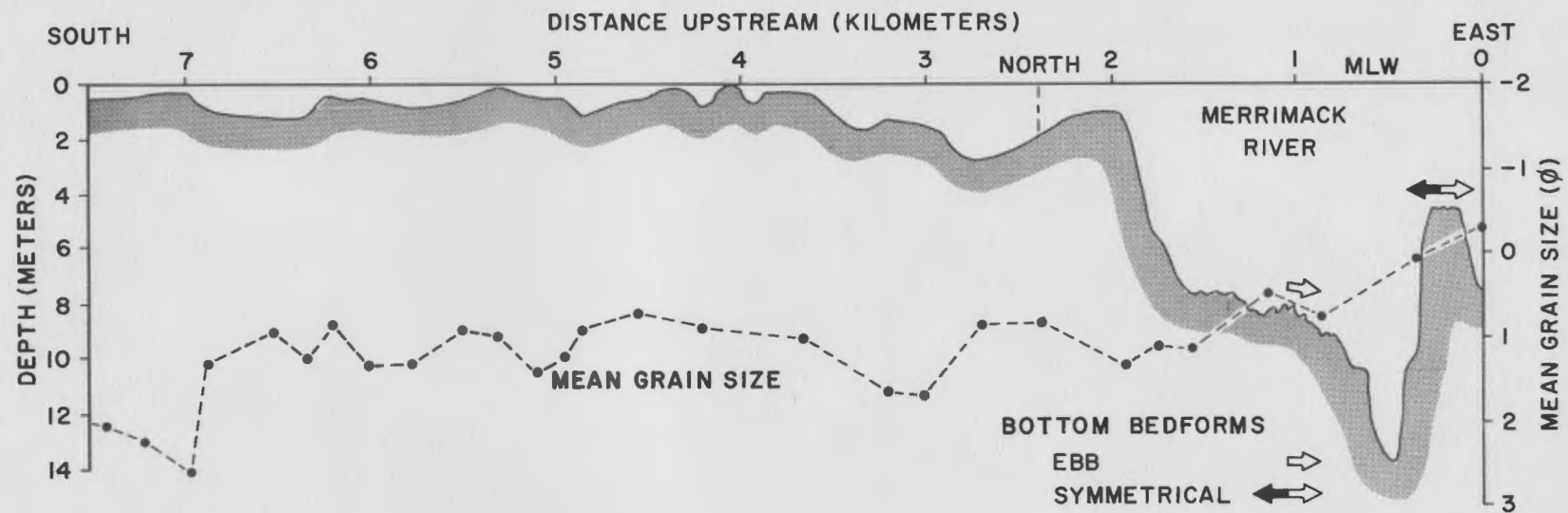


Figure 49

sand (mean 0.060 - 0.970), which underlies the marsh, is exposed in the tidal channel. Muddy sand (mean 2.00 - 2.60) is apparently being transported north out of the Parker River. Most of the sediment in the Plum Island River is sand from the gray feldspathic suite with little yellow-orange feldspar. Sediments are moderately sorted to poorly sorted (.40 - 1.80), generally near-symmetrical to coarse-skewed (+.1 to -.27) with some fine-skewed zones (.12 - .58), and mesokurtic to leptokurtic (1.11 - 2.67). Narrow, intertidal clam- and-worm flats composed of muddy sand border most of the channel. The absence of large mud flats suggests that the river is hydraulically active across its entire width.

Characteristic sedimentary structures in the Plum Island River include crossbedding, clam and worm burrows, mottling, hydrogen sulphide cells, and laminations of sand and mud. In places the laminae have been disrupted by vertical clam burrows (Figs. 43A and 43C). Thinner laminations (Fig. 50), resembling the rhythmites described by Reineck (1967) in the Weser and Elbe estuaries, Germany, are found on many of the flats bordering tidal channels. Origin of these laminations is uncertain, but they appear to be related to rhythmic sand transport from channel bottoms onto the flats during normal tidal flooding or during storms.

Because of the abundant sand supply, intertidal point bars are numerous in the Plum Island River. A plane-table map of a typical point bar located east of Woodbridge Island (Fig. 51) reveals that

- Figure 50. Rhythmite structures developed in an intertidal mud flat located near the southern end of the Plum Island River. These layers, or "rhythmites" (Reineck, 1967), appear to be due to rhythmic sand transport from channel bottoms onto the flats during normal tidal flooding or storm periods.
- A. Photograph showing distinctive sand layers.
 - B. X-ray radiograph of the same sample. Note the detail of the thin sandy layers.

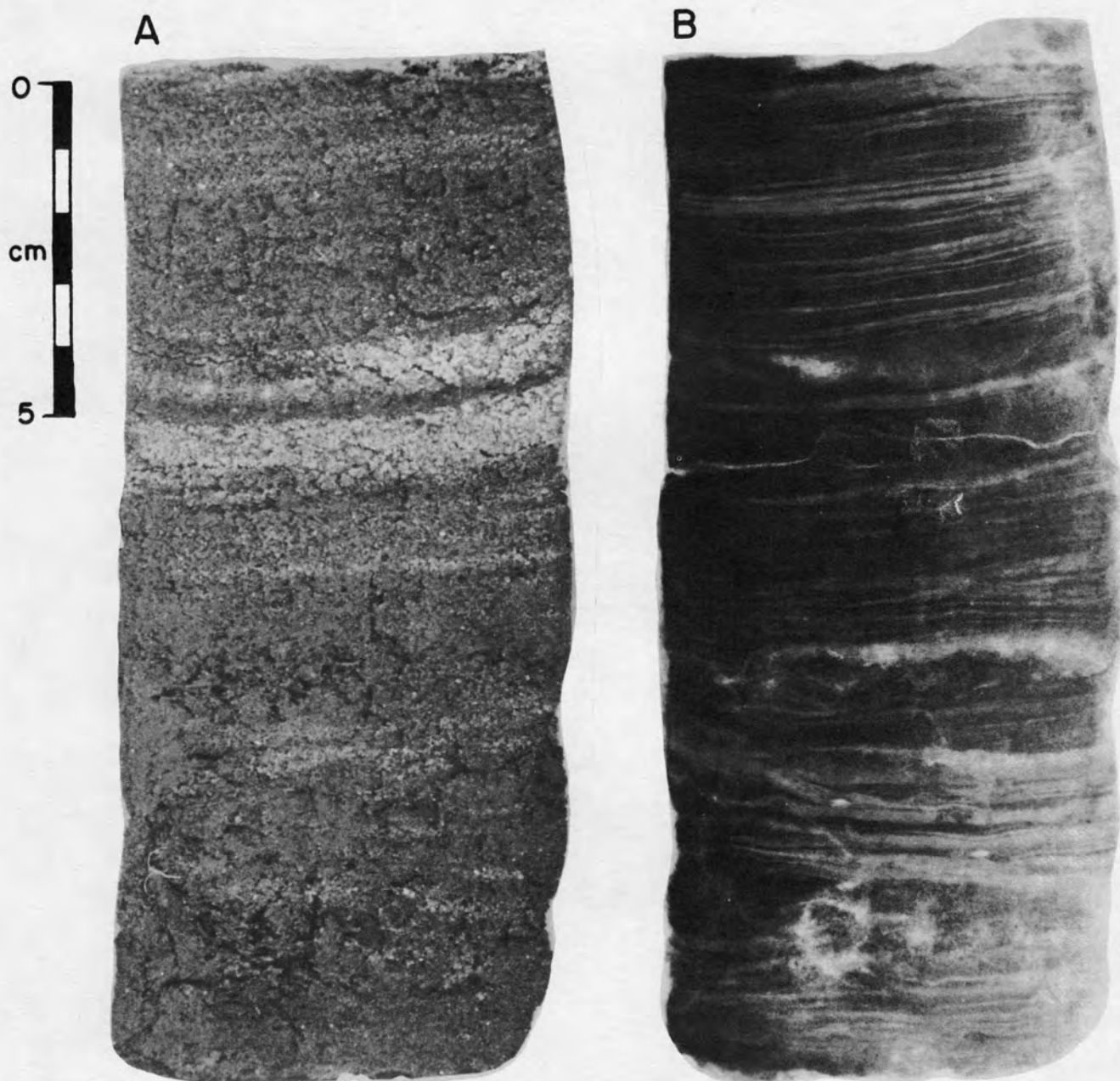


Figure 50

Figure 51. Plane-table map of point bar on eastern edge of Woodbridge Island, Plum Island River, at low tide (July 15, 1968). Datum is mean high water; contour interval 0.25 m. Dashed arrows near northern end of spit show azimuths of the ebb-oriented scour-megaripples shown in Figure 52. Solid curving arrows near base of spit show surface lineation patterns formed by ebb currents (lineation shown in Fig. 53).

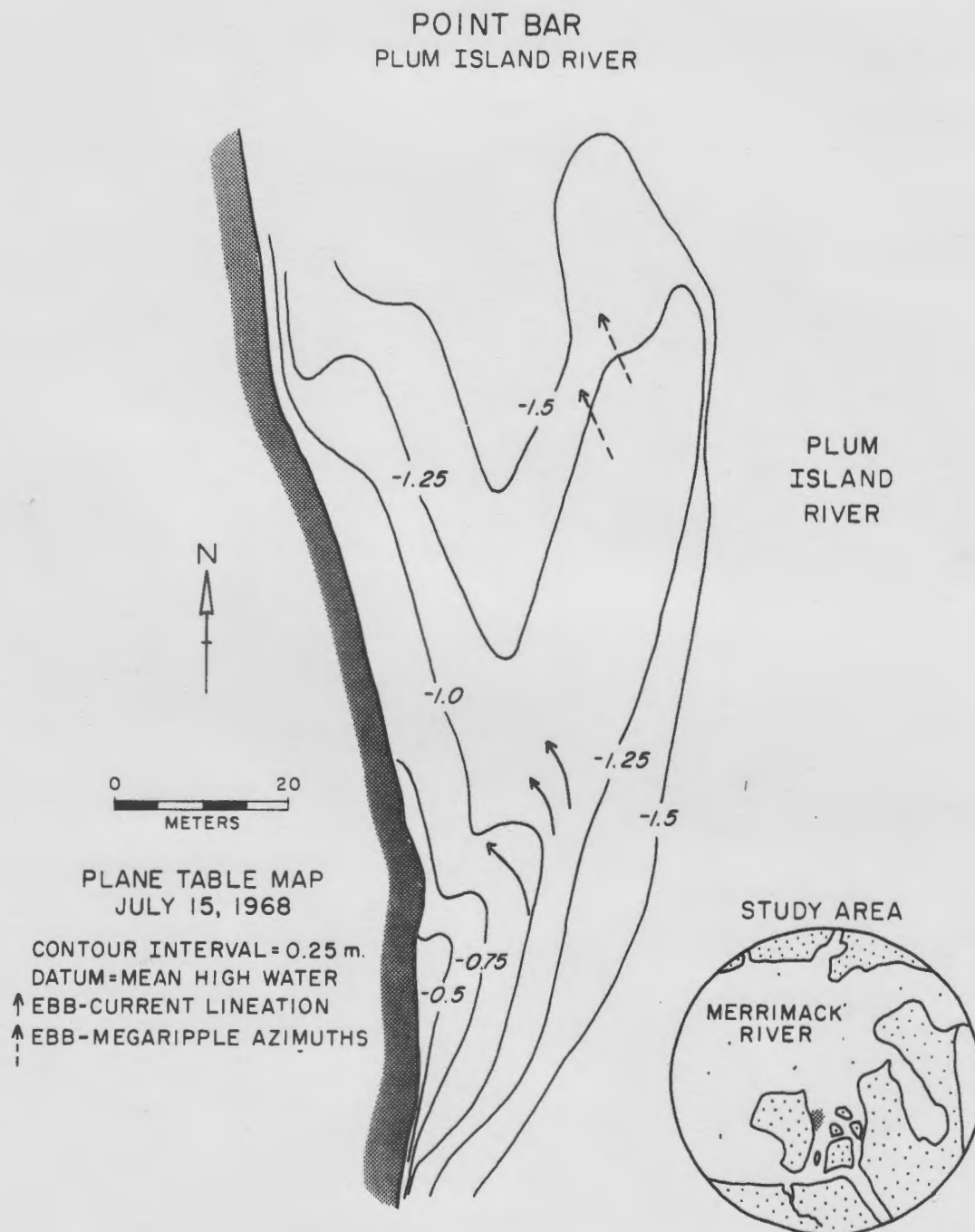


Figure 51

the dominant feature is a large northerly trailing ebb spit, which protects a muddy to sandy clam flat on the western side of the spit. During flood tide, currents funnel south across the clam flat and plane off the top of the ebb spit, building a southeasterly migrating slip face which deposits low-angle crossbeds. In general, flood currents do not appear to be as strong as ebb currents across this point bar. As the tide level drops, ebb currents sweep across the crest of the spit, forming upper-flow-regime planar beds in sheet flow across the leading edge of the spit. Behind the spit crest, scour-megaripples form as a result of a decrease in current velocity with increasing water depth (Fig. 52). Pronounced current lineation develops on top of the spit (Fig. 53). This lineation shows a drastic change in orientation from parallel with the trend of the spit on the up-channel margin to almost perpendicular to the spit on the west (Fig. 51). This change in orientation is due to early drainage of the clam flat as the tide level drops, while water tends to pond to the southeast behind the spit. Thus water flowing across the spit will take the shortest distance to the lower level clam flat behind, producing the perpendicular trend in lineation. Other sedimentary structures include worm burrows and clam burrows on the clam flat and herringbone crossbeds on the spit.

A similar point bar located about 1 km further south along the Plum Island River channel shows greater flood influence. This bar also is dominated by a large ebb spit oriented toward the northwest. At low tide two current lineations (S. 38° W. and S. 58° W.)

Figure 52. Low-tide photograph of ebb-oriented scour-megaripples on the spit of the point bar shown in Figure 51. View looking south-southeast up the main trend of the bar toward Woodbridge Island.

Figure 53. Low-tide photograph showing ebb-current lineations developed on the surface of the point bar shown in Figure 51. Note orientation of shells and current shadows behind coarse fragments. Current was flowing from bottom to top of photograph. Pencil for scale.



Figure 52



Figure 53

representative of different stages of draining were observed on the clam flat which forms the western portion of the point bar. Sedimentary structures include clam burrows and worm burrows on the flat, low-angle (5° - 8°) crossbeds on the ebb spit and higher angle planar crossbedding (10° - 15°) on the flood slip face. Coarsest sediments are found on the spit where tidal currents have winnowed out the finer material. Muddy sand has accumulated on the clam flat behind the spit. The sand is from the gray feldspathic suite with a small amount of yellow-orange feldspar. The geographic distribution of this sediment suite suggests derivation from a local deposit of glaciofluvial material that underlies the marsh south of the highway to Plum Island.

The Basin, located at the north end of Plum Island, is a large embayment where the mouth of the Merrimack was located during the early 1800's (note coastline changes on Plum Island since 1827, Fig. 62). The deep channel was dredged in 1962 but has shoaled rapidly during recent years. Sediments in the channel and on the intertidal flats are muddy sand (mean -0.3ϕ to 1.9ϕ , Fig. 19) of the yellow-orange feldspathic suite. Sand in the northeastern portion is well sorted ($.76\phi$), coarse-skewed ($-.17$), and leptokurtic (1.17 - 2.03), while that in the southwest section, where mud has accumulated, is poorly sorted (2.0ϕ - 2.3ϕ), fine-skewed ($.22$ - $.65$), and platykurtic (0.71 - 0.80). Common sedimentary structures include burrows, mottles, hydrogen sulphide cells, and zones where chemical reduction is apparently strong enough to lighten the color of some of the yellow-orange feldspar grains.

The other major secondary tidal channel is Black Rock Creek, located along the western side of the Salisbury Beach. Because this channel has little fresh-water discharge, it merely fills and drains with each tidal cycle. Nevertheless it influences the current velocities and hydrography of the lower estuary during ebb tide (note its effect on temperature and salinity at anchor station 167, Fig. 12). Tidal-current velocities are too weak to build point bars or bottom bedforms, even though abundant sand is present.

Sediments are generally muddy sand (mean 2.5ϕ - 3.9ϕ) with some mud accumulations (mean 4.8ϕ - 5.3ϕ) and include one zone of medium sand (mean 1.2ϕ) from a storm washover fan. The sand is from the gray feldspathic suite with an estimated mineralogy of 81 percent quartz, 9 percent gray feldspar, 3 percent yellow-orange feldspar, 6 percent rock fragments, and a trace of mica. Sediment is poorly sorted to very poorly sorted (1.5ϕ - 2.6ϕ) near-symmetrical to fine-skewed (-.04 to .43) and leptokurtic (1.22 - 3.35). Common sedimentary structures include mud and sand laminations, clam and worm burrows, mottles, and hydrogen sulphide cells with active chemical reduction. At several locations buried clam flats with large Mya arenaria shells in life position are present. During spring low tides, most of the channel bottom is drained.

Minor tidal channels. Minor tidal channels drain the marshes of the entire estuary (Fig. 2). The larger ones generally have muddy sloping

sides and intertidal flats, but in places are steep-sided with deep channels. Smaller ones are muddier and go dry at low tide. Sediment grain-size parameters are variable. Channels near the Plum Island River are of muddy sand (mean 1.08ϕ - 2.03ϕ) with a few scattered mud accumulations (mean 4.04ϕ). Sediment is poorly sorted to very poorly sorted (1.13ϕ - 3.10ϕ), near-symmetrical to fine-skewed ($-.02$ to $.57$), and leptokurtic (1.15 - 2.67). Sediments in the tidal channels of Salisbury Marsh and Town Creek Marsh are muddy sand to mud (mean 1.59ϕ - 5.72ϕ), poorly sorted to very poorly sorted (1.21ϕ - 2.33ϕ), fine-skewed ($.17$ - $.62$), and leptokurtic (1.21 - 2.33). Common sedimentary structures include small worm burrows, laminations, and rhythmites.

Salt marsh

The marshes, which constitute the third major sedimentary environment in the Merrimack River estuary, are composed of an intertidal zone occupied by Spartina alterniflora and a supratidal zone characterized by S. patens, Juncus gerardi, and Distichlis spicata. Recent work by McIntire and Morgan (1963) and McCormick (1968) has revealed many details of the marsh morphology, Holocene stratigraphy, and sea-level changes in the marshes south of the bridge to Plum Island, but until now little work had been done on the Merrimack marshes.

Using an aluminum rod 3.3 m long, the marshes were probed at 458 locations to determine peat thickness and to locate potential coring sites. A total of 17 cores, 5 cm in diameter and averaging 2.5 m in length, were obtained with a piston coring rig similar to that used by McCormick (1968).

The cores were sliced, described, photographed, and x-rayed in the laboratory. The cores reveal a general stratigraphic sequence from top to bottom of: (1) living high salt marsh dominated by S. patens, (2) high salt-marsh peat, (3) sandy to muddy low salt-marsh peat with abundant roots of S. alterniflora, (4) gray, silty to sandy intertidal facies believed to be analogous to the clam-flat and tidal-channel sediments in the present estuary, and (5) black peat composed of fresh- to brackish-water plant material.

The Holocene stratigraphy of the Merrimack marshes (details of core lithology are shown in Figs. 54 and 55 and core locations in Figs. 56 and 57) is similar to that observed by McCormick (1968) in the Parker River marshes. Almost everywhere the marsh is topped by a zone of living high salt marsh dominated by S. patens. This layer is generally underlain by a thick deposit of high salt-marsh peat which grades into a sandy to muddy low salt-marsh peat with abundant roots of S. alterniflora. Many of the cores bottomed in a gray, silty to sandy intertidal facies believed to be analogous to the clam-flat and tidal-channel environments in the present estuary. Cores H, I, O, and P (Figs. 54 and 55) all had layers of dark-brown to black peat believed to be deposited by fresh- to brackish-water plants. This peat is analogous to that found under the Parker River marshes (McCormick, 1968) and in many of the New England marshes (Bloom, 1964; Davis, 1910; Johnson, 1925; McIntire and Morgan, 1963; and Redfield and Rubin, 1962). All workers agree that this peat represents an accumulation of fresh- to brackish-water sedge-type plants,

Figure 54. Lithology of marsh cores A to I. Locations for these cores are shown in Figures 56 and 57.

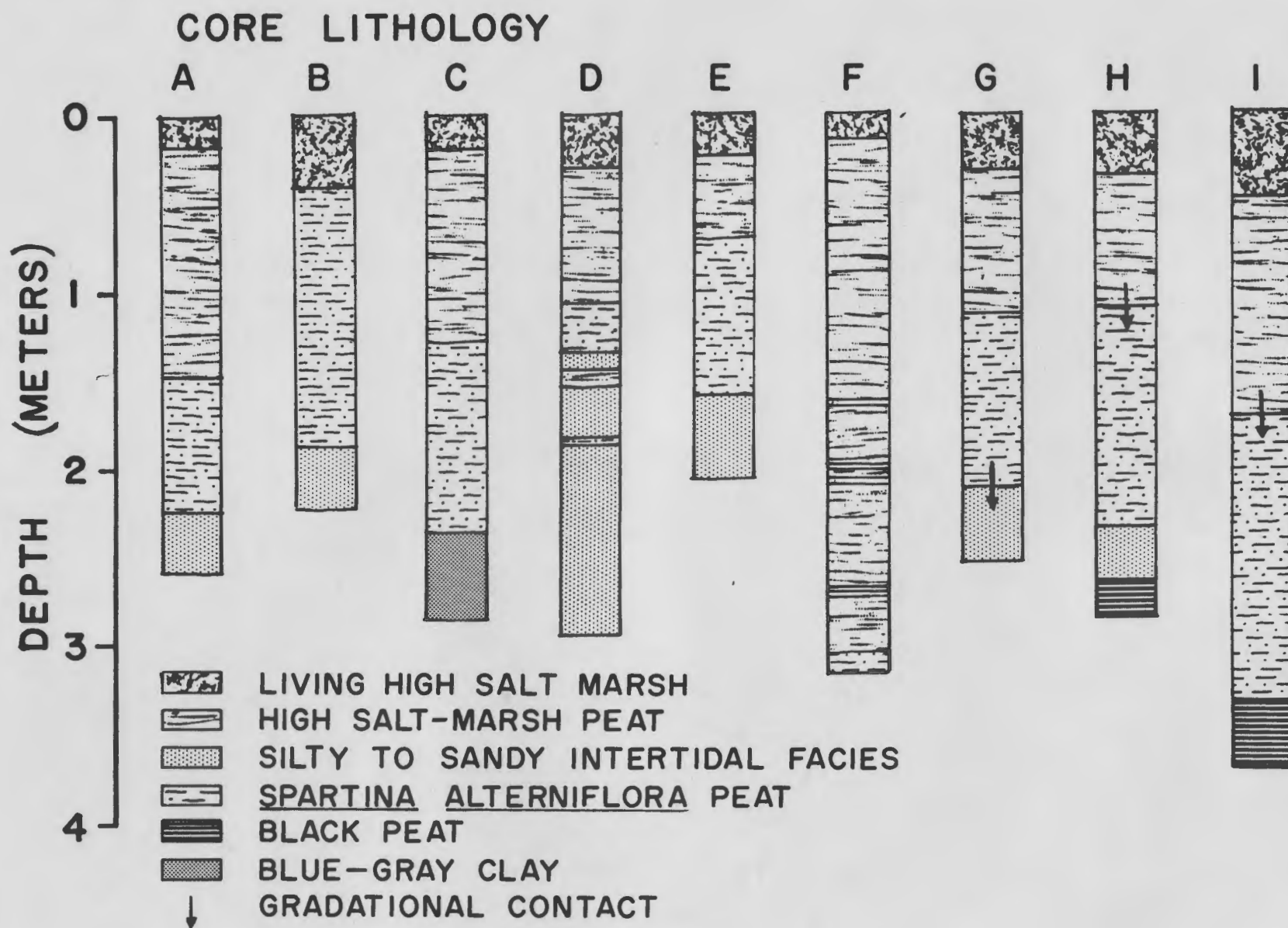


Figure 54

Figure 55. Lithology of marsh cores J to Q. Locations for these cores are shown in Figures 56 and 57.

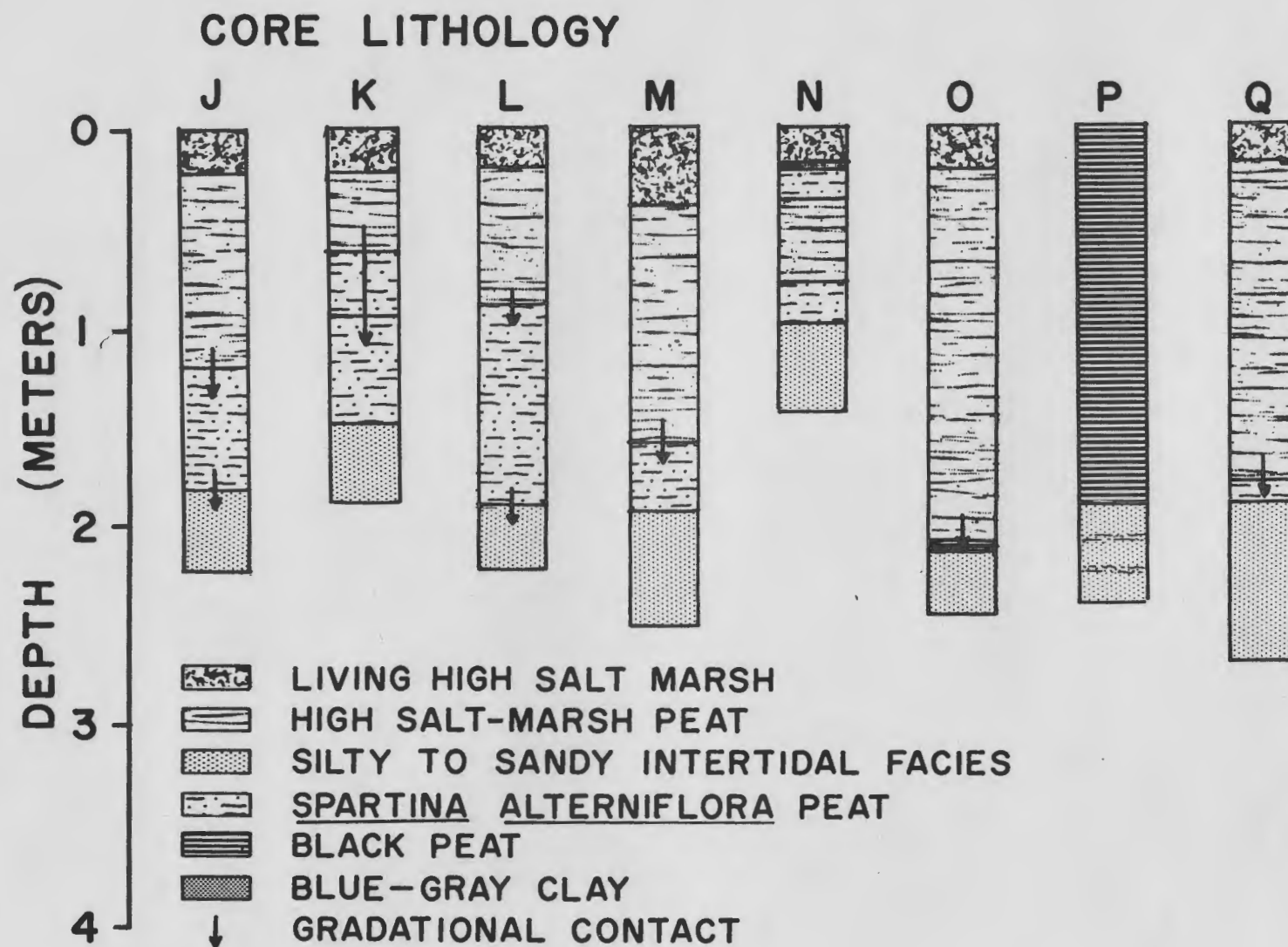


Figure 55

deposited in the zone of transition from salt marsh to normal highland vegetation or at very near mean high-water level. The base of core C consisted of 50 cm of blue-gray clay believed to be tidal-channel sediment. McIntire and Morgan (1963) and McCormick (1968) found late Pleistocene glaciomarine blue clay below the Parker River marshes; because of limited coring capability, the author was unable to confirm its presence in the Merrimack.

Details of the geometry of the marsh deposits are revealed in peat isopach maps (Figs. 56 and 57) and in stratigraphic cross sections (Figs. 58 and 59). In Salisbury Marsh (Fig. 56), a belt of peat 3-4 m thick extends from the northeast across most of the marsh, nearly parallel to a series of bedrock pinnacles in the northwest. Cores H and I bottom in black peat of the fringing fresh- to brackish-water marsh facies while most of the other cores bottom in the silty to sandy intertidal facies (Figs. 54 and 55). Core H reveals the general transgressive Holocene stratigraphy of black peat overlain by the intertidal facies and the S. alterniflora to S. patens marsh sequence. The presence of the silty to sandy intertidal facies under most of the S. alterniflora peat suggests that the latter did not develop until the sand- and mud-flats of the former open bay environment built up to approximately midtide level. This interpretation is in agreement with Bloom (1968) for the marshes of Connecticut.

A similar stratigraphic sequence is evident in the Plum Island River marsh (Figs. 57 and 59). The thickest peat is west of Plum Island. At

Figure 56. Peat isopach map of Salisbury marsh. Based on data from 215 probe rod stations and stratigraphy of nine cross sections (Figs. 58 and 59) shown with heavy black lines. Note bedrock pinnacles in the northwestern portion. The thickest peat (3-4 m) extends from northeast to southwest, well inland of present estuary shore.

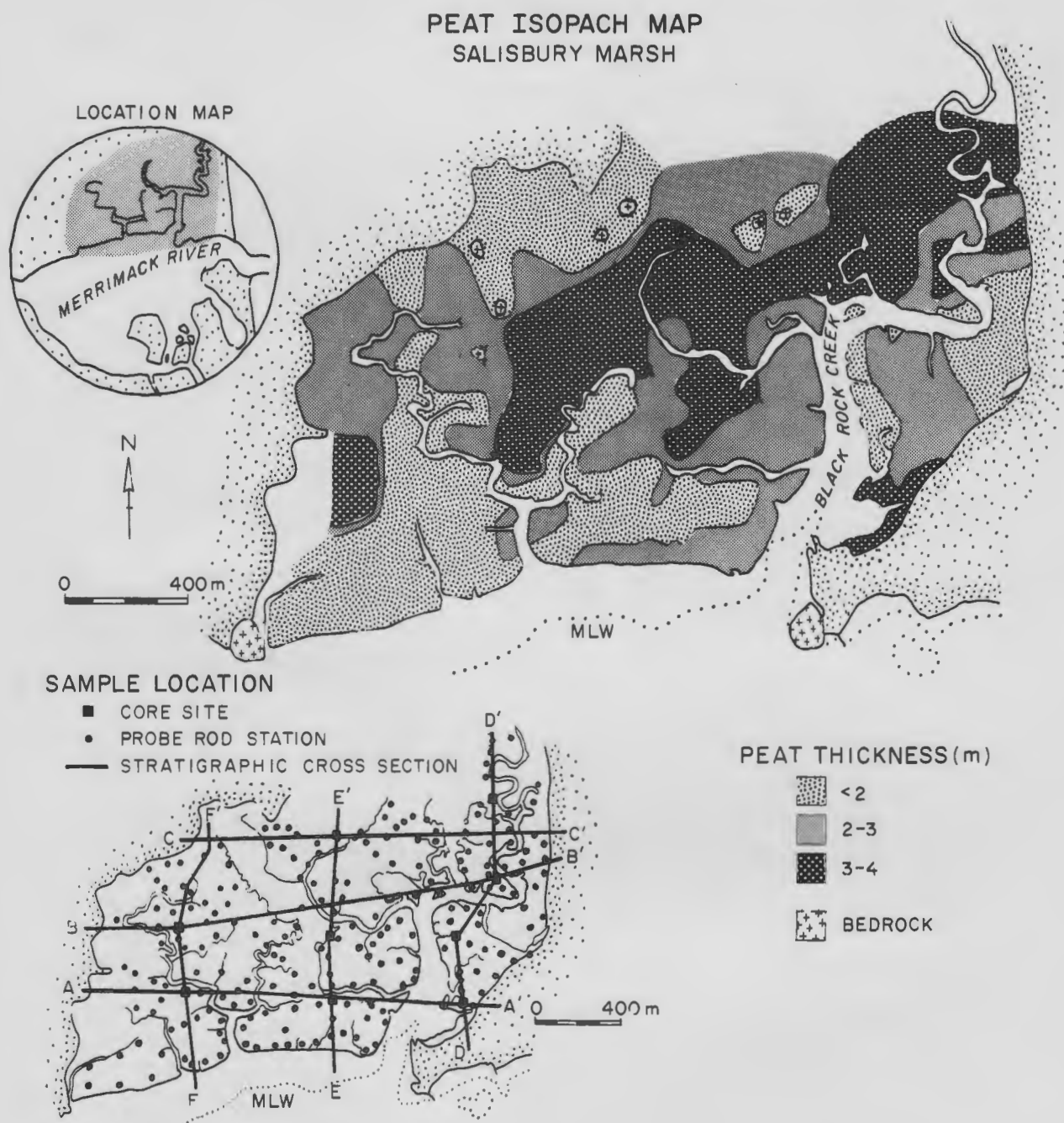


Figure 56

Figure 57. Peat isopach map of Plum Island River marsh. Based on data from 189 probe rod stations and stratigraphy of six cores. Locations of stratigraphic cross sections (Fig. 59) shown with heavy black lines. Note shallow sand body under northern end of Woodbridge Island.

PEAT ISOPACH MAP PLUM ISLAND RIVER MARSH

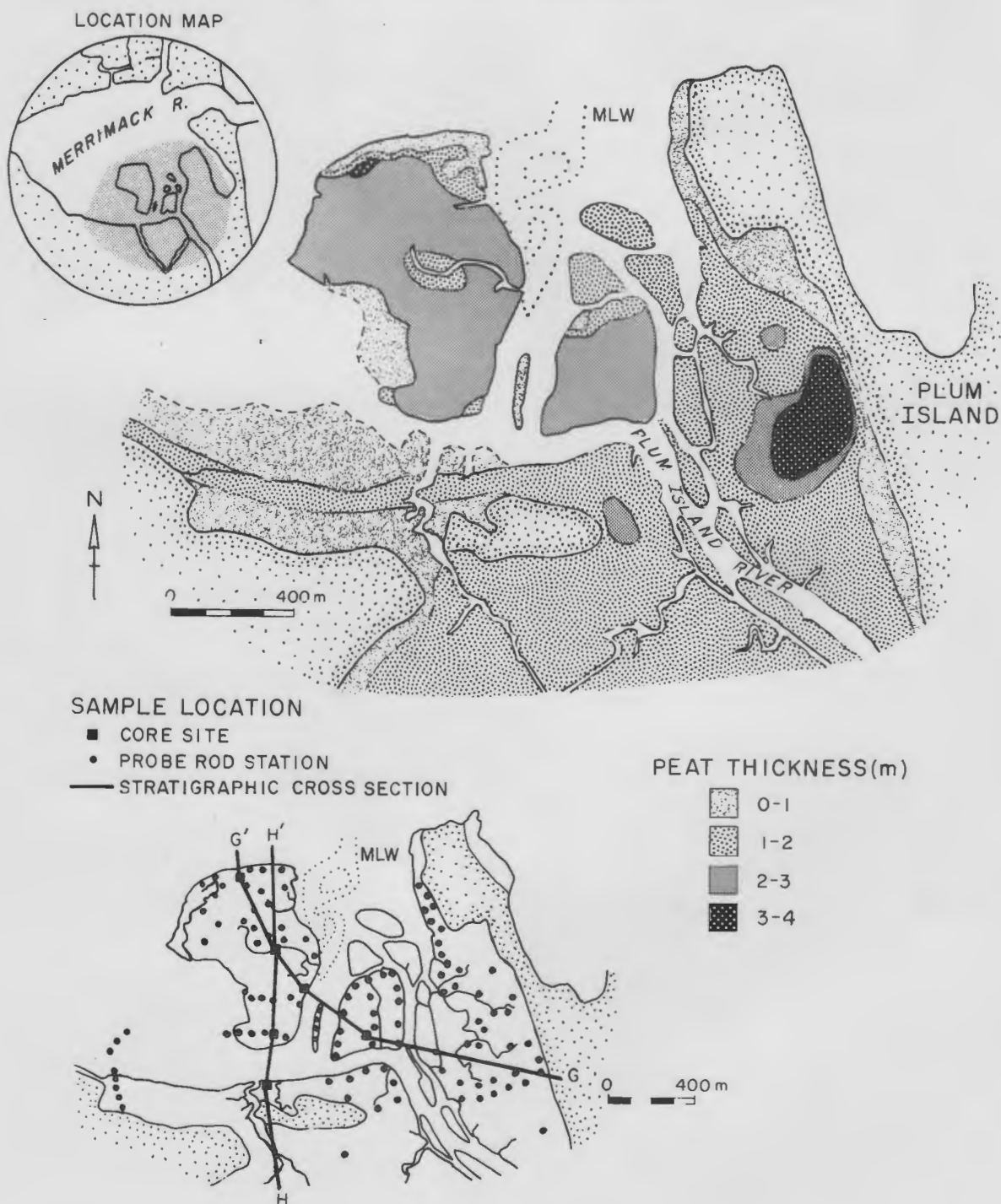


Figure 57

the south end of Woodbridge Island high salt-marsh peat is absent, reflecting rapid infilling of the existing channel. The north end of the island is underlain by an elongate, curving sand body (Fig. 57) composed of reworked glaciofluvial sediment similar to that found under the marshes south of the Plum Island highway. Angular cobbles were unearthed in several holes, and probe-rod data suggest a possible bedrock pinnacle at depth. Origin of this sand mass is still uncertain, but three possibilities have been suggested: it may be an old flood tidal-delta complex built when the river mouth was further south than at present, a deposit of glaciofluvial material which was reworked into a curved-spit complex by wave action as sea level rose, or artificial fill placed there to prevent erosion of the marsh.

The cores from Town Creek marsh reveal a slightly different stratigraphy. Much of the marsh is underlain by a peat section more than 3 m thick, but this material is largely fresh- to brackish-water peat (Core P; Fig. 55). Salty water rarely reaches this marsh and only along the Merrimack channel is *S. alterniflora* abundant. These marshes are in an early stage of marine transgression.

X-ray radiographs of the Merrimack cores reveal numerous laminations that may be partially due to the process of ice-rafting. During extended periods of subfreezing temperatures, the surface of the estuary freezes at high tide. During ebb, blocks of ice settle onto the mud flats, and layers of mud freeze to their bottoms. As the tide floods again, the blocks float off, carrying a coating of mud. If this process is repeated numerous times, the blocks become

Figure 58. Stratigraphic cross sections of the Salisbury marsh (for locations see Fig. 56). Note general thinness of the marsh peat and scattered bedrock pinnacles.

STRATIGRAPHIC CROSS SECTIONS

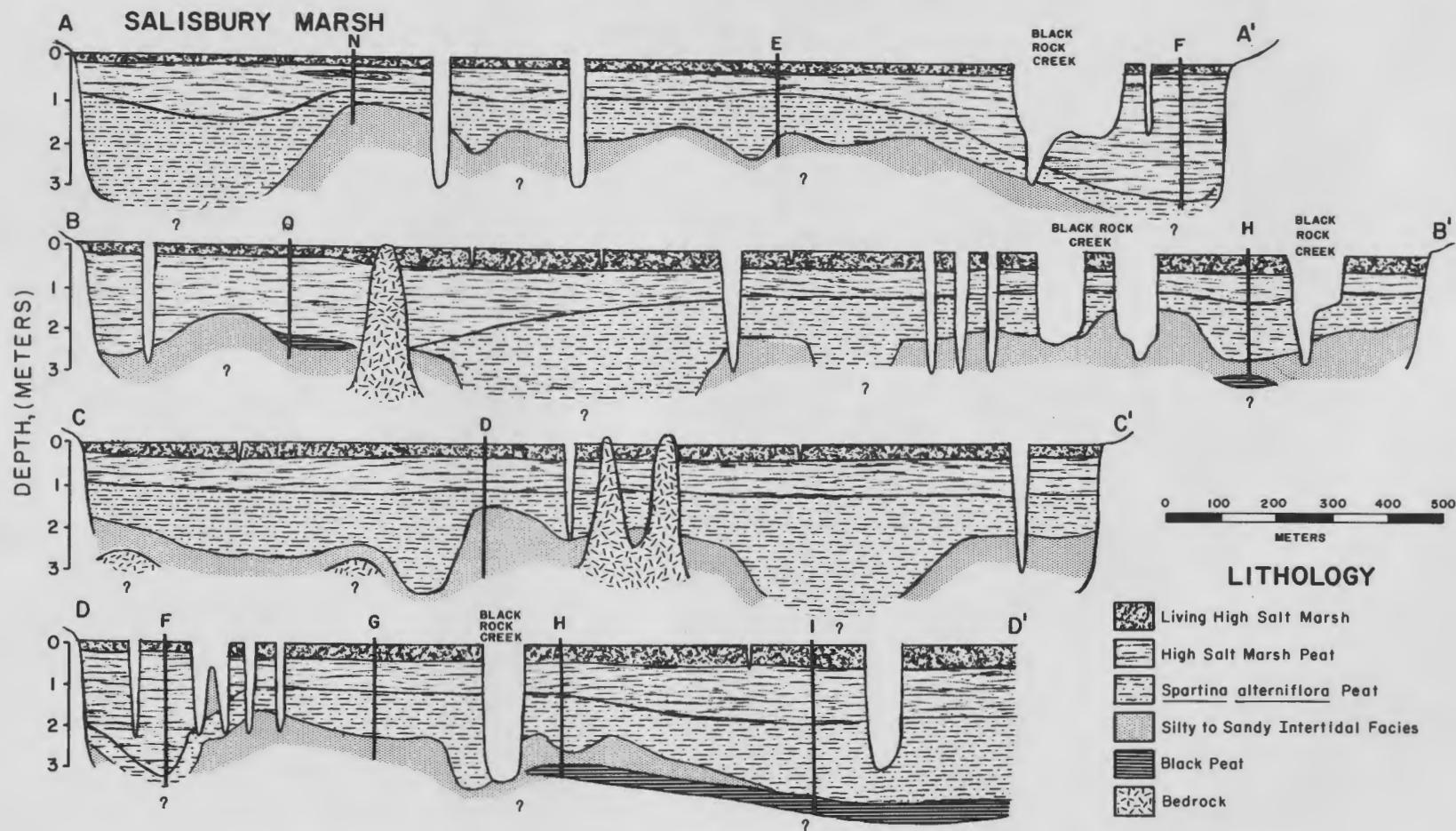


Figure 58

Figure 59. Stratigraphic cross sections of the Salisbury marsh (Fig. 56) and the Plum Island River marsh (Fig. 57). Thick black peat layer in Core C was probably deposited by fresh- to brackish-water plants at an early stage of marsh development.

STRATIGRAPHIC CROSS SECTIONS

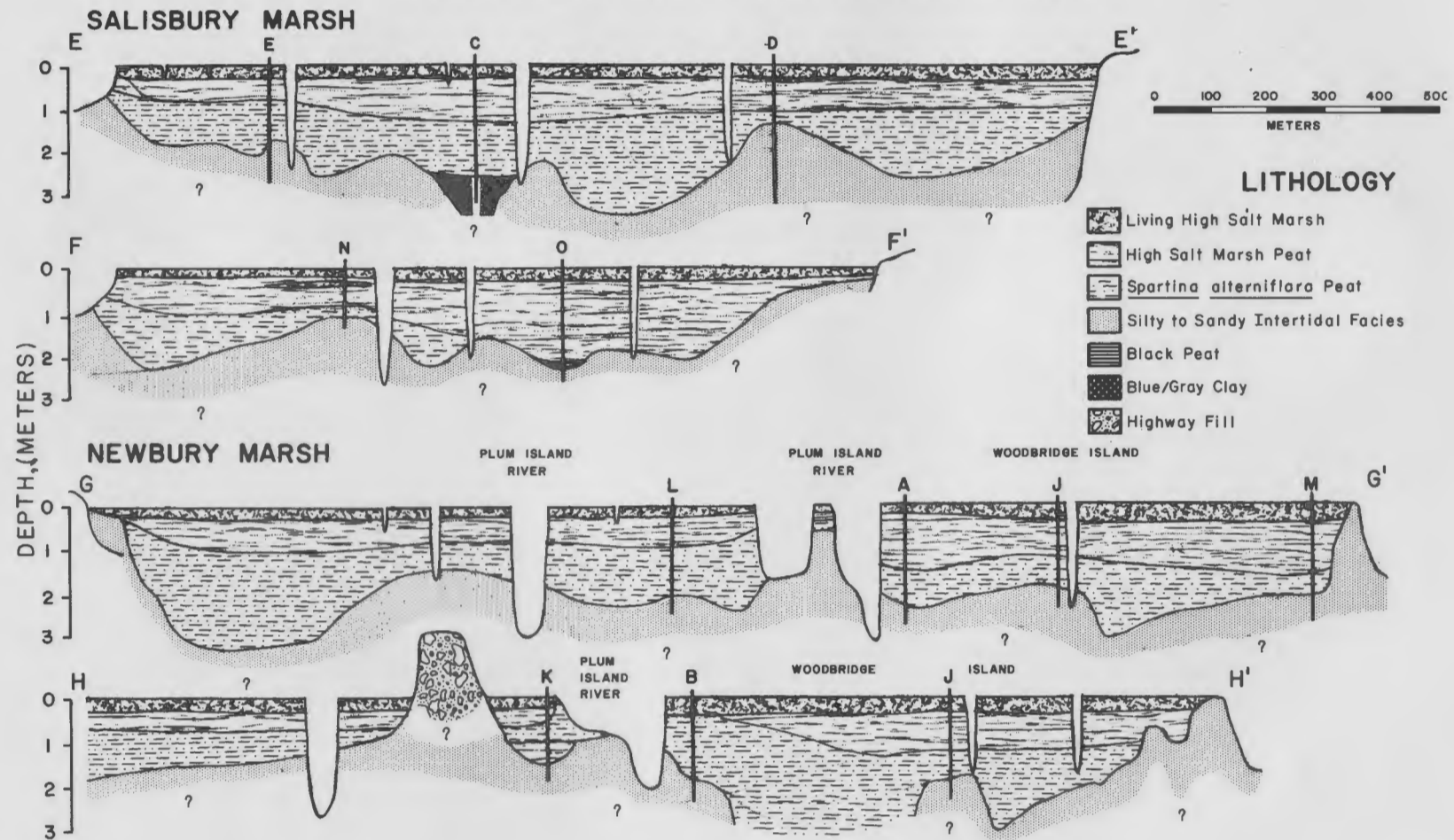


Figure 59

laminated with sediment (Fig. 60). During storm surges and exceptionally high spring tides, these ice blocks are transported out of the channels onto the marsh where many are stranded. When the blocks melt, a mud layer as much as 5 - 8 cm thick may be deposited. This mechanism is responsible for transport of muddy sediment, including shells of Mya arenaria and other infauna (Fig. 61), onto the marsh where it is later spread out by rainwater to form these observed laminations.

Figure 60. Blocks of ice carried out of the main channel of the Plum Island River during a spring tide (March 9, 1968). Note dark laminations of mud in the ice. Shovel for scale.

Figure 61. Close-up photograph of ice-rafted sediment deposited on marsh surface by melted ice block. Photograph taken March 9, 1968. Note Mya arenaria shells. Pocket knife for scale.



Figure 60



Figure 61

RECENT GEOLOGIC HISTORY OF THE MERRIMACK RIVER ESTUARY

The observed stratigraphy of the marshes is evidence of a gradual marine transgression and rising sea level since about 6300 B.P. (McIntire and Morgan, 1963). According to McIntire and Morgan, the blue clay was deposited during later Pleistocene time in an estuarine area at or near sea level. By 10,500 B.P., the ice had retreated and the land was rebounding more rapidly than sea level was rising. About 7500 B.P., the land reached its maximum uplift while sea level reached maximum regression. By 6300 B.P. the land began to subside and the sea started transgressing over the glaciomarine blue clay. Apparently the black peat was deposited as a time-transgressive unit in response to this relative sea-level rise. At about 3000 years B.P. a marked decrease in the rate of sea-level rise occurred along much of the New England coast (McIntire and Morgan, 1963; Bloom and Stuiver, 1963). Since then sea level appears to have reached stillstand while crustal downwarping in the Plum Island area continues at a rate of about 9.1 cm per century (McIntire and Morgan, 1963).

As early as 6000 B.P. an offshore barrier island was present in the vicinity of Plum Island. Fine-grained sediment accumulated behind the island in an open bay environment with a fringing fresh- to brackish-water marsh along the landward margin. With the gradual marine transgression, the gray, silty to sand intertidal facies overlapped the fringing black peat, but sedimentation was unable to keep pace with submergence. At approximately 3000 B.P. the rate of sea-level rise changed

so that the marsh sediments encroached over the open bay deposits. This accreting marsh sequence consists of S. alterniflora peat at the base and S. patens peat at the top. This interpretation is in agreement with that of Bloom (1968) for the marshes of Connecticut, Redfield (1965) for the Barnstable, Massachusetts, marsh, and McCormick (1968) for the marshes of the Parker River estuary.

During historic times, marked shoreline changes have occurred at the north end of Plum Island (Fig. 62). In 1827 the island was not forked, but in the next 24 years extensive changes occurred. The northeastern end retrograded almost 800 m southward and the mouth of the Merrimack occupied the area where the Basin is now. Storms and longshore currents then started to build a spit to enclose the Basin and the river mouth migrated northward. By 1851 the spit was almost 2 km long. From 1851 to 1880 the spit continued to prograde northward while Salisbury Beach retrograded. In the early 1880's the channel mouth was stabilized at the present location by means of two breakwaters. They were progressively lengthened until their present dimensions were attained (the north jetty in 1914 and the south jetty in 1906). Since then only minor shoreline changes have occurred. In view of these changes which occurred in 150 years, it is quite possible that the river mouth was once much farther south and that at that time the sand mass which now underlies the northern end of Woodbridge Island (Fig. 57) was a flood tidal-delta complex.

Much of Newburyport's early fame as a seaport was due to the fine harbor provided by the Merrimack River (Currier, 1906). Shoaling at the river mouth has been a persistent problem and is largely responsible for

Figure 62. Changes in the shoreline of the northern end of Plum Island and the southern end of Salisbury Beach from 1827 to 1940 (from Chute and Nichols, 1941, Pl. 3).

PLUM ISLAND-SALISBURY BEACH
SHORE LINE CHANGES
(At Mean High Tide)

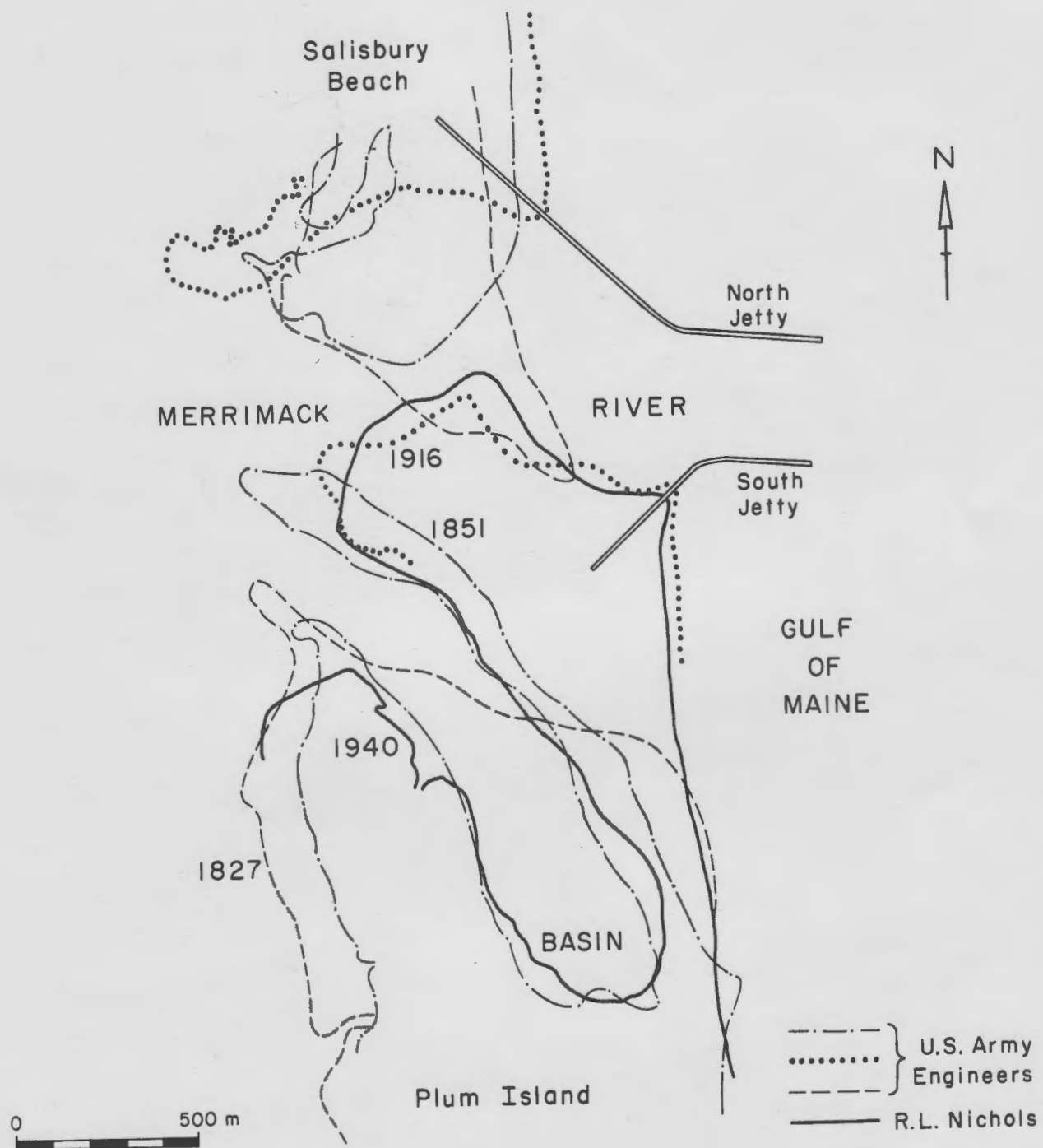


Figure 62

the decline in maritime activity in the area. A novel scheme by Col. John Anderson, topographical engineer for the U.S. Army Corps of Engineers, recommended construction of dikes across the Basin and the Plum Island River between Plum Island and Woodbridge Island and a break-water on the northwestern margin of Woodbridge Island. The structures were built in 1829-1831 in hopes of raising the current velocities at the mouth sufficiently to minimize shoaling. Unfortunately, the desired results were not achieved and periodic dredging has been necessary to keep the channel open.

SUMMARY AND CONCLUSIONS

The Merrimack River estuary is composed of three major sedimentary environments (Fig. 2). The main channel, which dominates the study area, consists of a subtidal channel, a flood-tidal delta near the estuary mouth, and extensive intertidal flats occupied by worms, clams, and mussels. A series of secondary tidal channels, including major channels such as the Plum Island River and Black Rock Creek and numerous minor tidal channels, drain the more than 16.9 km^2 of salt marsh in the Merrimack watershed.

The distribution of sediments in these sedimentary environments is closely related to the hydrographic circulation pattern, tidal-current velocities, bottom topography, and sediment source areas. During flood tides, salt water from the ocean is deflected to the north, or right side of the main channel, while fresh river water ponds up to the south across Joppa Flat causing marked horizontal stratification (Fig. 5). The salty ocean water carries small amounts of suspended sediment (up to 3-4 mg/l), while the fresh Merrimack water has a heavy load of fine-grained sediments and pollutant material (values up to 19 mg/l were observed but concentrations probably are much greater during spring runoff), much of which is deposited on Joppa Flat during high tide. During periods of below-normal discharge (less than about 3000 cfs), the stratification disappears and the estuary becomes partially mixed.

Because of the pronounced current-velocity asymmetry in the estuary (Fig. 15), there is a much longer period of low current velocities around

high tide than around low tide. Peak flood velocities, which occur 3 to 4 hours after low water and are concentrated near the bottom of the water column, scour the subtidal channel, winnowing out finer grained material and depositing it on the shoal intertidal flats. Maximum ebb velocities, which occur near the top of the water column, are nearly twice as strong as flood currents, but are not attained until 4 to 6 hours after high water when most of the intertidal areas are out of the water. Thus the effects of ebb currents are largely confined to the deeper channels. The current-velocity asymmetry is partly due to the residual ebb flow that must be overcome by flood currents during the rising tide.

Sediment types and textural parameters show excellent correlation with the sedimentary environments and the hydrographic circulation pattern of the estuary. Sediment in the main channel is gravelly to slightly gravelly sand, which is moderately sorted to well sorted, coarse-skewed to near-symmetrical, and mesokurtic. On the intertidal flats, where tidal currents are weaker, sediments are finer grained (muddy sand to mud), poorly sorted to very poorly sorted, fine-skewed, and leptokurtic. Textural parameters of sediments from the secondary tidal channels are somewhat variable due to differences in local source areas but the sediments are generally fine grained and poorly sorted.

The flood-tidal delta is a dynamic sediment body composed of well-sorted sand and gravelly sand (mean 1.1 ϕ to 2.5 ϕ) and covered by bedforms. The highest part of the tidal delta forms an ebb shield which protects flood-oriented sand waves along the northeastern margin from modification

by ebb currents. The bedforms are largest and show greatest migration rates during spring-tidal conditions when current velocities across the delta are above normal. When river discharge drops below about 3000 cfs, flood-tidal currents tend to dominate the entire delta complex.

Three types of sand are present in the Merrimack estuary. A yellow-orange feldspathic suite (modal size $0.5\phi - 1.0\phi$) occupies the main channel and is apparently being transported downstream, possibly from an upland glacial sediment source. The second type is a gray feldspathic suite (modal size $1.1\phi - 1.5\phi$) which underlies the marshes of the lower estuary and seems to be derived locally, possibly from erosion of the Newburyport Quartz Diorite. The third sand is finer grained (modal size $2.4\phi - 2.9\phi$) with subequal amounts of gray and yellow-orange feldspar. This sand is present in the central part of the main channel and in several tidal channels, but its origin is uncertain.

Characteristic sedimentary structures are found in each sedimentary environment of the estuary. Structures in the sediments on the bottom of the main subtidal channel include crude laminations of estuarine sediment overlying organic detritus which was probably deposited during above-normal discharge conditions, large-scale crossbedding developed in large channel bedforms, and small-scale crossbedding in ripples developed in zones of medium-grained sand. Crossbedding is well developed on the flood-tidal delta; large flood sand waves deposit high-angle beds (27° - 32°), while smaller sand waves on the ebb shield have low-angle beds (5° - 15°). Scour-megaripples on the ebb spit produce festoon crossbeds. The inter-

tidal flats in the main channel and in secondary tidal channels are characterized by burrows of worms and clams, black hydrogen sulphide cells, laminations, organic mottles, and buried clam flats with large Mya arenaria shells in life position. Buried shell slumps are present beneath the mussel banks in the lower estuary. Several of the small tidal channels have rhythmite structures of interbedded mud and sand. Some of the high salt-marsh peat deposits are laminated, possibly due to deposition of sediment on the marsh surface by ice-rafting during the winter. None of these sedimentary structures or organic deposits alone would be conclusive proof of an estuarine environment if this study area were to be preserved in the rock record; however, taken together, they probably would be excellent clues for reconstructing the paleogeography of the area and making paleoecological interpretations.

An offshore barrier island was present in the vicinity of Plum Island as early as 6000 B.P. Fine-grained sediment accumulated behind the island in an open bay environment with a fringing fresh- to brackish-water marsh. With rising sea level, these sand-flat and mud-flat sediments transgressed landward over a black peat layer deposited by fresh- to brackish-water plants. At about 3000 B.P. the rate of sea-level rise slowed down enough to allow the fringing S. alterniflora marsh to accrete seaward over the open bay sediments. Once the marshes grew above the intertidal zone, high salt marsh plants such as S. patens were able to establish themselves. As a result of this regression of marsh deposits, the original open bay environment was transformed into the present marsh system with tidal channels and islands.

REFERENCES CITED

- Bloom, A.L., 1964, Peat accumulation and compaction in a Connecticut coastal marsh: Jour. Sed. Petrology, v. 34, p. 599-603.
- _____, 1968, Postglacial stratigraphy and morphology of central Connecticut, p. A-1-1 - A-1-7, in Orville, P.M., Editor, Guidebook for field trips in Connecticut; New England Intercol. Conf., 60th Ann. Mtg., Oct. 1968, New Haven, Connecticut, 305 p.
- _____, and Stuiver, M., 1963, Submergence of the Connecticut coast; Science, v. 139, P. 332-334.
- Chute, N.E., 1964, Geology of the Norfolk Basin Carboniferous sedimentary rocks and the various igneous rocks of the Norwood and Blue Hills quadrangles, p. 91-114, in Skehan, J.W., Editor, Guidebook for New England Intercollegiate Geological Conference: New England Intercol. Geol. Conf., 56th Ann. Mtg., Oct. 1964, Chestnut Hill, Massachusetts, 120 p.
- _____, and Nichols, R.L., 1941, Geology of northeastern Massachusetts: Mass. Dept. Public Works and U.S. Geol. Survey Cooperative Geology Project, Bull. 7, 48 p.
- Clapp, C.H., 1921, Geology of the igneous rocks of Essex county, Mass.: U.S. Geol. Survey Bull. 704, 132 p.
- Coastal Research Group, Univ. of Mass., 1969, Coastal environments, N.E. Massachusetts and New Hampshire, Field Trip Guidebook: Eastern Section of Soc. of Econ. Paleo. and Min., Field Trip, May, 1969, 462 p.
- Commonwealth of Massachusetts, 1964, Special report of Dept. of Public Health relative to the preparation of plans and maps for the disposal of sewage in the Merrimack River valley: Comm. of Mass. House Doc. No. 3733, 219 p.
- Currier, J.J., 1906, History of Newburyport, Massachusetts- 1764 to 1905: Newburyport, Mass., 412 p.
- DaBoll, J.M., 1969, Holocene sediments of the Parker River estuary, Massachusetts: M.S. Thesis, Univ. of Massachusetts, Amherst, Massachusetts, Coastal Research Group Contribution no. 3-CRG, 138 p.
- Davis, C.A., 1910, Salt marsh formation near Boston and its geological significance: Econ. Geology, v. 5, P. 623-639.
- Dexter, R.W., 1947, Marine communities of a tidal inlet at Cape Ann, Mass. a study in bio-ecology: Econ. Monographs, v. 17, p. 261-294.

- Emerson, B.K., 1917, Geology of Massachusetts and Rhode Island: U.S. Geol. Survey Bull. 597, 289 p.
- Folk, R.L., 1968, Petrology of Sedimentary rocks: Austin, Texas, Hemphills, 170 p.
- _____ and Ward, W.C., 1957, Brazos River bar- a study in the significance of grain size parameters: Jour. Sed. Petrology, v. 27, p. 3-26.
- Haven, D.S. and Morales-Alamo, R., 1969, Biodeposition as a factor in estuarine sedimentary processes (abs): Southeastern Section, 18th Ann. Mtg. Geol. Soc. America, p. 33.
- Jerome, W.C., Jr., Chesmore, A.P., Anderson, C.O., Jr., and Grice, F., 1965, A study of the marine resources of the Merrimack River estuary: Mass, Div. of Marine Fisheries, Mono. Ser. No. 1, 90 p.
- Johnson, D.W., 1919, Shore processes and shoreline development: New York, John Wiley and Sons, Inc., 584 p.
- _____ 1925, New England-Acadian Shoreline: New York, John Wiley and Sons, Inc., 608 p.
- McCormick, C.L., 1968, Holocene stratigraphy of the marshes at Plum Island, Massachusetts: Ph.D. thesis, Univ. of Mass., 104 p. (unpublished).
- McIntire, W.G. and Morgan, J.P., 1963, Recent geomorphic history of Plum Island, Massachusetts, and adjacent coasts: Louisiana State Univ., Coastal Studies Ser. No. 8, 44 p.
- Nichols, R.L., 1942, Shoreline changes on Plum Island, Massachusetts: Am. Jour. Sci., v. 240, p. 349-355.
- Postma, H., 1967, Sediment transport and sedimentation in the estuarine environment, p. 158-179, in Lauff, g.H., Editor, Estuaries: Amer. Assoc. for the Advancement of Sci., Washington, D.C., 757 p.
- Pritchard, D.W., 1955, Estuarine circulation patterns: Amer. Soc. Civil Engineers, Proc. 81, 717/1-717/11.
- Redfield, A.C., 1965, Ontogeny of a salt marsh estuary: Science, v. 147, p. 50-55.
- _____ and Rubin, M., 1962, The age of salt marsh peat and its relation to recent changes in sea level at Barnstable, Mass.: Proc. Natl. Acad. Sci., v 48, p. 1728-1734.

- Reineck, H.E., 1967, Layered sediments of tidal flats, beaches, and shelf bottoms of the North Sea, p. 191-206, in Lauff, G.H., Editor, Estuaries: Amer. Assoc. for the Advancement of Sci., Washington, D.C., 757 p.
- Sammel, E.A., 1962, Configuration of the bedrock beneath the channel of the lower Merrimack River, Massachusetts: U.S. Geol. Survey Prof. Paper 405-D, p. D125-D127.
- , 1963, Surficial geology of the Ipswich quadrangle, Massachusetts: U.S. Geol. Survey Geol. Quad. Map GQ-189.
- Sears, J.H., 1905, The physical geography, geology, mineralogy, and paleontology of Essex county, Massachusetts: Salem, Mass., Essex Institute, 418 p.
- U.S. Geological Survey, 1968, Water resources data for Massachusetts, New Hampshire, Rhode Island, Vermont-1967: Water Resources Division, U.S. Geological Survey, 305 p.
- Wiesnet, D.R. and Cotton, J.E., 1967, Use of infrared imagery in circulation studies of the Merrimack River estuary, Massachusetts: U.S. Geological Survey open-file report, 11 p., (reprinted as National Aeronautics and Space Administration Tech. Letter NASA-78).

